



# QEX

INCLUDING:  
COMMUNICATIONS  
QUARTERLY

Forum for Communications Experimenters

March / April 2001

Build K2QHE's  
Compensated, Modular  
RF Voltmeter



**ARRL** *The national association  
for AMATEUR RADIO*  
225 Main Street  
Newington, CT USA 06111-1494

# You have questions...

How many microvolts is 85 dBm at 50 ohms?  
What is the spectral content of QPSK?  
What the resistor color code and standard values?  
How do digital IIR and FIR filters work?  
What mixer spurs result from 70 MHz RF and 18.1 MHz LO?  
How does an active filter work?  
How do I wind a 120 nH inductor?  
What capacitor resonates with 2.2  $\mu$ H at 10.7 MHz?  
What VSWR corresponds to 12 dB return loss?  
What s the effect of reducing Q from 300 to 100?  
What is Miller effect?  
How do I perform two-port transformations?  
How is bias set on bipolar transistors and FETs?  
What are the basics of SPICE analysis?  
What do all those noise parameters mean?  
How do I make a 700 Hz active bandpass filter?  
What are Maxwell s equations?  
Can I graph the  $\sin(x)/x$  curve?  
What dimensions do I need for a 50 ohm microstrip?  
How do I match 25 +j40 ohms to my 75 ohm system?  
Where can I find a review of Kirchoff s Laws?  
How much antenna gain does my system need?  
How do I bias a BFR91 or 2N2222 transistor?  
Will I get bad crosstalk between lines on my p.c. board?  
Can I perform basic transfer function math?  
How can a beginner learn about components at RF?  
What s the difference between linear and non-linear?  
What is the capacitance of two 11 cm plates spaced 1 mm?  
Why do we use feedback?  
I know RF, but where can I find digital basics?  
Can I do vector to scalar conversons?  
What is the AC impedance of a parallel R-C network?  
What is a conductor's skin depth at 900 MHz?  
What do those thermal resistance numbers mean?  
Can I visualize the field lines between capacitor plates?  
What is the mismatch loss of a 5.22:1 VSWR?  
How do I simulate a darlington pair amplifier?  
What are the resistor values for a 50 ohm 6 dB pad?  
Should I use a pi or tee matching network in my circuit?



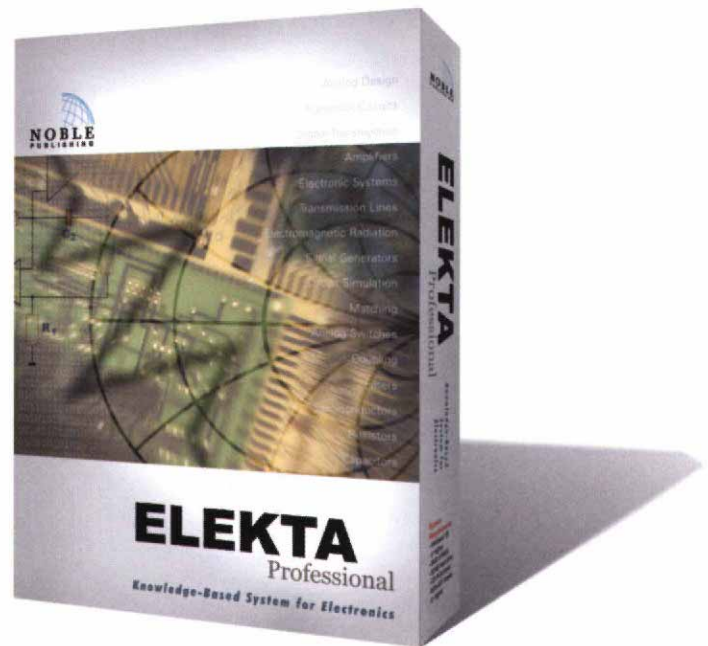
For information or to order contact:  
Noble Publishing, 630 Pinnacle Court, Norcross, GA 30071  
Tel: 770-449-6774 • Fax: 770-448-2839  
[www.noblepub.com](http://www.noblepub.com)

The Deal is Back!

# ELEKTA

Professional

has the  
answers!



SPECIAL OFFER

**\$89**

shipped FREE within US and Canada  
(\$109 shipped worldwide)

*This Offer Expires 3/31/01*

\* Dealer inquiries invited



**INCLUDING: COMMUNICATIONS  
QUARTERLY**

QEX (ISSN: 0886-8093) is published bimonthly in January, March, May, July, September, and November by the American Radio Relay League, 225 Main Street, Newington CT 06111-1494. Yearly subscription rate to ARRL members is \$22; nonmembers \$34. Other rates are listed below. Periodicals postage paid at Hartford, CT and at additional mailing offices.

POSTMASTER: Send address changes to: QEX, 225 Main St, Newington, CT 06111-1494 Issue No 205

David Sumner, K1ZZ  
*Publisher*

Doug Smith, KF6DX  
*Editor*

Robert Schetgen, KU7G  
*Managing Editor*

Lori Weinberg  
*Assistant Editor*

Peter Bertini, K1ZJH  
Zack Lau, W1VT  
*Contributing Editors*

**Production Department**

Mark J. Wilson, K1RO  
*Publications Manager*

Michelle Bloom, WB1ENT  
*Production Supervisor*

Sue Fagan  
*Graphic Design Supervisor*

David Pingree, N1NAS  
*Technical Illustrator*

Joe Shea  
*Production Assistant*

**Advertising Information Contact:**

John Bee, N1GNV, *Advertising Manager*  
860-594-0207 direct  
860-594-0200 ARRL  
860-594-0259 fax

**Circulation Department**

Debra Jahnke, *Manager*  
Kathy Capodicasa, N1GZO, *Deputy Manager*  
Cathy Steпина, *QEX Circulation*

**Offices**

225 Main St, Newington, CT 06111-1494 USA  
Telephone: 860-594-0200  
Telex: 650215-5052 MCI  
Fax: 860-594-0259 (24 hour direct line)  
e-mail: [qex@arrl.org](mailto:qex@arrl.org)

Subscription rate for 6 issues:

In the US: ARRL Member \$22,  
nonmember \$34;

US, Canada and Mexico by First Class Mail:  
ARRL member \$35, nonmember \$47;

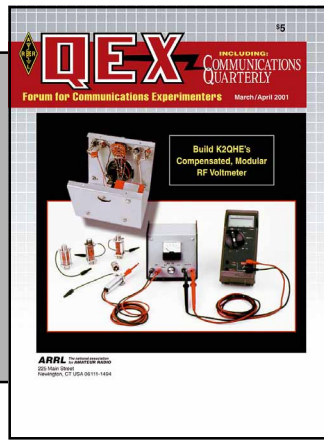
Elsewhere by Surface Mail (4-8 week delivery):  
ARRL member \$27,  
nonmember \$39;

Elsewhere by Airmail: ARRL member \$55,  
nonmember \$67.

Members are asked to include their membership control number or a label from their QST wrapper when applying.

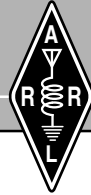
In order to ensure prompt delivery, we ask that you periodically check the address information on your mailing label. If you find any inaccuracies, please contact the Circulation Department immediately. Thank you for your assistance.

Copyright ©2001 by the American Radio Relay League Inc. For permission to quote or reprint material from QEX or any ARRL publication, send a written request including the issue date (or book title), article, page numbers and a description of where you intend to use the reprinted material. Send the request to the office of the Publications Manager ([permission@arrl.org](mailto:permission@arrl.org))



**About the Cover**

K2QHE's voltmeter can work with or without an external DVM. The article begins on [page 26](#).



**Features**

**3 The ATR-2000: A Homemade, High-Performance HF Transceiver, Part 3**

*By John B. Stephensen, KD6OZH*

**9 PTC: Perceptual Transform Coding for Bandwidth Reduction of Speech in the Analog Domain, Part 2**

*By Doug Smith, KF6DX*

**18 Beyond Fractional-N, Part 1**

*By Cornell Drentea, KW7CD*

**26 A Compensated, Modular RF Voltmeter**

*By Sid Cooper, K2QHE*

**35 The Rectangle Family of Antennas, Part 1: The Not-So-Simple Rectangle**

*By Dan Handelsman, N2DT*

**47 The Quad Antenna Revisited, Part 4: Effects of Ground on Quad Loops**

*By R. P. Haviland, W4MB*

**Columns**

**55 RF** *By Zack Lau, W1VT*

**60 Letters to the Editor**

**59 Upcoming Conferences**

**62 Next Issue in QEX**

**Mar/Apr 2001 QEX Advertising Index**

Active Electronics: [59](#)  
American Radio Relay League: [46](#), [63](#),  
[64](#), [Cov III](#), [Cov IV](#)  
Atomic Time, Inc.: [8](#)  
Roy Lewallen, W7EL: [34](#)  
Nemal Electronics International, Inc.: [34](#)

Noble Publishing: [Cov II](#)  
Palomar: [46](#)  
Tucson Amateur Packet Radio Corp: [62](#)  
TX RX Systems Inc.: [58](#)  
Universal Radio, Inc.: [34](#), [58](#)





The American Radio Relay League, Inc. is a noncommercial association of radio amateurs, organized for the promotion of interests in Amateur Radio communication and experimentation, for the establishment of networks to provide communications in the event of disasters or other emergencies, for the advancement of radio art and of the public welfare, for the representation of the radio amateur in legislative matters, and for the maintenance of fraternalism and a high standard of conduct.

ARRL is an incorporated association without capital stock chartered under the laws of the state of Connecticut, and is an exempt organization under Section 501(c)(3) of the Internal Revenue Code of 1986. Its affairs are governed by a Board of Directors, whose voting members are elected every two years by the general membership. The officers are elected or appointed by the Directors. The League is noncommercial, and no one who could gain financially from the shaping of its affairs is eligible for membership on its Board.

"Of, by, and for the radio amateur," ARRL numbers within its ranks the vast majority of active amateurs in the nation and has a proud history of achievement as the standard-bearer in amateur affairs.

A bona fide interest in Amateur Radio is the only essential qualification of membership; an Amateur Radio license is not a prerequisite, although full voting membership is granted only to licensed amateurs in the US.

Membership inquiries and general correspondence should be addressed to the administrative headquarters at 225 Main Street, Newington, CT 06111 USA.

Telephone: 860-594-0200  
Telex: 650215-5052 MCI  
MCIMAIL (electronic mail system) ID: 215-5052  
FAX: 860-594-0259 (24-hour direct line)

#### Officers

**President:** JIM D. HAYNIE, W5JBP  
3226 Newcastle Dr, Dallas, TX 75220-1640

**Executive Vice President:** DAVID SUMNER, K1ZZ

The purpose of *QEX* is to:

- 1) provide a medium for the exchange of ideas and information among Amateur Radio experimenters,
- 2) document advanced technical work in the Amateur Radio field, and
- 3) support efforts to advance the state of the Amateur Radio art.

All correspondence concerning *QEX* should be addressed to the American Radio Relay League, 225 Main Street, Newington, CT 06111 USA. Envelopes containing manuscripts and letters for publication in *QEX* should be marked Editor, *QEX*.

Both theoretical and practical technical articles are welcomed. Manuscripts should be submitted on IBM or Mac format 3.5-inch diskette in word-processor format, if possible. We can redraw any figures as long as their content is clear. Photos should be glossy, color or black-and-white prints of at least the size they are to appear in *QEX*. Further information for authors can be found on the Web at [www.arrl.org/qex/](http://www.arrl.org/qex/) or by e-mail to [qex@arrl.org](mailto:qex@arrl.org).

Any opinions expressed in *QEX* are those of the authors, not necessarily those of the Editor or the League. While we strive to ensure all material is technically correct, authors are expected to defend their own assertions. Products mentioned are included for your information only; no endorsement is implied. Readers are cautioned to verify the availability of products before sending money to vendors.

# Empirically Speaking

In college, I took an introductory course in digital electronics. After having learned the basics of logic gates, shift registers, adders and so forth, we proceeded to our first project: the design of a desktop calculator. Hand-held calculators were already popular at the time and many students wondered why we should bother with such a seemingly mundane exercise. But many of those same students were in the habit of accepting the answer their calculators gave them without question. "The machine can't lie," they'd say. "Does the answer make sense, though?" was my standard response; and that was often when the thinking process began—after an answer had been obtained.

These days, we have many design aids in software and a nearly universal platform for their execution: the personal computer. Tremendous progress has been made in modeling structures such as antennas, amplifiers and filters. Those models arise from direct application of the scientific method. Measurement is logically the first step in the search for the truth, but it is too easy to leave out that step. In addition, I might be tempted to add a new last step to the method that should be self-evident: Repeat it until you're satisfied your theory agrees with reality.

My point is that omission of actual measurements may leave us short of complete solutions. A theory is only a theory until it is shown to explain all observations. Making measurements, though, is perhaps not as easy—or fun—as crunching numbers. Specifically, it may not be fun when the measurements show that your theory is wrong, or when they prove a competing theory right. We therefore especially encourage the publication of your data as well as your analysis.

Mathematical proofs are fine and some theories even defy proof by measurement. For example: I read a proof many years ago that  $\sqrt{2}$  is an irrational number. An irrational number is one that cannot be written down exactly; its numerical representation contains an infinite number of digits and so can never be precisely depicted

on paper. A colleague argued that in base- $\sqrt{2}$ , the number may be simply written as 1; hence, it is not an irrational number in that base. I looked again at the proof. I found it did not mention base anywhere and that it made no assumptions about how things are written down: I could not refute it. The proof began with the assumption that  $\sqrt{2}$  is a rational number and finished with an equation that was obviously untrue. That kind of disproof is known as "reduction to absurdity."

So even though measurement is not always possible, I believe a way to understanding how things really work always is. That's what keeps me going.

#### In This Issue

**John Stephensen, KD6OZH**, returns with the final segment of his homebrew transceiver project. We got a lot of good feedback on this series, and I think you'll find the conclusion was worth the wait. Having finished the initial work on my Perceptual Transform Coding codec, I offer an explanation of how it functions, as well as some results. *You* are going to make the measurements on it by listening to it and deciding, albeit subjectively, whether there is any merit to it.

**Cornell Drentea, KW7CD**, discusses contemporary synthesizer design approaches in the first part of his two-part series. He explains how he's taken DDSs to certain limits in various applications. **Sid Cooper, K2QHE**, presents an RF voltmeter you can build. It's a very valuable measurement tool and a welcome addition to most ham shacks.

**Dan Handelsman, N2DT**, has been working with rectangular antennas and he discloses some interesting findings in the first segment of his series. In the same vein, **Bob Haviland, W4MB**, discusses the effects of ground on loop antennas.

In **RF**, Zack explores the application of an off-center-fed dipole for HF QRP work. He presents construction information for a balun and transformer.—73, **Doug Smith, KF6DX**; [kf6dx@arrl.org](mailto:kf6dx@arrl.org). □□



# *The ATR-2000: A Homemade, High-Performance HF Transceiver, Part 3*

---

*Part 3 completes this series with details of the power amplifier,  
noise blanker, control circuitry and power supplies*

---

By John B. Stephensen, KD6OZH

This is the last of three articles about a homemade HF transceiver. The transceiver was designed to provide high performance with minimal complexity and previous articles<sup>1</sup> have covered the signal-processing path of the receiver, including the local oscillator, mixer, IF amplifier, product detector/balanced modulator and AGC. This part covers the power amplifier, noise blanker, control circuitry and power supplies.

## **Power Amplifier Circuit**

The linear amplifier increases the

<sup>1</sup>Notes appear on [page 6](#).

---

153 Gretna Green Way  
Los Angeles, CA 90049  
[kd6ozh@amsat.org](mailto:kd6ozh@amsat.org)

output of the mixer and band-pass filter described in Part 1 (about -12 dBm) to the 100-W level. The initial three stages, shown in Fig 1, operate class A and provide 38 dB of gain. Each uses collector-to-base feedback and emitter degeneration to achieve approximately 50-Ω input and output impedances. The circuit is derived from one shown in Chapter 8 of *Solid State Design for the Radio Amateur*<sup>2</sup> and is capable of 800 mW of output with -40 dBc third-order distortion products. The TO-5 case 2N3553 transistors used in the last stage are no longer manufactured, but TO-220 case RF power transistors, such as the MRF475, may be an acceptable substitute. The driver was constructed on copper-clad epoxy-glass Vectorboard.

A Motorola MRF151 power FET is

used in the final amplifier, as shown in Fig 2. This transistor was selected because of its excellent linearity and ruggedness. It also requires a much simpler circuit than would a bipolar transistor. The device can withstand a 30:1 SWR so protection circuits are not needed. The circuit used is based on the Motorola data sheet and provides 26 dB of gain at 14 MHz, 24 dB at 28 MHz. The gate of a power FET is almost purely capacitive at HF and is 350 pF for the MRF151. Series and shunt resistors are added to provide a reasonable input impedance and enhance stability. It is matched to 50-Ω by a broadband 9:1 transformer. The input transformer is noncritical; it is wound on a small ferrite balun core.

The PA was constructed with a simple PC board made by cutting-

away unused areas of copper. The circuit board is mounted on a 1/4-inch-thick aluminum plate that is then bolted to a large heat sink. The layout is not critical except for the short leads from the two FET emitters to ground. The MRF151 operates with 40-50 V dc on the drain and its drain current can reach 4 A. The relatively high voltage provides three benefits:

- The optimal output impedance is higher than that of a low-voltage de-

vice, and it is more easily matched to 50  $\Omega$ .

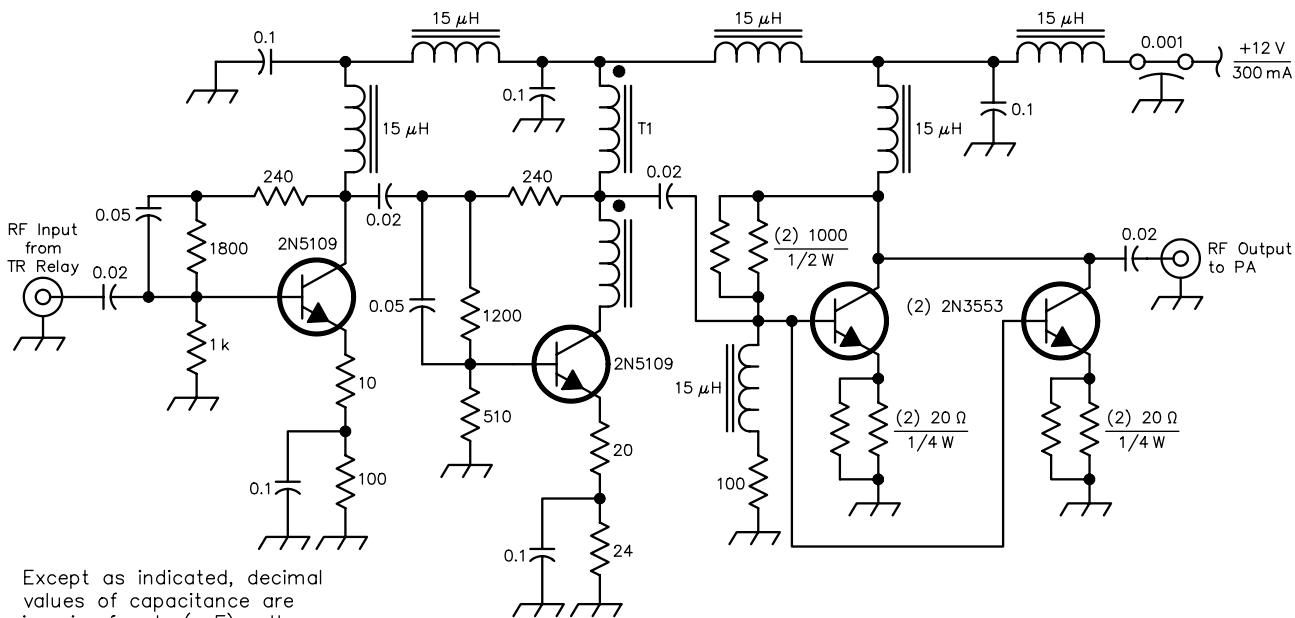
- The smaller dc current flowing through the primary winding requires less ferrite to withstand the dc magnetizing force and prevent core saturation.

- The device is more linear and produces less intermodulation distortion (IMD) than devices operating at lower voltages.

The 9:1 output matching trans-

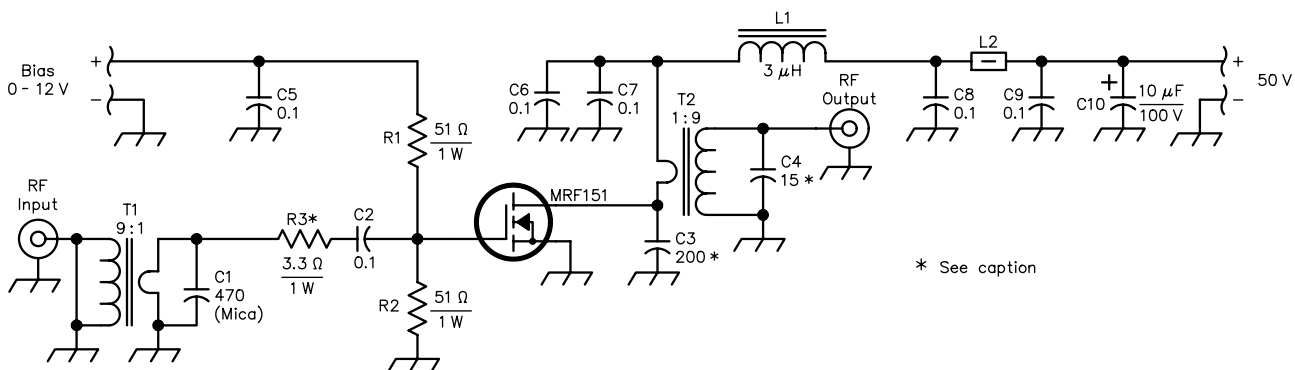
former is built from two sets of ferrite cores mounted on brass tubes that serve as the primary winding. The primary winding is completed by a copper shorting plate at one end. Three turns of #18 AWG wire insulated with Teflon tubing are threaded through the tubes to make the secondary winding. The MRF151 is biased for 500 mA of standing current to minimize distortion at low power levels.

A diplexer filter follows the amplifier.



Except as indicated, decimal values of capacitance are in microfarads ( $\mu\text{F}$ ); others are in picofarads (pF); resistances are in ohms; k = 1,000.

Fig 1—Schematic of the class-A driver. T1 is 7 bifilar turns of #26 AWG enameled wire on an FT37-43 ferrite core.



\* See caption

Fig 2—Schematic of the class-AB1 power amplifier.

C2, C5-C9—0.1  $\mu\text{F}$  ceramic chip or monolithic with short leads.  
C3—200 pF unencapsulated mica or dipped mica with short leads.  
C4—15 pF unencapsulated mica or dipped mica with short leads.

L1—3  $\mu\text{H}$  VK200/4B ferrite choke or equivalent  
L2—2 ferrite beads 2  $\mu\text{H}$   
R3—3.3  $\Omega$ , 1-W carbon (made from 2 parallel connected 6.8  $\Omega$ , 1/2-W components)

T1—Amidon BLN-61-202 binocular core with 1-turn 1/8-inch OD brass tubing primary, 3-turns #24 AWG secondary.  
T2—4 stacked Amidon FT50B-61 toroid cores with 3-turn #18 AWG primary and 1-turn 9/32-inch OD brass tubing secondary.

The circuit is unique in that it requires only three inductors but provides more than 50 dB of harmonic suppression and low return loss to reduce IMD. This level of harmonic suppression is required to meet the proposed spurious output limits that may go into effect in 2003.<sup>3</sup> A good return loss is required with power FETs to minimize distortion. Otherwise, harmonics are reflected back into the drain circuit to mix with the output signal, producing odd-order IMD products. A typical filter/diplexer for this application is composed of parallel connected low and high-pass filters; however, even a minimal filter such as that used by WO1YH<sup>4</sup> to reduce IMD in a push-pull amplifier requires five inductors. This is inadequate for use with a single FET as it provides only 25 dB of second-harmonic attenuation. A Cauer filter, such as the WB6BLD design,<sup>5</sup> can provide over 50 dB of second- and third-harmonic attenuation with only two inductors, but provides no termination for harmonics.

The filter used here is unconventional in two ways. Its passband is modified to provide low attenuation only over the actual Amateur Radio bands, and the input circuit is a diplexer that improves linearity by routing amplifier harmonics to a suitable load. The first section of the filter consists of a termination resistor in series with the input (to provide a good return loss at harmonic frequencies) and a series-tuned circuit ( $Q=1$ ) to bypass the termination at the fundamental frequency. The next two sections are similar to a low-pass Cauer filter, but the component values are modified to compensate for the addition of the series-tuned circuit. The return loss at the second harmonic is over 12 dB and increases to over 20 dB at the third harmonic. The predicted attenuation and return loss for the 20 and 10-meter versions are shown in Figs 4 and 5.

The power amplifier was tested with a two-tone audio input to the transceiver and the drive level was increased until the third-order IMD product was at the -30 dBc level. The

fifth- and seventh-order IMD products were considerably lower, and higher-order products were not measurable. The CW power output was 110 W with 42.5 V dc on the drain. See Table 1.

The amplifier was initially tested with a low- $Q$ ,  $\pi$ -network filter on the output, and harmonic distortion was worse than shown above. The diplexer circuit reduced distortion products by 5 dB.

### Noise Blanker

The noise blanker differs from most

in that it has a separate receiver to pick up the noise and operate the blanker. The noise receiver (see Fig 6) is a wideband TRF amplifier followed by an envelope detector. The blanking level is set via a simple attenuator (R1) at the input of the receiver. The first RF stage (Q1) is a common-source dual-gate MOSFET amplifier with a high- $Q$  tuned circuit to provide some selectivity. The drain is terminated in a low-impedance broadband transformer to ensure stability. This is followed by a 5 to 30 MHz band-pass filter to prevent

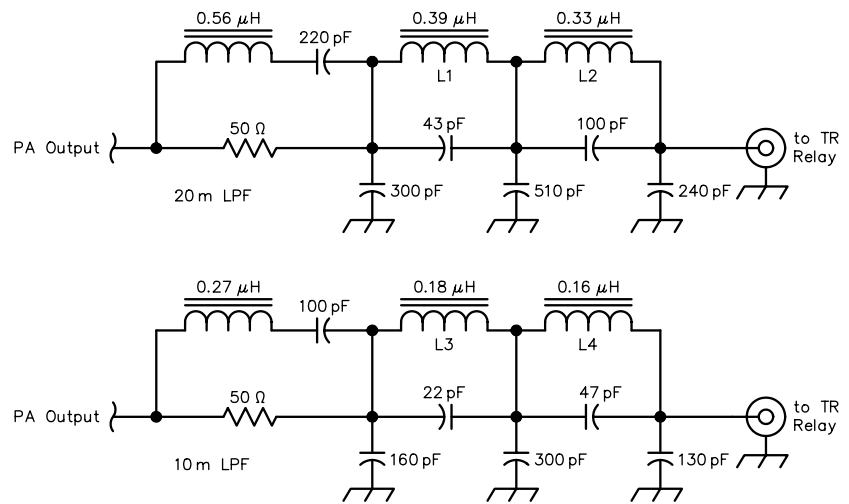


**Fig 3—Schematic diagram of 10- and 20-meter low-pass filters. All capacitors are DM19 silver mica  $\pm 5\%$ , 500 V. Resistors are Caddock MP930 50  $\Omega$ ,  $\pm 1\%$ . Adjust inductors for best return loss by compressing turns.**

**L1—16 turns of #18 AWG enameled wire on a T130-0 toroid core.**

**L2—15 turns of #18 AWG enameled wire on a T130-0 toroid core.**

**L3—11 turns of #18 AWG enameled wire on a T130-0 toroid core.**

**L4—10 turns of #18 AWG enameled wire on a T130-0 toroid core.**

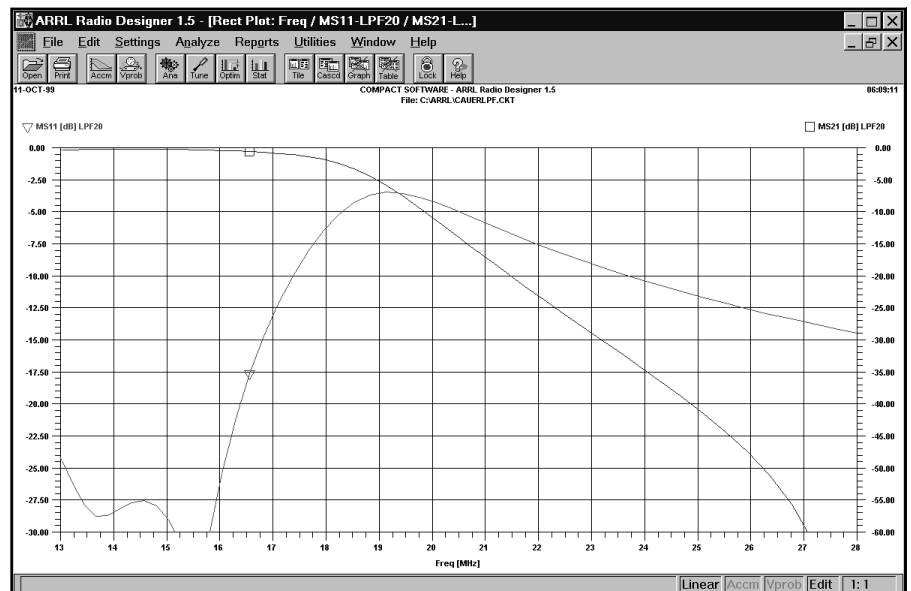


**Fig 4—Attenuation (S21) and return loss (S11) of 20-meter filter.**

**Table 1—Measured IMD**

Product Level	
Order	(dBc)
3	-30
5	-40
7	-48
9-11	-58



strong VHF-TV or AM-broadcast stations from activating the blanker. The final three gain stages are broadband resistive-feedback bipolar amplifiers. The total gain of the noise receiver is approximately 60 dB.

The final noise amplifier (Q4) is capable of 200 mW of output and drives a low-impedance detector circuit, Q5, through a 9:1 step-up transformer. Positive cycles of noise pulses cause this transistor to conduct. Its collector is attached to the blanker circuitry (described in Part 2 of this article series) where it discharges a timing capacitor to control the noise gate. Negative cycles of noise pulses are clipped by a diode to prevent base-emitter breakdown on strong pulses.

In my neighborhood, either noise is absent or it is present at S7-S9 levels. This noise blanker has worked very effectively, reducing noise to S1 levels. I use a length of wire about 15 feet above the ground to sample the noise. When enabled, the noise receiver is tuned to the frequency where noise is loudest but away from any high-powered stations that might accidentally activate the blanker. The gain is set to maximize blanker effectiveness and does not require adjustment as the signal receiver is tuned within the amateur band. Consequently, I have not attempted to computerize the noise blanker tuning or gain controls.

When viewing the noise on a spectrum analyzer, the strength of the broadband noise varies considerably with frequency, going through peaks and nulls. At my location, the noise peaks near 17 MHz, and the blanker is most effective with the noise receiver tuned near this peak. When first developing this blanker, I tried using a superheterodyne noise receiver with a multipole, 150-kHz-bandwidth IF filter as I had done in a VHF receiver several years ago. The noise reduction on the S-meter was only 20-30 dB, while the broadband TRF noise receiver allows 40-50 dB of reduction. The key to the effectiveness of this design seems to be minimizing the delay in the noise receiver in order to activate the noise gate as early as possible. The broad bandwidth also collects as much noise as possible, which enhances the amplitude of the noise spikes compared to other signals.

### Power Supply

The power supply for the 100-W amplifier is extremely simple. As

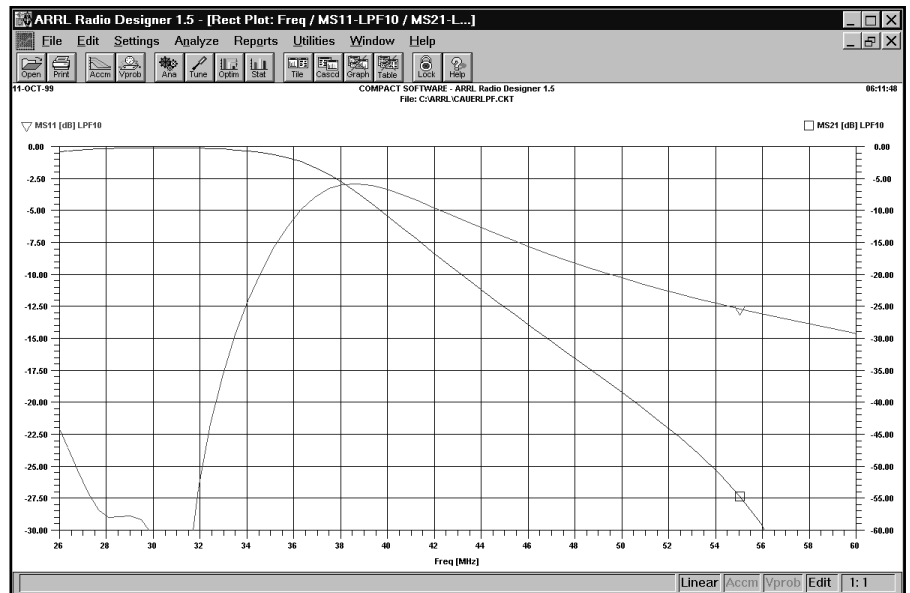


Fig 5—Attenuation (S21) and return loss (S11) of 10-meter filter.

shown in Fig 7, it consists of an unregulated supply that provides 42-48 V dc (for 110-120 V ac input) from a full-wave rectifier for the power FET. It also supplies 21-24 V from the transformer center tap to operate the antenna-changeover relay. An IC voltage regulator provides +12 V dc for the class-A driver stages.

The supply voltage for the power FET must not vary significantly during operation, as that would cause IMD. For this reason, two large aluminum electrolytic capacitors are used to filter the 48-V output to eliminate any audio-frequency ripple. The transformer and rectifiers are protected by a series resistor in the transformer primary circuit to limit inrush current as the capacitors charge. A 48 V dc relay is activated as the capacitors charge to short out the current-limiting resistor during normal operation.

The power supply for the rest of the transceiver is shown in Fig 8. Three voltages are supplied: +28 V, +15 V and -15 V. The 28-V supply uses a full-wave voltage doubler and linear voltage regulator to supply a few milliamperes for the transceiver VCO. The  $\pm 15$ -V supplies power the rest of the transceiver and each consists of a full-wave rectifier and linear regulator. Less than 1 A is required from each supply, with the bulk being converted to  $\pm 5$  V by local voltage regulators to power the DDS.

### Conclusions

This project provided an interesting experience in optimizing analog circuit design for me (I spent much of my working life designing digital circuits) and resulted in a very useful transceiver. One of the pleasant surprises was the simplification of the frequency-synthesizer circuit afforded by current technology. A single-loop PLL combined with a DDS provides a very simple and attractive local oscillator for SSB transceivers when the PLL multiplication factor is low, the loop bandwidth is small and VCO frequency range is narrow.

### Notes

- <sup>1</sup>J. B. Stephensen, KD6OZH, "The ATR-2000: A Homemade, High-Performance HF Transceiver," *QEX*, Mar/April 2000, pp 3-15; Part 2, May/June 2000, pp 39-51. The firmware for the ATR-2000 consists of SYNTHCTL.ZIP (code for the synthesizer PIC) and RADIOCTL.ZIP (code for the PC interfaced PIC). You can download this package from the ARRL Web [www.arrl.org/qexfiles/](http://www.arrl.org/qexfiles/). Look for ATR2000.ZIP.
- <sup>2</sup>W. Hayward, W7ZOI, and D. DeMaw, W1FB, *Solid State Design for the Radio Amateur*, (Newington: ARRL, 1977).
- <sup>3</sup>L. Price, W4RA, and P. Rinaldo, W4RI, "WRC 97—An Amateur Radio Perspective," *QST*, Feb 1998, pp 31-34.
- <sup>4</sup>W. E. Sabin, W0IYH, "Diplexer Filters for an HF MOSFET Power Amplifier," *QEX*, Jul/Aug 1999, pp 20-26.
- <sup>5</sup>J. L. Tonne, WB6BLD, "Harmonic Filters, Improved," *QEX*, Sep/Oct 1998, pp 50-53.



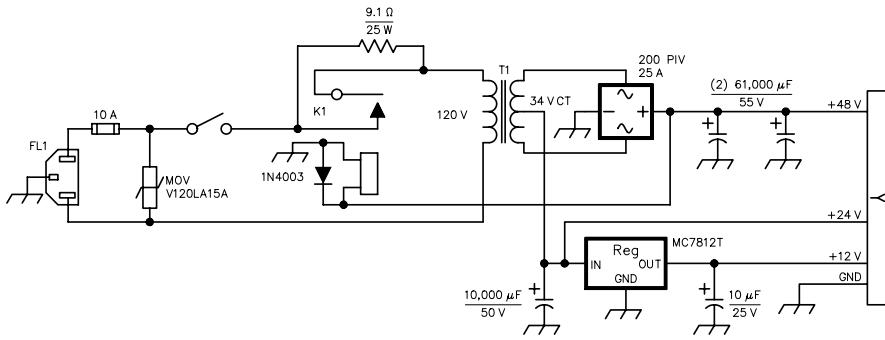


**Fig 7—Schematic of the PA power supply.**  
 FL1—250 V ac, 10 A IEC receptacle and line filter  
 K1—SPST relay with 48 V dc coil and normally open 10 A contacts  
 T1—Transformer, 120-V primary, 34-V center tapped secondary from Surplus Sales (Col-662-0650-020).

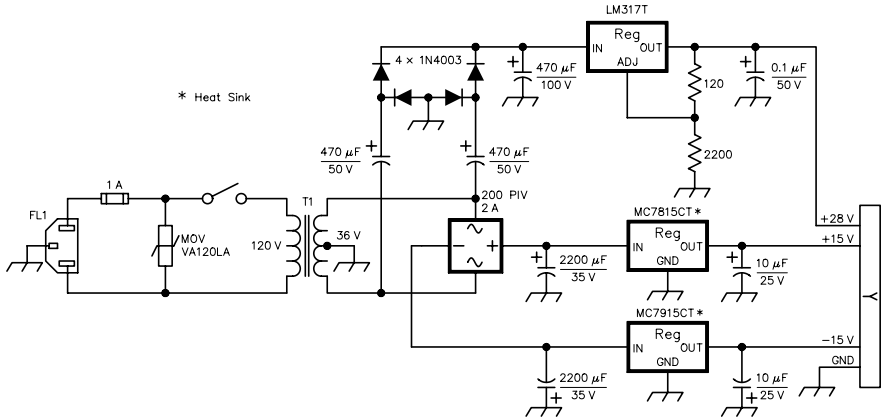


**Fig 8—Schematic of the main power supply.**  
 FL1—250-V, 3-A IEC receptacle and line filter  
 T1—transformer, 120-V primary, 36-V, 0.8 A center tapped secondary (All Electronics TX-3608)

 <p><b>SALE</b></p>	<h2 style="text-align: center;">ATOMIC TIME™</h2> <p style="text-align: center;">...self setting ...correct time ...atomic clock</p> <p style="text-align: center;">World's most exact time... atomic clocks, atomic watches and weather stations</p> <ul style="list-style-type: none"> <li>• for any time zone</li> <li>• synchronized to the u.s. atomic clock in colorado</li> <li>• accurate to 1sec. in 1 mil. years</li> <li>• engineered in germany</li> </ul> <p><b>complete line of atomic clocks</b>          JUNGHANS MEGA CERAMIC Watch          JUNGHANS MEGA CARBON Watch          JUNGHANS MEGA CLOCKS          JUNGHANS SOLAR WATCHES          ATOMIC SPORTS WATCHES          ATOMIC SCHOOL/OFFICE CLOCKS          ATOMIC INDUSTRIAL CLOCKS          Oregon Scientific Weather Stations,          Weather Forecast, World Time, NOAA          Radios, Radio Controlled Clocks...          call for our FREE Brochure          or go to <a href="http://www.atomictime.com">www.atomictime.com</a>          credit card orders call toll free  <b>1-800-985-8463</b>          30 Day Money Back Guarantee          send checks incl. s&amp;h \$6.95 to          ATOMIC TIME, INC.          1010 JORIE BLVD.          OAK BROOK, IL 60523</p>	 <p>atomic dual alarm clock w. temperature day and date, black 3.5x4.5x2 \$29.95</p>
 <p>atomic radio with 2 alarms and temperature, day, date, LCD \$39.95</p>		 <p>jumbo digit atomic clock w. temperature &amp; day and date, wall or desk 8.5 x8.5 x1 • \$49.95</p>
<p><b>NEW</b></p>  <p>Junghans atomic carbon, stainless bezel, sapphire lens LCD day, date - carbon/leather band • \$279.00</p>	 <p>black arabic 12 wall clock for home or office • \$59.95 (wood \$69.95)</p>	



# *PTC: Perceptual Transform Coding for Bandwidth Reduction of Speech in the Analog Domain, Part 2*

---

*Our exploration continues with an experimental codec,  
downloadable .WAV files and examination of the coded signals.*

---

By Doug Smith, KF6DX

*[Note: The author apologizes for the length of time between Parts 1 and 2. He will, no doubt, blame it on the editor—Ed.]*

## **Recapitulation of Part 1**

In Part 1 of this article,<sup>1</sup> properties of human speech and hearing were examined for quantization effects that may be exploited in bandwidth-reduction schemes. When we left off, we were ready to choose methods of efficiently representing speech signals. Here in Part 2, we'll take a look at the actual implementation of a PTC codec, beginning with principles of subband

---

PO Box 4074  
Sedona, AZ 86340  
[kf6dx@arrl.org](mailto:kf6dx@arrl.org)

decomposition. We'll finish with tests and analysis of the resulting frequency-companded signals.

## **Subband Decomposition**

Choosing how to represent a signal is an important problem in DSP—just as important as how a signal is manipulated. In this section, I'll show how *subband decomposition* helps meet the requirement for frequency resolution proportional to frequency (see Part 1) while minimizing the computational burden of analysis and synthesis operations. This technique is moderately well documented in contemporary literature but is poorly understood in general. Most of the texts currently available were written by mathematicians for other mathematicians. That often results in stuff

that's too insensible and that rarely comes close to the goal of explaining things clearly. I went through a lot of brain wracking doing this and I don't expect you to get it right away. Let me know if you have questions.

Mathematical language can be concise and elegant; it is also frequently ambiguous and sometimes reveals little of its underlying usefulness at first glance. I will use it where I have to, but I will also try to blow away some of the fog surrounding what should be part of Amateur Radio's repertoire.

## *Review of Traditional Spectral Analysis Methods for Speech*

The fast Fourier transform (FFT) has traditionally played a major role in speech communications research. Portions of speech such as sustained

vowel sounds or fricatives, for example, can be modeled as the output of a linear system excited by a source either periodically or randomly varying with time. The output of such a system is simply the product of the frequency response of the vocal tract and the spectrum of the excitation. Fourier analysis is useful in extracting these separate factors from speech waveforms (see Rabiner and Schafer, Reference 7 in Part 1). Over the long term, though, speech signals are considerably more complex than this simple model. Thus, standard Fourier-transform representations that are satisfactory for periodic, stationary signals are not necessarily appropriate for speech signals whose properties rapidly and distinctly change with time.

For reasons that will become apparent, it is reasonable and convenient to assume that the spectral content of speech doesn't change much over short time intervals, say 30 ms or so. This key unlocks a door to some of the redundancy we're seeking as a target for

bandwidth-reduction algorithms (more on this later). First, let's consider how certain properties of spectral analysis systems pertain to an analog perceptual speech coder.

In a previous series,<sup>2</sup> I described the FFT and showed that it is a *block transform*; it operates on a block of input samples and produces a block of output samples that portray the frequency content of the input. In another segment,<sup>3</sup> I showed how the damn-fast Fourier transform (DFFT) produces a nearly identical spectral analysis on a sample-by-sample basis. Note that the FFT has fixed frequency resolution directly proportional to the sampling frequency,  $f_s$ , and inversely proportional to the length of the input block,  $N$ :

$$\Delta f = \frac{f_s}{N} \quad (\text{Eq 1})$$

DFFT frequency resolution, on the other hand, can be different for each bin and we don't have to calculate all the bins to get a result.

We are seeking a method of spectral analysis that falls in line with what was shown previously for human hearing: Differential frequency threshold is somehow proportional to frequency. In other words, it is more difficult to detect differences in frequency the higher the frequency of the sounds. It is reasonable to suspect that an algorithm exploiting this fact will be more efficient than a straight FFT for

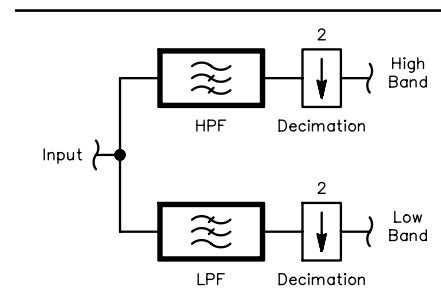


Fig 1—The first stage of subband decomposition.

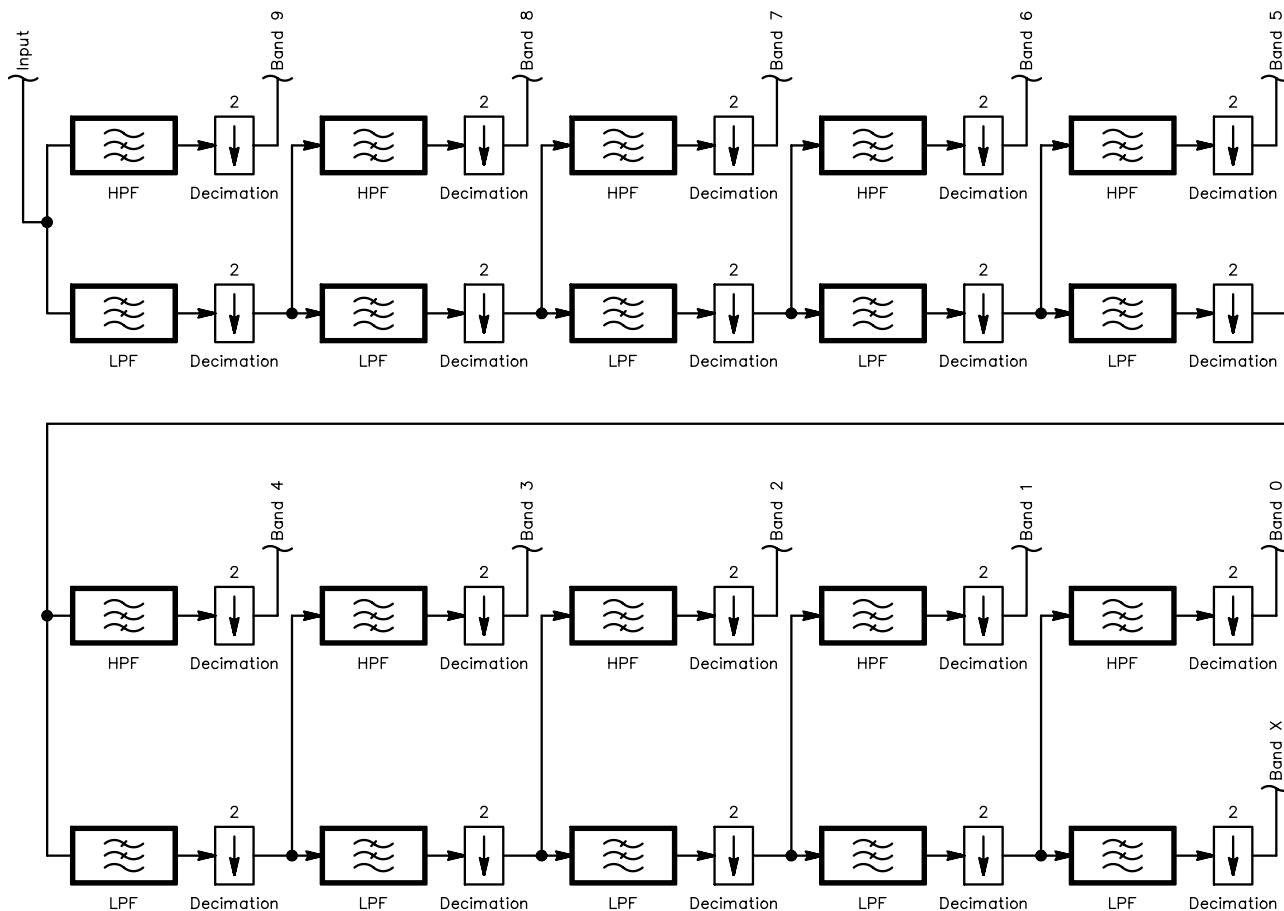


Fig 2—Complete 10-stage subband decomposition.

the analysis of speech signals, because the total number of bins calculated would be greatly reduced. The DFFT seems to meet the requirements of variable resolution and local calculation of selected bins, but the total computational burden can be reduced still further, where facilities exist for high-speed DSP filtering.

### Critically Sampled Filter Banks

Digital signal processors are optimized for the computation of *convolution sums* of the form:

$$y_n = \sum_{k=0}^{L-1} h_k x_{n-k} \quad (\text{Eq 2})$$

Such calculations are called multiply-and-accumulate (MAC) calculations. Those are exactly what are required to implement finite-impulse-response (FIR) filters in DSP. FFT and even DFFT algorithms don't necessarily make good use of MACs, so any filtering operation that reduces the complexity of subsequent FFTs is usually beneficial.

Rabiner and Schafer at Bell Labs worked on what are now called *multi-rate filter banks*.<sup>4, 5</sup> In the first step of one such scheme, the signal under analysis first passes through two filters: a high-pass and a low-pass. See Fig 1. These filters have nearly identical cutoff frequencies and thus separate the input spectrum into high- and low-frequency bands. Since each filter's bandwidth is half the original signal's bandwidth, the sampling rate at each filter's output may be reduced by a factor of two without destroying information. This is Nyquist's criterion. The process of lowering the sampling rate is called *decimation*. In it, every other sample is simply discarded. We could calculate the filter outputs at the higher rate before decimating them, but we save time by calculating only those we intend to keep.

Decimation filters with bandwidth equal to half of the input bandwidth (one quarter of the sampling frequency) are called *half-band* filters. When correctly designed, they have certain properties that lead to further computational savings.

In the second step, the decimated high-pass output is saved for later processing. The decimated low-pass output is further split into two subbands using half-band filters as before. The high-pass output is saved and the low-pass output split again. This process continues until no further band splitting can occur. The result is shown as the block diagram of

Fig 2. This is known as a *tree-structured* filter bank. The output of each filter is *maximally decimated* or *critically sampled* because its sampling rate is minimized.

Note that the sampling frequency is halved at each step; hence, the number of samples available in any particular time span is also halved. Band splitting must end when we are left with only a single sample. Except for the final division, outputs from the system all come from the high-pass filters. These are further processed by FFTs that compute frequency content. This decomposition has made it easier to achieve good frequency resolution at the lower frequencies since fewer samples represent fewer frequency bins of an FFT applied there. Because the FFT is a block transform, the size of input blocks for each FFT (that is, the time span) is directly related to the size of blocks coming through the filters. Perhaps this is easier to fathom by studying the following example.

Refer to Fig 2. Let's say the system's raw sampling rate is 31,250 Hz. The input bandwidth is, therefore, half that or 15,625 Hz. In keeping with our premise that speech doesn't change much over time spans on the order of 30 ms, we'll take that to be the length of the input block at the left-hand side of the diagram. To get the whole thing to work nicely, it would be nice if the input block contained a number of samples equal to an integral power of two. By inspection,  $2^{10}$  input samples looks like a good number, since:

$$\begin{aligned} \text{time span} &= \frac{\text{number of samples}}{\text{sampling frequency}} \\ &= \frac{N}{f_s} \\ &= \frac{2^{10}}{31,250} \\ &= 32.768 \text{ ms} \end{aligned} \quad (\text{Eq 3})$$

At the output of the first stage of filters, the sampling rate is reduced to  $f_s/2 = 15,625$  Hz; the number of samples in 32.768 ms is now  $2^9$ . The input signal is split into two bands: 0-7812.5 Hz and 7812.5-15,625 Hz. At the next stage, the number of samples in the low-pass path is reduced to  $2^8$  and the signal is split into bands 0 to 3906.25 Hz and 3906.25 to 7812.5 Hz. This pattern shows that we are going to perform  $\log_2 N = 10$  iterations of band splitting before we get down to a single sample.

Now we have ten 32.768-ms blocks of samples to analyze, each with a different number of samples. Let's start

with the highest-frequency block, which I'll call Band 9. Its bandwidth is 7812.5 Hz and its sampling frequency is twice that. Were we to apply an  $M$ -point FFT to these data, we'd have a frequency resolution of  $f_s/2M$ . Since the block length is  $N/2$ , we may perform  $N/(2M)$  FFTs on adjacent sub-blocks. In other words, we're confronted with a trade-off between good *temporal resolution* and frequency resolution. We're only interested, though, in the content of the entire 32.768-ms block: Its content doesn't change significantly during this period. From what we know about differential frequency threshold, we decide a frequency resolution of about 500 Hz is adequate for this subband. FFT size  $M$  therefore need only be:

$$\begin{aligned} M &= \frac{f_s}{\Delta f} \\ &= \frac{15,625}{500} \\ &\approx 32 \end{aligned} \quad (\text{Eq 4})$$

For a real input signal, this produces 16 analysis frequencies or bins. Actually, 32 bins are produced, but the bins in the top and bottom groups of 16 are just the complex conjugates of one another, and so are redundant. Here we are with a block of  $2^9 = 512$  samples and needing only 32 for our frequency analysis. Simple and direct would be to compute the  $512/32 = 16$  FFT blocks and average them. Nevertheless, as it turns out, we may select virtually any contiguous 32-sample block from within the input block, since frequency content doesn't change much over the input block.

So, for band 9, a 32-point FFT taken on the 32-sample block that was harvested. See Fig 3. We now know the frequency content of this band over a 32.768-ms period to a resolution of:

$$\begin{aligned} \Delta f &= \frac{f_s}{M} \\ &= \frac{15,625}{32} \\ &\approx 488 \text{ Hz} \end{aligned} \quad (\text{Eq 5})$$

The same process is performed on bands 6-8. At band 5, no block harvesting is necessary since the decimated block is already 32 samples in length. When we get to band 4, we run into a little snag: The block is only 16 samples long. It is tempting to just perform a 16-point FFT on this block, but then the frequency resolution would be  $f_s/16 = 488/16 \approx 30.5$  Hz, or the same as for Band 5. This is a getting a bit higher than the Weber fraction (see Part 1), so we decide to analyze this subband over



a time period twice that of band 5, or 65.536 ms. We then have our 32 samples and twice the frequency resolution.

Likewise, with band 3, doubling again requires a block-length increase to 131.072 ms to get the 32 samples and a frequency resolution of about 7.6 Hz. This band represents a frequency range of roughly 122 to 244 Hz—getting pretty low. For frequencies below 122 Hz (Bands 0-2), 7.6 Hz is deemed to be sufficient resolution and smaller FFTs are performed on 131.072-ms blocks. Band X, an 11th band, is just the left-over LPF output from the split that produces band 0.

This alteration of subband block lengths reflects the main axiom under which the system operates: Good temporal resolution is more valuable than good frequency resolution at higher frequencies; at low frequencies, good frequency resolution is more impor-

tant. This is supported by many of the studies cited previously and by common sense.

A conclusion is that above a certain level, improvement in temporal resolution is useless because speech doesn't contain information changing so rapidly; further, the human hearing system cannot distinguish the rapid changes in spectral content that would be produced. Below a certain frequency threshold, improvement in frequency resolution is useless because the information contained in low frequencies is limited. The theory of natural selection<sup>6</sup> seems to indicate that animals do not develop their senses beyond what is necessary. It is therefore no surprise that our hearing matches our ability to communicate verbally. Animals in the wild present a somewhat different story, since they must be able to detect the presence of their enemies through subtle sounds, smells and visual attributes. Still, it

is found that surviving species acquired the necessary tools and many of those that are extinct did not.

### Perceptual Transforms

Perhaps some readers have experienced Internet audio systems, many of which use perceptual audio coders in one form or another. A data stream at 33.6 kbps occupies a bandwidth of  $33.6/2 = 16.8$  kHz (when reconstructed) and we know this can be coded in an analog format to fit through a 3-kHz-bandwidth telephone line. This approximately 5.5:1 compression ratio shows that there is hope!

As early as 35 years ago, attempts were made to reduce speech bandwidth by brute-force methods that squeezed all spectral components closer together in frequency.<sup>7</sup> At that time, the fast Fourier transform (FFT) was undergoing a rebirth.<sup>8</sup> I guess it should have been evident from the nature of the beast that such frequency compres-

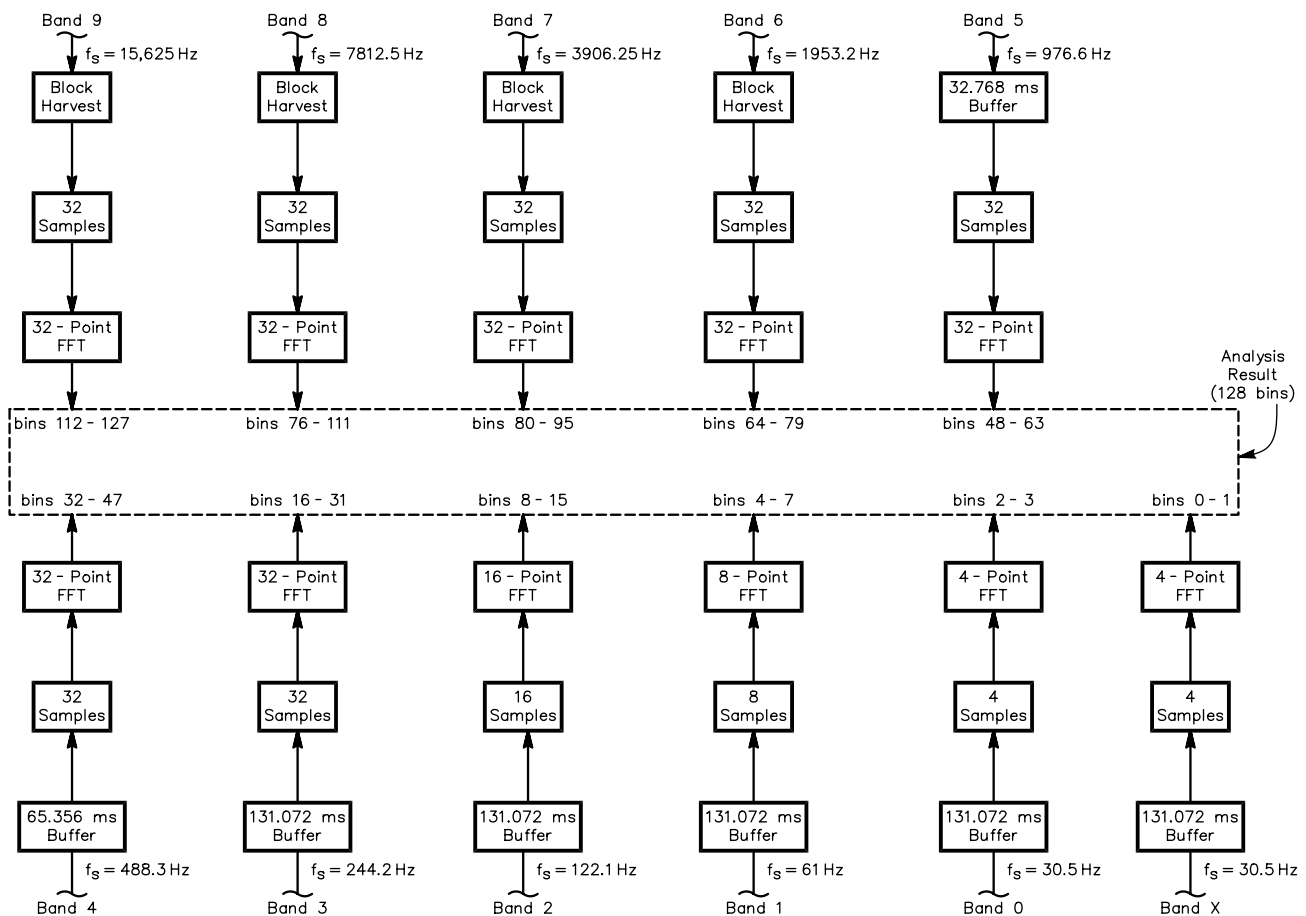


Fig 3—The processing details of subband analysis. Note: Although FFT results are identified only by bin numbers 0-127, each of those bins has a complex-conjugate mate in the range 128-255; mating bins are implied where they are needed to compute inverse transforms. Bin numbers 0-127 correspond to the 128 analysis frequencies.

sion forces discrete transform elements to overlap, resulting in rather serious distortion. Perceptual coding cannot be obtained quite this simply. More-recent efforts utilizing subband coding and other methods<sup>9</sup> must have achieved at least some success, but we still don't see such schemes being employed generally.

Amateurs have also undertaken the quest for analog bandwidth compression. John Ash, KB7ONG, Fred Christiansen, KA6PNW, and Rob Frohne, KL7NA, wrote about a system somewhat similar to mine in *QEX* a few years ago.<sup>10</sup> Their premise was along the same lines that I've explained above: Certain parts of speech are redundant or irrelevant and so may be discarded. I've not heard what their results sound like and I cannot comment on the viability of their approach. I can only write that my tactics are a bit different from theirs in that spectral information is generally preserved across the frequency band of interest.

Anything reducing speech bandwidth by at least a factor of two ought to find immediate application in many services worldwide. It would reduce congestion on our crowded amateur bands as well as on commercial and military channels. It might increase telephone-circuit traffic manifold. It would not play in Peoria, though, unless it met the quality goals set in Part 1. I reluctantly infer, therefore, that previous bids have fallen short.

We have produced samples in the frequency domain of a signal sampled in blocks 32.768 ms long. Now I propose to construct an analog signal from those frequency-domain samples that is also 32.768 ms long but has a greatly reduced bandwidth. I will use the bins obtained from the subband decomposition above as the inputs to a

256-point inverse FFT (FFT<sup>-1</sup>). The sampling frequency of the output will therefore be:

$$f_s = \frac{\text{number of samples}}{\text{time span}} = \frac{256}{0.032768} = 7812.5 \text{ Hz} \quad (\text{Eq 6})$$

In so doing, the bins will represent frequencies spaced  $1/0.032768 \text{ s} \approx 30.5 \text{ Hz}$  apart. The highest-frequency bin will correspond to the highest-frequency bin of the FFT done on band 9. The next-highest-frequency bin will represent the second-highest-frequency bin of the FFT done on band 9, and so on until all analysis bins have been *down-shifted* to their respective places in the coder's *synthesis FFT<sup>-1</sup>*. Note that no temporal-resolution rules have been violated since each bin represents a 32.768-ms block in both FFTs. See Fig 4.

Frequencies of analysis bands are listed in Table 1; synthesis frequencies are listed in Table 2. Frequency resolution in synthesis is proportional to frequency. A speech signal of  $\text{BW} = 15.625 \text{ kHz}$  has been coded into  $\text{BW} \approx (30.5)(128) = 3.90625 \text{ kHz}$ ! The frequency compression ratio is four. Note that this system, when restricted to half the input bandwidth, produces ap-

proximately the same compression ratio. An input bandwidth of 3.90625 kHz, for example, produces output bandwidth of about 977 Hz.

An additional, significant benefit of the system is that it may remove the restrictions placed on high- and low-frequency response by the characteristics of IF and AF filters in transceivers. Table 2's data reveal that very low frequencies are shifted upward by several hundred Hz. That means the low-frequency response of the system is preserved even when the coded signal passes through two bandwidth-limiting filters: one in the transmitter and one in the receiver.

#### PTC Decoder

The decoder reconstructs the signal using exactly the reverse of the process used in the coder. See Fig 5. It first translates the signal to the frequency domain using a standard, 256-point FFT at the sampling rate of 7812.5 Hz. Input block length for each FFT is 256 samples or 32.768 ms. This produces analysis bins corresponding to 128 discrete frequencies. These samples are then inverse-Fourier transformed by band, with an additional provision for generating time-domain sequences longer than 32 samples for bands 6-9 in that synthesis operation. The

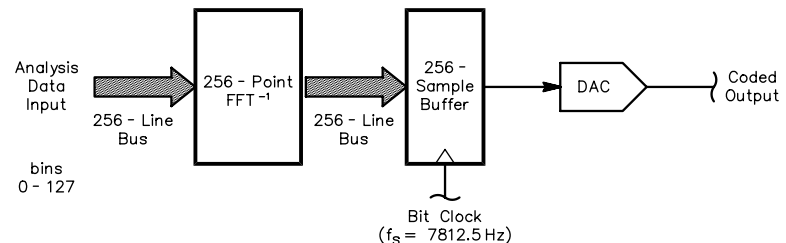


Fig 4—Final processing of the coded analog signal.

Table 1—PTC Codec Example with  $\text{BW}_{\text{IN}} = 15,625 \text{ Hz}$ ,  $\text{BW}_{\text{OUT}} = 3906 \text{ Hz}$

Band	Low-Pass Range (Hz)	High-Pass Range (Hz)	Sampling Rate (Hz)	Samples per 32.768 ms	Frequency Resolution (Hz)
9	0-7812.5	7812.5-15,625	15,625	512	488.3
8	0-3906.3	3906.3-7812.5	7812.5	256	244.2
7	0-1953.2	1953.2-3906.3	3906.3	128	122.1
6	0-976.6	976.6-1953.2	1953.2	64	61
5	0-488.3	488.3-976.6	976.6	32	30.5
4	0-244.2	244.2-488.3	488.3	16 (32 in 65 ms)	15.3
3	0-122.1	122.1-244.2	244.2	8 (32 in 131 ms)	7.6
2	0-61	61-122.1	122.1	4 (16 in 131 ms)	7.6
1	0-30.5	30.5-61	61	2 (8 in 131 ms)	7.6
0	0-15.3	15.3-30.5	30.5	1 (4 in 131 ms)	7.6
X	0-15.3	NA	30.5	1 (4 in 131 ms)	7.6

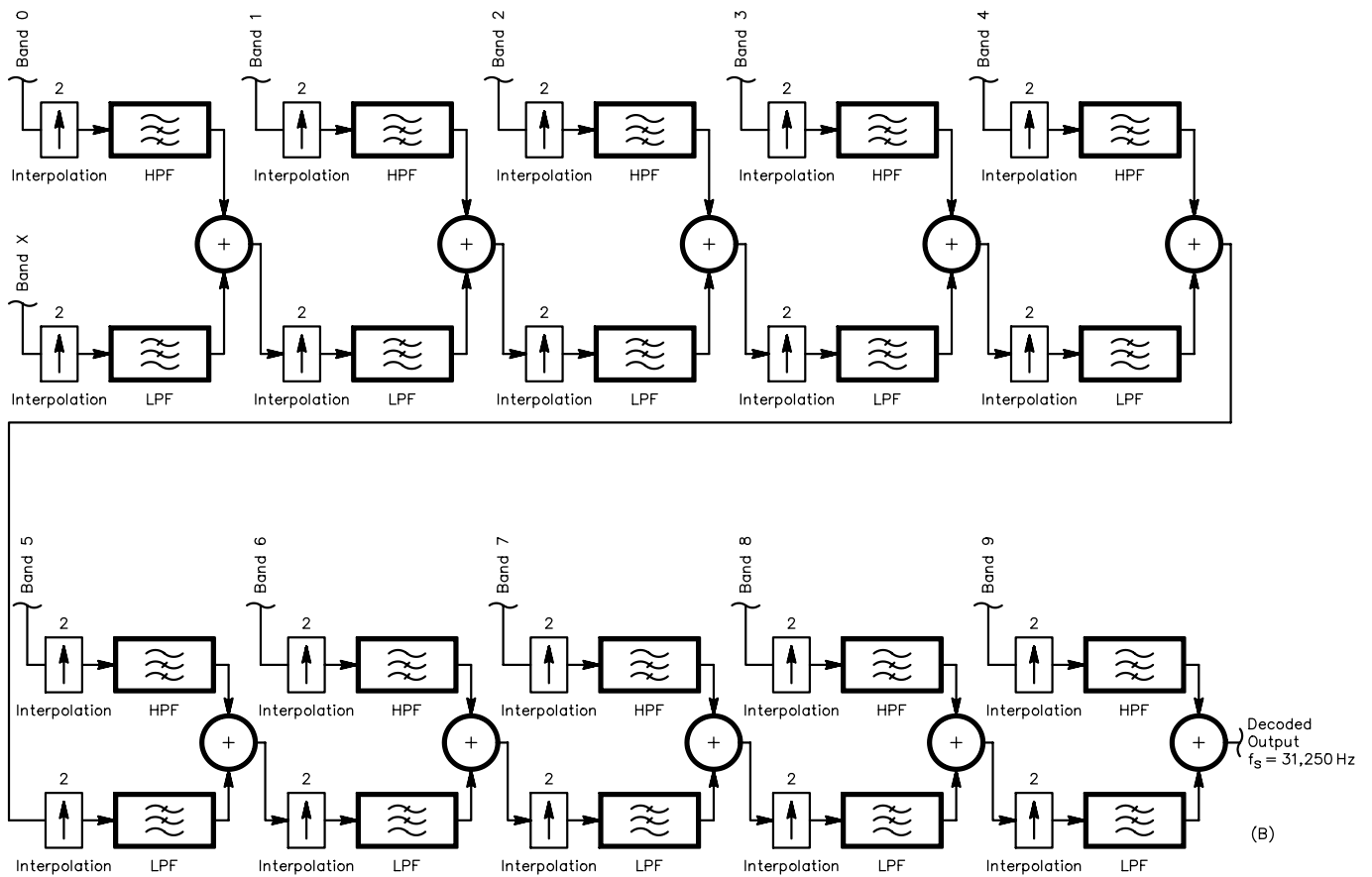
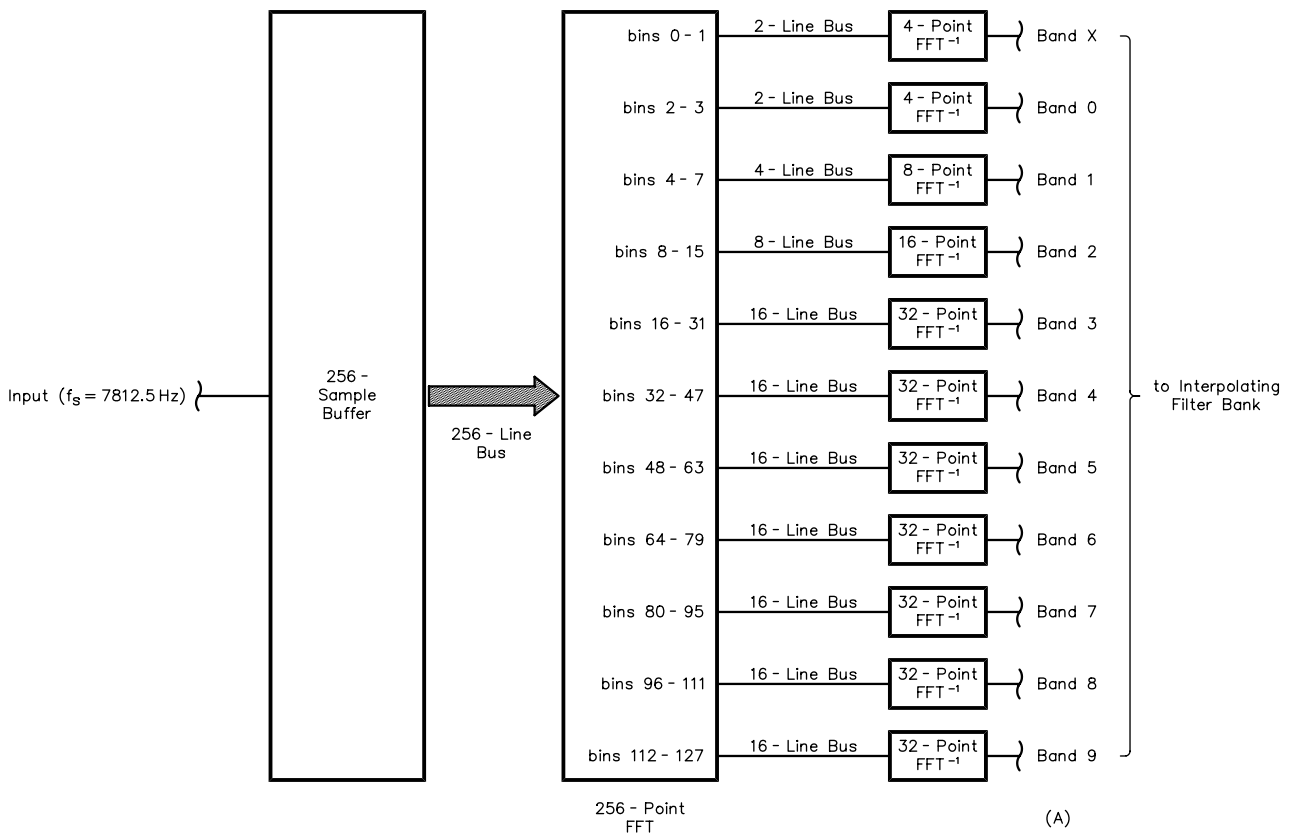


Fig 5—A complete 10-band subband decoder.

sequences are interpolated (interpolation is the inverse of decimation), filtered and combined in a manner opposite to that of the coder. The net result is a 32.768-ms block of output samples at the original sampling frequency of 31,250 Hz. Notice that the bin order of each FFT<sup>-1</sup> must be reversed; the subsequent interpolation and HPF operations (in Fig 5B) invert the spectrum of the band being processed. The final output is obviously not a perfect reconstruction of the original input, since a compromise has been made between temporal and frequency resolution. In fact, it is quite remarkable how different it looks on a 'scope compared with the original and yet sounds so remarkably the same!

#### Computational Details

Now let's look at some other details of the processing algorithms. Emphasis will be placed on computational efficiency. My PTC system is currently implemented on a fast PC and does not come close to operating in real time. Chunks of speech may be coded and decoded only after initial recording. Obviously, the next step is to build a codec that processes speech on the fly. One heck of a lot of computation goes on in these algorithms. I calculate that a PTC codec may be implemented on a dedicated DSP platform that has only modest processing power by today's standards. Without the shortcuts outlined below, much more horsepower would be required. Alternatively, increased processing capability would allow greater frequency resolution and therefore improved quality.

In the coder, the output of one filtering stage forms the input to the next. Notice that enough output samples from one stage must be accumulated before the next stage's output can be

computed. Further, the input buffer for a particular filter stage must grow beyond 32.768 ms by the length of the filter's impulse response. Finally, the filter's impulse response must be long enough to achieve *orthogonality* between subbands. This term means that no frequency component appearing in either the high- or low-pass subbands appears at significant amplitude in the other filter's output. That is, the filters must be sharp enough not to let frequency components appear simultaneously in both the high-pass and low-pass outputs. This requirement obviously presents itself most critically in and near the transition regions of the filters' frequency responses. Either some overlap or some exclusion of analysis frequencies must be tolerated, since short filters are not very sharp-skirted.

FIR half-band filters can be designed in DSP with impulse responses having odd-numbered coefficients equal to zero. See Fig 6. This is achieved using Fourier design methods when the total number of taps is

odd.<sup>11</sup> The significance of this is that the total computational burden is reduced by a factor of two, since those taps with coefficients equal to zero don't need to be computed or added to the convolution sum. In addition, it turns out that half-band, high-pass and low-pass filters may be designed so that their impulse responses are nearly the opposites of one another. For a filter of length  $L$ , the coefficients of a half-band high-pass filter,  $h_k$ , are simply the negative of the coefficients of a half-band low-pass filter, except for the coefficient at the center of the filter,  $h_{(L-1)/2}$ . See Fig 7. This further reduces computational complexity by a factor of two, since the output of either filter is just the convolution sum using coefficients  $\pm h_k$  plus the term produced with the center coefficient.

Filters of length  $L = 33$  designed using a rectangular window barely meet the requirements above. To avoid having to insert delays in the FFT paths, it is well to store all the input samples for both coder and decoder before calculating all the filter

**Table 2—Frequency Mapping in Synthesis of a 4:1 PTC Coder**

Band	Input Frequency Range (Hz)	Output Frequency Range (Hz)	Number of Frequencies
9	7812.5-15625	3418.0-3906.25	16
8	3906.3-7812.5	2929.7-3418.0	16
7	1953.1-3906.3	2441.4-2929.7	16
6	976.6-1953.1	1953.1-2441.4	16
5	488.3-976.6	1464.8-1953.1	16
4	244.2-488.3	976.6-1464.8	16
3	122.1-244.2	488.3-976.6	16
2	61-122.1	244.2-488.3	8
1	30.5-61	122.1-244.2	4
0	15.3-30.5	61-122.1	2
X	0-15.3	0-61	2
TOTALS	0-15625 Hz	0-3906.25 Hz	128 frequencies

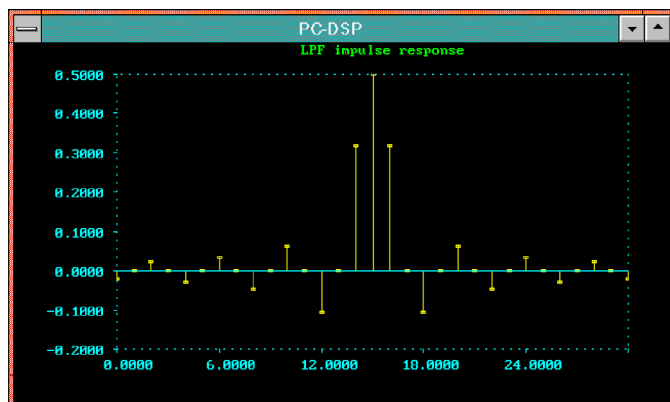


**Fig 6—The impulse response of a 33-tap, half-band low-pass filter. Notice that odd-numbered coefficients have a value of zero, save the center coefficient.**

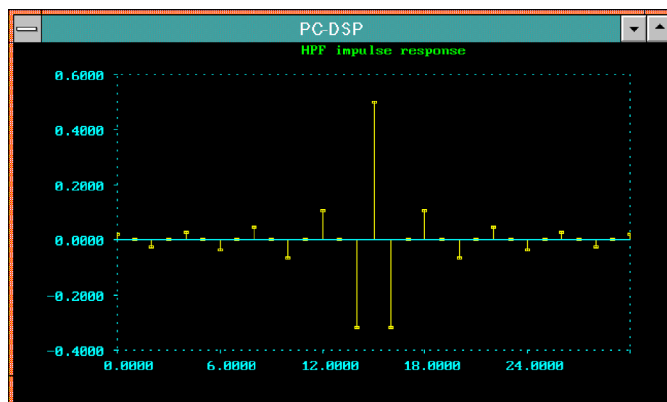


**Fig 7—The impulse response of a 33-tap, half-band high-pass filter. Notice that, except for the center coefficient, all the coefficients are simply the negative of the filter depicted in Fig 6.**



outputs. This isn't always possible, though, since it results in significant throughput delay. Note that a small delay is always precipitated by the wait for buffers to fill. A complete filter stage using this *polyphase* approach is shown in Fig 8A. The frequency responses of the FIR filters I actually use are shown in Fig 8B.

Either the FFT or DFFT may be used in spectral analysis, depending on the processor. I emphasize again that the DFFT allows independent spectral-leakage control for each bin, although it may incur greater computational burden under certain circumstances. The usual rules regarding scaling of input and output data apply.

## Results

The coder and decoder are not synchronized. Because the 32.768-ms frames in the coder are not likely to be aligned in time with those in the decoder, a spectral-smearing effect always occurs. The magnitude of the effect depends heavily on how much the high-frequency content of adjacent frames changes. As stated above, the low-frequency content is not liable to change very much from frame to frame. In the worst imaginable case, high-frequency content changes markedly between frames and half the energy appears in one frame, the other half in the next. Total energy content is preserved, but the temporal resolution is compromised to the tune of half the analysis-block length. This effect has not presented itself as a perceptual problem during testing.

When I started this project, I believed that PTC-coded speech compressed to one fourth of its original bandwidth would still be intelligible, but it is not. The main reason for that

seems to be that frequencies corresponding to the pitch of a person's voice are shifted upward in frequency too much to allow the ear to discern them. Formant energy resides much closer to the pitch energy, rendering them indistinguishable from one another. That is not to say you can't still tell that it's speech; it just sounds—well, different.

You may download an example of PTC codec performance from the *QEX* Web site.<sup>12</sup> The package includes some .WAV files: an original, digital recording of my not-so-melodious voice, a PTC-coded version of same with a compression ratio of four and the decoded result. I cannot guarantee they will play exactly right on all systems because of the non-standard sampling rates, but you will get the idea. Also, notice that some work still needs to be done to restore all the naturalness of the original recording after decoding. Application of windowing to time-domain data in analysis and synthesis is the subject of ongoing experimentation. I find it is difficult to tell the difference, though, between coded/decoded speech and the original, at least over HF SSB. After years of listening to 2.4-kHz audio, it astonishes me how much the addition of some sibilance and presence improves perceived speech quality.

Many acquaintances of mine enjoy listening to SSB signals by using a much greater receiver bandwidth than that used in the transmitter. I attribute this to the IMD products appearing beyond the transmitter's bandwidth that pass for sibilance at the receiver. Good thing they can't listen to the IMD products on the other side because I don't think the results would be quite so pleasing.

You may say someone sounds like

FM, but the trouble has been that the high-pass filters necessary to eliminate CTCSS tones have had a very deleterious effect on voice signals. More often, I think we're referring to the degree of quieting that is apparent. In the finish, my scheme has some effect on signal-to-noise ratio as well.

Not only have we reduced bandwidth by a factor of four, but we've also gained a signal-to-noise ratio (SNR) advantage of:

$$\Delta SNR = 10 \log_4 \approx 6 \text{ dB} \quad (\text{Eq } 7)$$

Note that we've also avoided approximately 6 dB of QRM in the process (using appropriate IF filters) and that we've relieved our neighbors in frequency by the same margin. These factors apply to the on-the-air signal, not to the result. Statistical noise from signal processing algorithms usually offsets the reduction in atmospheric noise. The system is subject to a magnified effect from any on-channel interference, if it is polyphonic. That is to say: If polyphonic, on-channel interference occupies bandwidth  $m$ , I will demodulate it with  $BW=4m$ . Selective-fading effects are also amplified by the same amount. PTC-coded speech is also a bit more susceptible to frequency errors.

As stated in Part 1, the ear seems to be sensitive to the relative phase of components lying within the same critical band. I postulate this is because such components may produce a beat frequency of greater than the critical bandwidth, resulting in an audible effect. It is interesting to hear how audio waveforms having different phase relationships between their spectral components—and that look quite different on the 'scope—sound remarkably the same.

PTC doesn't process singing, music,

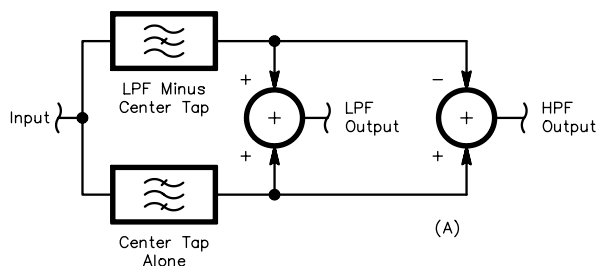
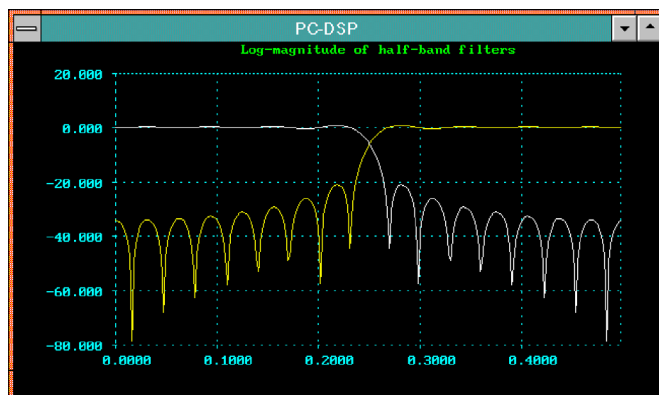


Fig 8—(A) shows a complete polyphase filter stage. The term *polyphase* refers to the process of computing partial convolution sums for the filter in question. (B) shows frequency responses of half-band filters.



(B)

slow-scan signals or audio containing strong, discrete-frequency components very well, although the concept could certainly be optimized for that purpose. In the form of an external audio processor, PTC would be compatible with virtually any transceiver. The prospective uses of the bandwidth savings are alluring, to say the least. Transmitting unintelligible signals, though, raises a few red flags. Read on.

### Is PTC Legal on Amateur Bands? In Commercial Services?

To a non-PTC-equipped receiver, a coded USB signal appears to be several hundred hertz higher in frequency (lower for LSB) than it really is. At low compression ratios ( $\leq 2$ ), the coded speech is still understandable without being decoded. An uncoded signal applied to the decoder can still be copied. This is a desirable situation in view of the FCC rules, which are clear when it comes to encryption of signals.<sup>13</sup>

As mentioned, compression ratios of greater than three make coded speech unintelligible. Now I must ask whether those signals may be transmitted legally on the ham bands. If the answer is "No, you can't," then another question presents itself: "How much intelligibility do I can lose before I cross the legal line?" If you hope the answer is "Yes, you can," then certain arguments may come into play.

First, there is an analogy to the legality of unspecified digital modes that have been publicly documented, as outlined in the FCC rules.<sup>14</sup> Digital voice modes have been legal on the phone bands for a long time: They are just as unintelligible as high-compression, PTC signals to the unequipped—maybe more so. PTC coding carries a bandwidth-reduction feather in its cap, which many current digital-voice modes do not. However, the SNR advantage of PTC is minimal compared to that of digital modes.

That brings me to an admonishment about this stuff: *Don't play the coded .WAV file from the Web site on the air just yet!* If I hear them there or have good reason to believe they were there, I'll yank the whole thing and the game will be over; however, play the before and after .WAV files as much as you want.

PTC codecs allow four or more times as many voice signals to occupy a given band as compared with uncoded signals. While this may not destroy all QRM, it sure seems to offer a better chance for radio operators to happily coexist. Application of PTC to other

services, such as FM land mobile, is not quite so simple. Transceivers usually have synthesizer tuning steps of 12.5 kHz or 25 kHz to match the channel spacing and IF filters. New or heavily modified designs would have to be fielded to take advantage of greater spectral occupancy. Other uses may be made of the saved spectrum without changing channel spacing. Full-frequency-range stereo or four-channel speech, for example, is possible in typical voice bandwidths. With two or more independent channels, more information can be communicated. I can't see very much reason PTC cannot legally be employed in commercial services.

Since the vast public telephone network has already gone digital, I have to wonder whether it is useful there to increase traffic-handling capacity. Certainly, PTC coding could be applied prior to digitization to achieve a boost; however, large-scale rearrangement of multiplexing equipment would be necessary and lots of new gear would have to be purchased. In addition, it may be that speech-compression coding in digital form (after digitization) would be more cost-effective.

### Summary

This work was motivated by the principle that no signal should occupy more bandwidth than necessary to convey the information it contains. Peter Martinez, G3PLX, and the immediate popularity of PSK31 drove that point home.

From the foregoing data, it's evident that not all components of human speech are necessary to achieve high perceptual quality. Irrelevant components are sometimes made inaudible by masking or critical-band effects and therefore can be eliminated. Many modern digital coding methods make extensive use of these factors to achieve their efficiencies. We also find that speech doesn't change much from one short time frame to the next, and so contains redundancies. This is also used to reduce bandwidth.

It was shown that if the ear is less sensitive to differences in frequency as frequency increases, then the high-frequency territory is prime ground for bandwidth compression. The underlying principle of PTC is to create an analog signal of lesser bandwidth and frequency resolution in three steps:

1. Analyze the frequency content of the input signal with non-uniform

frequency resolution

2. Combine adjacent frequency bins that are closer together than the differential frequency threshold

3. Down-shift some of the bins in frequency

The processing power required to implement PTC is moderate by today's standards. I see no reason why affordable codecs cannot be built and put to use reducing QRM. Outboard DSP units are already common equipment at many Amateur Radio stations; many have sufficient number-crunching power for this application. While thinking about digital audio modes, I ask you to also consider this bandwidth-efficient scheme.

Thanks to Bob Heil, K9EID, and Warren Bruene, W5OLY, for their valuable input and assistance. See you in the soup, guys!

### Notes

- <sup>1</sup>D. Smith, KF6DX, "PTC: Perceptual Transform Coding for Bandwidth Reduction of Speech in the Analog Domain, Part 1," *QEX*, May/June 2000.
- <sup>2</sup>D. Smith, "Signals, Samples, and Stuff: Part 3," *QEX*, Jul/Aug, 1998.
- <sup>3</sup>D. Smith, "Signals, Samples, and Stuff: Part 4," *QEX*, Sep/Oct, 1998.
- <sup>4</sup>R. W. Schafer and L. R. Rabiner, "Design of Digital Filter Banks for Speech Analysis," *Bell System Technical Journal*, Vol 50, No. 10, December 1971.
- <sup>5</sup>R. W. Schafer, L. R. Rabiner and O. Herrmann, "FIR Digital Filter Banks for Speech Analysis," *Bell System Technical Journal*, Vol 54, No. 3, March 1975.
- <sup>6</sup>R. C. Stauffer, Ed., *Charles Darwin's Natural Selection*, 1975.
- <sup>7</sup>US Patent No. 3,349,184, Morgan, 1967; also see J. L. Flanagan and R. M. Golden, "Phase Vocoder," *Bell System Technical Journal*, Vol 45, No. 9, November 1966.
- <sup>9</sup>J. W. Cooley and J. W. Tukey, "An Algorithm for the Machine Calculation of Complex Fourier Series," *Mathematics of Computation*, American Mathematical Society, Vol 19, April, 1965; [www.ams.org/mcom](http://www.ams.org/mcom).
- <sup>10</sup>US Patent No. 4,374,304, Flanagan, 1983; also see US Patent No. 3,510,597, Williamson, 1970.
- <sup>11</sup>J. Ash, KB7ONG, F. Christiansen, KA6PNW, and R. Frohne, KL7NA, "DSP Voice Frequency Compandor for use in RF Communications," *QEX*, July, 1994.
- <sup>12</sup>W. E. Sabin and E. O. Schoenike, Eds., *Single Sideband Systems and Circuits*, Second Edition, (New York: McGraw-Hill, 1995).
- <sup>13</sup>You can download the .WAV files from [www.arri.org/qexfiles](http://www.arri.org/qexfiles). Look for PTCWAVE.ZIP.
- <sup>14</sup>47 CFR 97.113 (a): "No amateur station shall transmit: . . . (4) . . . messages in codes or ciphers intended to obscure the meaning thereof . . ."
- <sup>15</sup>47 CFR 97.309 (b). □□

# *Beyond Fractional-N, Part 1*

---

*Eliminating the PLL remains the last step in utilizing the DDS solely as the main LO in radios.*

---

By Cornell Drentea, KW7CD

Unlike what some manufacturers would have us believe, today's direct digital synthesizers (DDSs) are not used alone to generate VHF/UHF local oscillators (LO) frequencies in up-converting HF radios. Although much progress has been made in the past 10 years in the area of high-resolution frequency synthesis, today's synthesizers use additional techniques (such as PLL and others) to function as high-frequency, high-resolution LOs.<sup>1</sup> Although using a straight DDS as the first LO in an up-converting radio is quite desirable and technologically feasible today, there are still obstacles in the way of implementation.

This article is a synthesizer-technology report combined with a practical construction article directed at ham experimenters, as well as professionals. Although the work contains ample tutorial material, it is not meant to be an exercise in basic concepts, but

rather an advanced applied-technology update. I therefore assume that the reader is familiar with basic DDS (Reference 7) and PLL concepts (References 2, 3, 6, 8, 9, 10, 11 and 12) This article discusses state-of-the-art synthesizer technology as applied to the first conversion of an up-converting HF radio. It explores the feasibility of using a super-DDS (SDDS) to achieve direct LOs without using the PLL technique.

The article also presents other synthesis approaches, particularly the DDS-driven PLL. In addition, new cost-effective DDS synthesizers are introduced to the industry utilizing simple brute force multipliers to achieve performance equal to, or better than, that of today's popular DDS-driven PLL technique.

A final goal of this article is to discuss an advanced DDS-driven PLL synthesizer as a state-of-the-art approach to high-resolution, wide-bandwidth synthesis. A modern implementation of this approach will be presented in Part 2, operating at 10 times the required LO frequency (L-band) in an up-converting 75-MHz-IF HF transceiver. This synthesizer was designed and developed

specifically for my Star-10 transceiver. It offers new ideas on what can be done to improve the traditional DDS-driven PLL technique, which I introduced in 1988 (Reference 1).

## **The Many Faces of Frequency Synthesis**

LOs have come a long way from free-running implementations. They take the form of complex synthesizers that use new techniques to answer many conflicting requirements. Some of these are fine step resolution, frequency agility, low spurious and phase-noise performance, to name just a few.

In addition, wide-band, high-resolution synthesizers have been notoriously expensive to produce. Although progress has been recently made in simplifying frequency synthesis, there is a need today to produce even lower-cost, yet high-performance synthesizers to simplify transceiver design overall.

There are many forms of frequency synthesis being used today. See Fig 1. Among them are brute-force-direct and indirect techniques, combined with PLLs and several others. At microwave frequencies, harmonic-mixer techniques have also been used.<sup>2</sup>

<sup>1</sup>Notes appear on page 25.

Recognizing this complexity and its associated cost, new synthesizer techniques have evolved over the past 10 years as extensions of existing techniques. As such, the direct digital synthesizer (DDS) has served as an essential player in today's transceiver designs.

Although the DDS idea was introduced a long time ago, the first practical DDS became a reality only in the early 1980s. It was then that the DDS was first used as a numerically controlled oscillator (NCO), first at audio frequencies and later at RF.

#### The DDS-Driven PLL

In the synthesizer world, there is a proverb: "There are synthesizers, and then there are synthesizers!" This means that while it is relatively easy to design a high-performance synthesizer that generates a few frequencies over a limited bandwidth (such as used in a dedicated-channel radio or radar), synthesizers designed for wide-band, high-resolution up-converting HF radios have proved to be very demanding. This is so because of their ultra-wide cover-

age and very fine resolution, which are conflicting requirements. Let's now look at those requirements.

In today's up-converting HF radios (2 to 30 MHz), synthesizers are required to generate clean, high-resolution, VHF to UHF LO frequencies to cover over four octaves of RF bandwidth.<sup>3</sup> Generally, a step resolution of one to 10 hertz is required over this entire bandwidth. Imagine a synthesizer that can tune such a range in one band with a resolution of 1 Hz. Although there are many ways to achieve this kind of performance, doing so with a single loop presents an interesting challenge. In addition, our synthesizer must have a superior phase-noise and spurious performance over the entire bandwidth. Until the late 1980s, this performance was attempted (but not necessarily accomplished) by using a complex combination of techniques from Fig 1. Multiple PLLs and brute-force synthesis approaches (such as mixers and digital dividers) were used in various loop arrangements to obtain wide coverage and fine step resolution. These arrangements introduced unique prob-

lems. In addition to being expensive and difficult to control in manufacturing, their phase-noise and spurious performance left a lot to be desired because of problems introduced by their complexity. See Fig 2.

#### A New Deal

In February 1988 at RF-Technology Expo in Anaheim, California, I publicly introduced a practical new synthesis technique, the DDS-driven PLL (References 1 and 13).<sup>4</sup> This is a significantly less-complicated approach to obtaining high-resolution, variable-frequency LOs for fully synthesized radios than the multiple-loop PLL approach shown in Fig 2.

The idea is simple. Instead of using a combination of multiple brute-force approaches combined with fractional-N, multiple-loop synthesizers (Reference 2), a new device—the direct digital synthesizer—could be used as a high-resolution variable reference in a fixed, divide-by-N PLL multiplier. Fig 3 shows this concept in its original proposed form.

Since it wasn't yet possible to use the

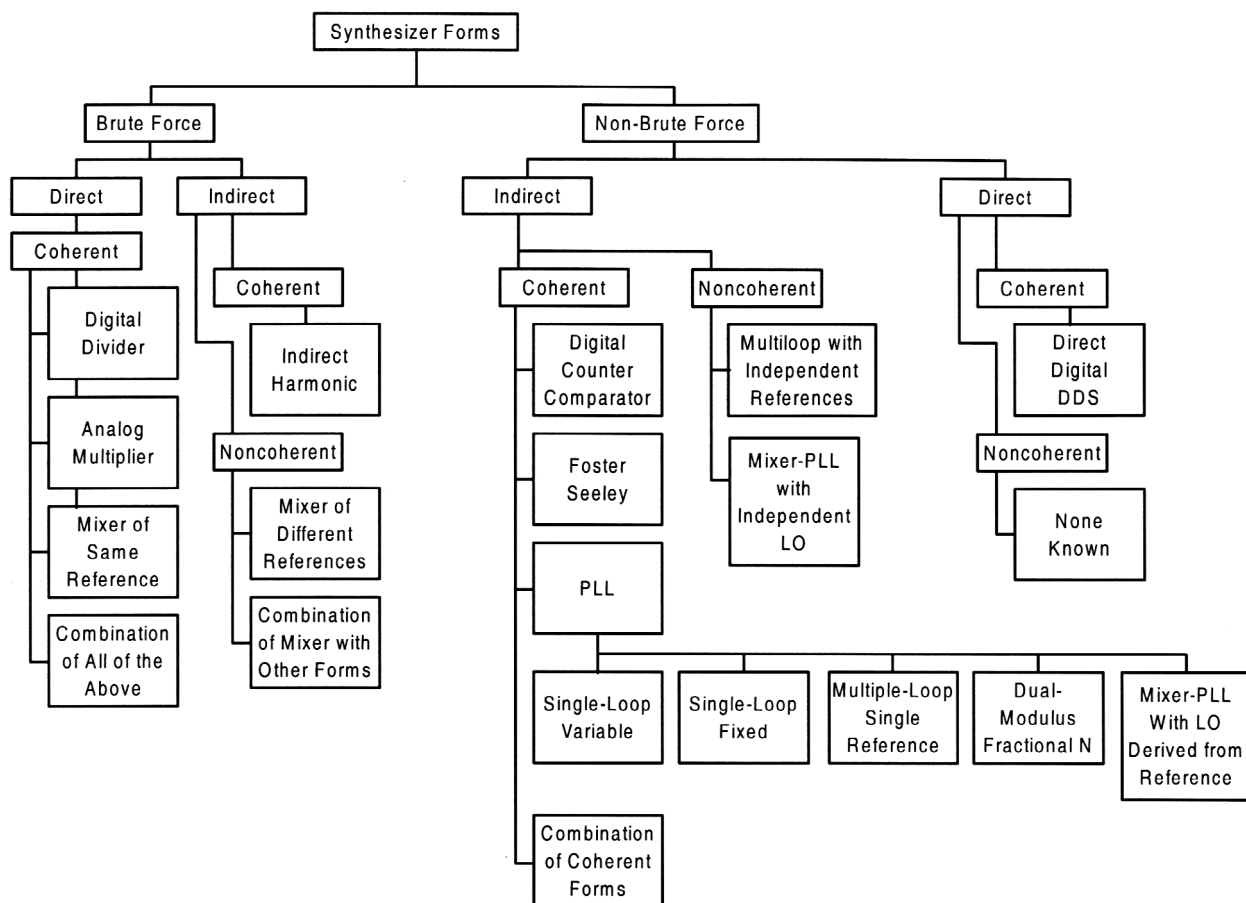
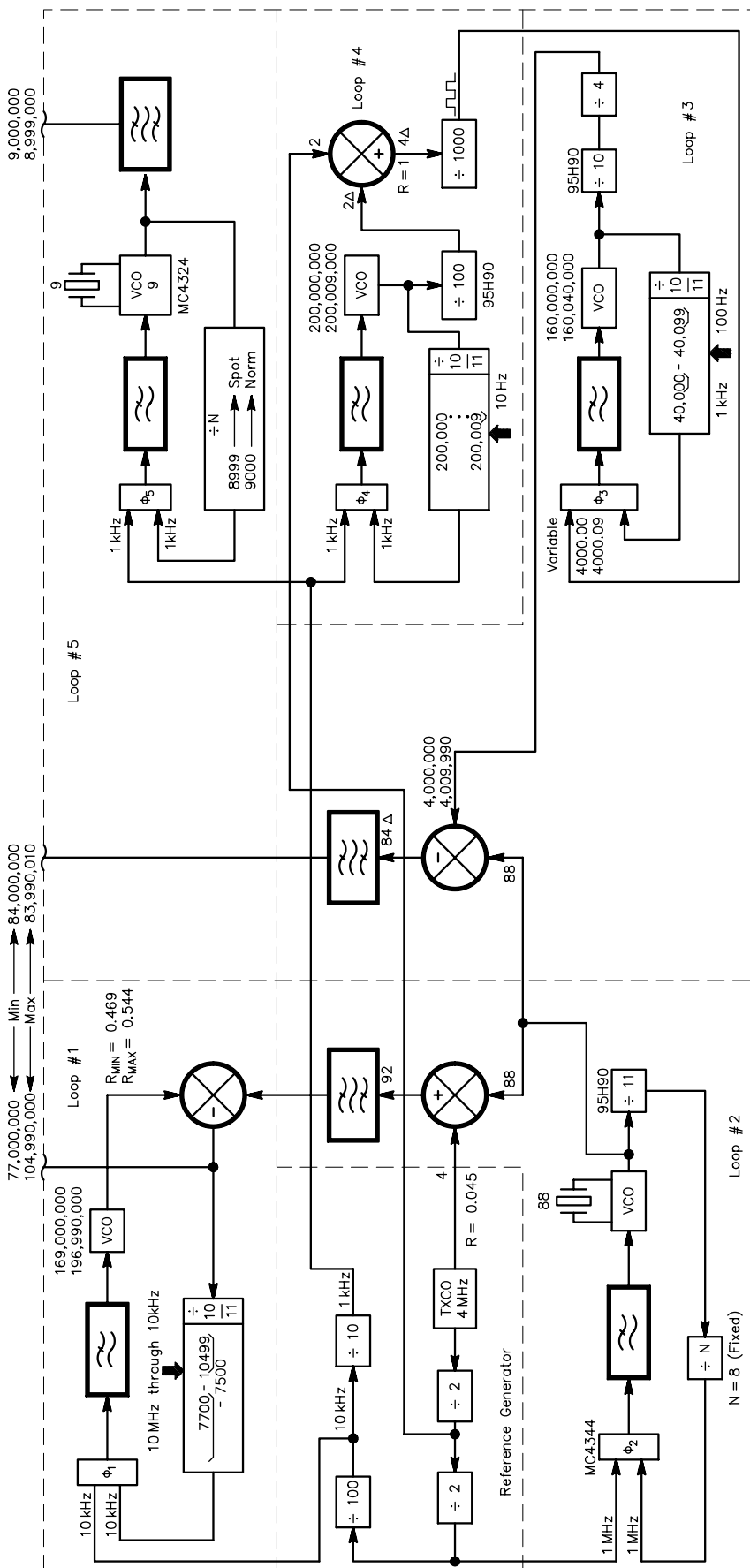


Fig 1—Many forms of frequency synthesis are available to modern designers.





DDS directly at the high LO frequencies needed in HF radios, the big idea was to cleverly modify the traditional PLL. In the DDS-driven PLL, the modification replaces the PLL's previously fixed reference with a variable-frequency, high-resolution DDS. This, in turn provides a coherent source that steers the PLL in fine steps over its entire bandwidth, while maintaining a high-frequency reference. By using the variable DDS and a tight loop bandwidth in the PLL, the fine resolution of the DDS is effectively transferred to the PLL output, while improving the synthesizer's phase-noise and spurious performance.

This allows for even further simplification. Because the high-frequency reference (the DDS) now provides the fine resolution, the traditional programmable, dual-modulus, fractional-N mechanism (also known as the Digiphase approach, see [References 2 and 3](#)) used in the feedback loop could be eliminated altogether. It is replaced with a simple, less expensive fixed divide-by-N digital divider, as shown in [Fig 3](#). What could be simpler? By streamlining a single-loop PLL to a DDS-driven PLL, high resolution and coherency to a high-stability reference is finally obtained in a single-loop synthesizer, a previously nearly-impossible task.

So far, we have seen that the DDS-driven PLL has streamlined high-resolution synthesizer design by using the DDS' inherent fractional-division ability, while maintaining a high reference frequency, which is a desirable factor in achieving high performance. The implications are, by now, clearly significant: reduced spurious signals, low reference-sideband levels, good phase-noise performance and fast switching, all in one simple synthesizer.

At the turn of the last decade, this solution spelled almost instant success. Two years after the RF-Expo paper, and up to this day, most synthesized HF radios on the market use the DDS-driven PLL idea as their major synthesizer approach. It has proved itself the industry's workhorse. In addition, the cost of synthesizers has been dramatically reduced. New LSICs combining the DDS and PLL techniques on a single chip are now evolving.

**Fig 2**—Example of a typical high-resolution synthesizer dating before the introduction of the DDS (early 1980s). Multiple PLLs were used in concert with brute-force methods to provide high-resolution LOs. The high division ratios used in the programmable dividers meant inferior phase-noise and spurious performance.



using them in such radios impractical.

### Low-Cost DDS Technology

We have seen how DDS technology has come a long way since the 1980s—and even during the 1990s. New, low-cost DDS devices that can generate precision waveforms above 10 MHz (higher frequency implies less performance) using reference frequencies of up to 120 MHz are commonplace today. They are being used in DDS-driven PLLs by most ham radios on the market. As such, the AD-9850 has proven to be the workhorse of the low-cost DDSs and is at the heart of many DDS-driven PLL systems. While we wait for low-cost DDS chips with outputs above 100 MHz, there are ways to eliminate PLLs and still maintain performance similar to that of DDS-driven PLLs.

### Practical DDS-Only LOs

As previously mentioned, we would like to use existing low-cost DDS technology directly and without PLLs in typical up-converting HF radios with a first IF around 75 MHz. As we have seen, such a DDS would need to operate at much higher reference frequencies than do currently available low-cost parts, in order to provide the required performance. So, how could we use existing low-cost devices as DDS-only LOs without those demanding reference-frequency requirements?

Let's analyze a no-PLL LO application using existing DDS technology, such as the AD-9850. Unlike the DDS-driven PLL, we'll take the brute-force multiplier method from Fig 1. This is shown in Fig 5. In this approach, a standard low-cost DDS can produce a high-resolution frequency range of 7.7 MHz to 10.5 MHz in very fine steps. The step resolution is 10 times finer than the final resolution required (that is, 1 Hz for 10-Hz ultimate resolution). This is not a problem for our DDS, which is inherently a good fractional-N, high-resolution RF source.

The output of the DDS is then conditioned and amplified according to standard RF techniques, and finally multiplied by 10—first by 5, then by 2. This output is then filtered and amplified again to serve as the high-resolution 77 to 105 MHz LO for our modern transceiver.

Notice that the brute-force nature of this synthesizer makes it a very attractive solution from a cost point of view; however, there is a price to be paid for this simplicity. Unlike a DDS-driven PLL (which has a built-in loop filter that eliminates various spurious and

phase noise problems outside the PLL bandwidth), a DDS-only multiplier tends to propagate—and even enlarge—spurious and phase-noise problems produced by the DDS. To counter this problem, it's best to select a high-performance DDS (more bits) and a reference oscillator of superior phase-noise characteristics for the design.

I have implemented several DDS-multiplier designs with good results using the AD-9850 and various multiplying and conditioning techniques. With reference frequencies above 80 MHz, the in-band spurious performance of those designs has been predicted and measured at  $-70$  dBc. In one particular design, the spurious response has been tamed to  $-85$  dBc over the 75 to 105 MHz range. This is more than sufficient in most HF applications, considering that many typical radios on the market today may exhibit synthesizer spurious responses between  $-40$  dBc and  $-70$  dBc. In addition, the phase-noise performance of DDS-only synthesizers using multiplier techniques is virtually identical to that obtained with an equivalent multiplier DDS-driven PLL approach if care is exercised in design. The multiplier-type DDS-only synthesizer should become more popular in ham radios in the future because of its simplicity and low cost.

### DDS-Based Design Review

We have seen how the DDS can produce high-resolution LOs for HF equipment. Fig 6 compares DDS-based synthesizers that could be used in up-converting HF radios with 75 MHz first IFs. Let's review the at-

tributes of those solutions.

The DDS-driven PLL design at Fig 6A is economical because it works directly at the LO range (77 to 105 MHz). Such implementations are popular in today's radios. Phase-noise performance in this design is generally adequate ( $-100$  to  $-110$  dBc/Hz at 1 kHz separation). This despite the fact that designers no longer use multiple, switchable VCOs in PLLs, an old technique of using several high-Q ranges in order to meet a tight phase-noise performance specification (References 3 and 6). A single wide-band VCO is commonly used today in these synthesizers to reduce cost.

The DDS-driven PLL at B operates at 10 times the required frequency range, or 770-1050 MHz. This takes advantage of the reduction in percentage bandwidth of a single VCO used over a higher frequency set. The idea here is to obtain even better phase-noise performance than at Fig 6A by digitally dividing by 10 to obtain the required 77 to 105 MHz LO. A good consequence is that this division improves the phase-noise performance of the output by 20 dB.<sup>6</sup> Although the superiority of the design at Fig 6B was initially disputed, experience shows a 6-dB phase-noise improvement—over that of the design at Fig 6A—with this design. We will discuss this implementation in more detail in Part 2 of this series.

The design at Fig 6C shows the use of a super-DDS directly as a 77 to 105 MHz LO. Although feasible with today's DDS technology, such a DDS would require a reference frequency of 840 MHz to maintain good spurious

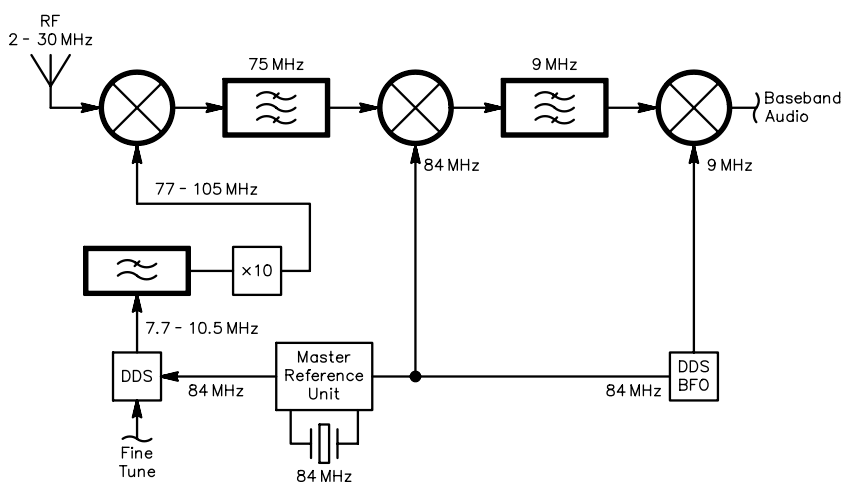


Fig 5—DDS-multiplier techniques can be used efficiently to generate high-resolution LO signals in up-converting transceivers. See text.

performance, making this technology expensive and impractical in our applications.

One last way of producing a 77 to 105 MHz LO using a DDS is shown at Fig 6D. It uses a low-cost DDS from above, as equipped with a master reference unit (MRU) of superior phase-noise performance. The output is multiplied directly by 10 using common brute-force-multiplier techniques from Fig 1. This has the advantage of eliminating the need for a PLL from the previous DDS-Driven PLL, reducing the complexity and cost associated with it. However, while the phase-noise performance of such a synthesizer would be comparable with the other types, its spurious performance will be inferior to that of the DDS-Driven PLL. As previously discussed, the latter offers dampening of the spurious response by the usually tight loop filter included in the PLL.

### Phase-Noise Requirements of DDS LOs

Let's now look at the phase-noise requirements for a DDS LO. Receiver analysis shows that for a high-dynamic-range HF receiver, a phase-noise performance of  $-90$  dBc/Hz to  $-100$  dBc/Hz at 1 kHz would be sufficient to ensure a reasonably "quiet" receiver (see Fig 7). In this context, a quiet receiver is defined as a receiver that receives a single-tone signal at a reasonable MDS level, consistent with HF receiver noise figure (NF). In other words, the receiver is reasonably quiet when there are no other signals to produce intermodulation distortion in our receiver.<sup>7</sup>

Consequently, the  $-90$  dBc number

from above is not really the synthesizer's phase-noise requirement, but rather the first mixer's output performance obtained by computing the entire front-end behavior for the system, operating under ideal linear conditions (no competing signals). The

problem is much more complex with multiple signals, though. To account for intermodulation distortion and reciprocal mixing in the front end of our radio, an improved phase-noise margin is required of the synthesizer under severe operating conditions. To

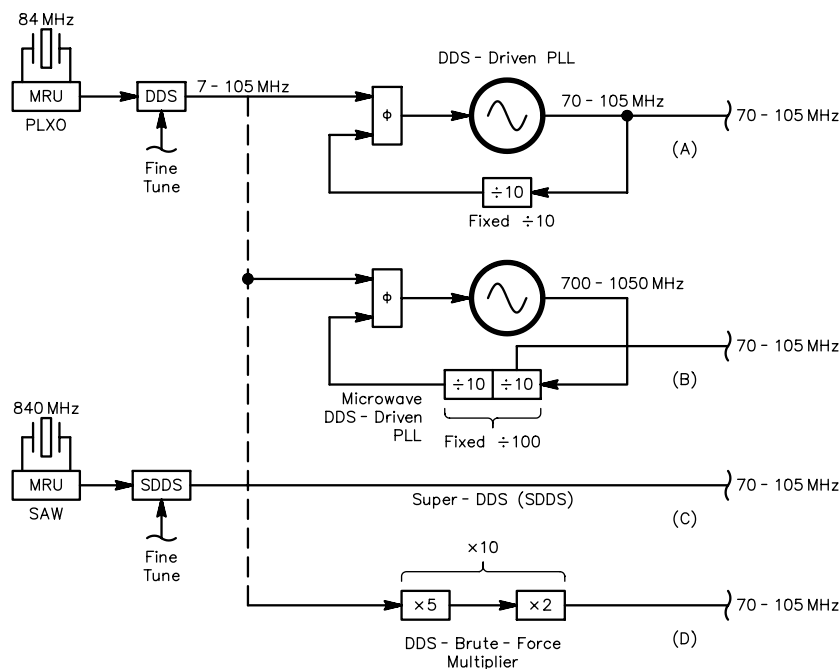


**Fig 6—Comparing several ways of implementing wide-band, high-resolution frequency synthesizers for up-converting HF radios with first IF at 75 MHz: (A) DDS-driven PLL with output directly at the LO range of 75-105 MHz. (B) A DDS-driven PLL operating at 10 times the required range (750-1050 MHz). Dividing the output by 10 can improve the performance (see text). (C) The ideal case for providing LOs at 75-105 MHz requires a DDS with a high reference frequency of 840 MHz. Although technology exists today to produce such a synthesizer, the implementation is not yet economically feasible for ham equipment. (D) An alternative synthesizer solution uses frequency multiplication of a good, low-frequency reference to obtain comparable LO performance at 75-105 MHz (see text).**

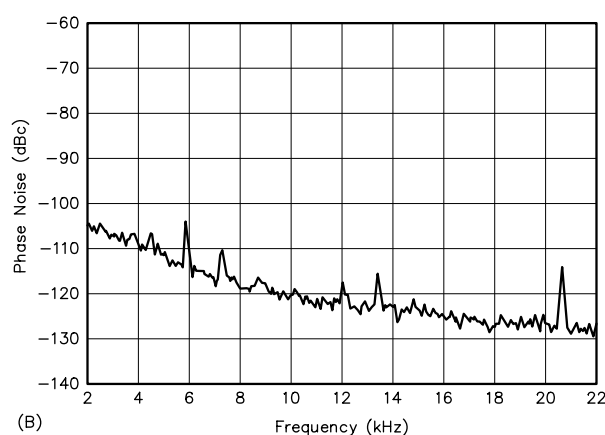
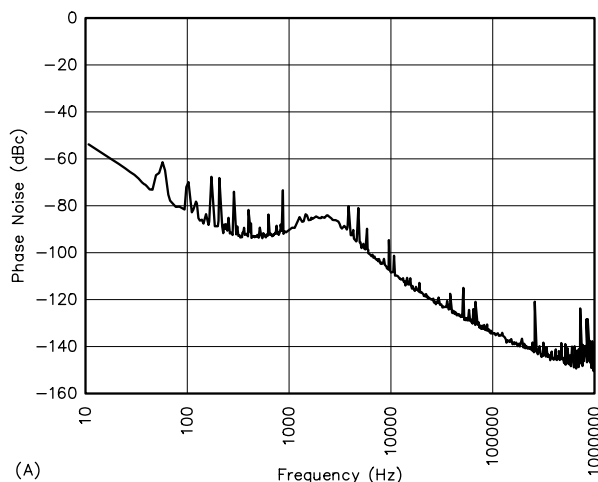


**Fig 7—The synthesizer performance at (A) is from a top-of-the-line transceiver of the past. The synthesizer at (B) is from one of today's low-cost transceivers using a DDS-driven PLL.**



build up this margin, it is customary to add at least 10 dB to the above phase-noise number in order to figure out the synthesizer's phase-noise requirement for third-order intercept (IP3) spurious-free dynamic ranges (SFDR) in excess of 100 dB.

This translates into a phase-noise requirement of better than  $-110$  dBc/Hz at a 1-kHz offset for a 77 to 105 MHz high-resolution synthesizer. Anything more than  $-110$  dBc (if it can be done) helps, but only to a point, since the noise figure of the receiver ultimately

prevails. By this, I mean that in a DDS, the phase-noise figure is affected by the actual noise floor of the digital part itself, which is usually around  $-135$  dBc in a commercial part such as the AD-9850.

Although phase-noise performance of  $-110$  dBc/Hz at 1 kHz is a very demanding requirement in a 75 to 105 MHz synthesizer with steps of 1 or 10 Hz, such performance is typical of DDS-driven PLL synthesizers today. A high-resolution, wide-bandwidth DDS-driven PLL can achieve  $-120$  dBc/Hz at

1 kHz. To achieve such a design, superior phase-noise performance is required of the DDS reference oscillator, the master reference unit (MRU), as shown in Fig 8.

### Spurious Performance in DDS LOs

The above discussion demonstrates clearly that while the phase-noise performance of today's synthesizers has been improved by using DDS technology, the nonharmonic and harmonic spurious performance has been lim-

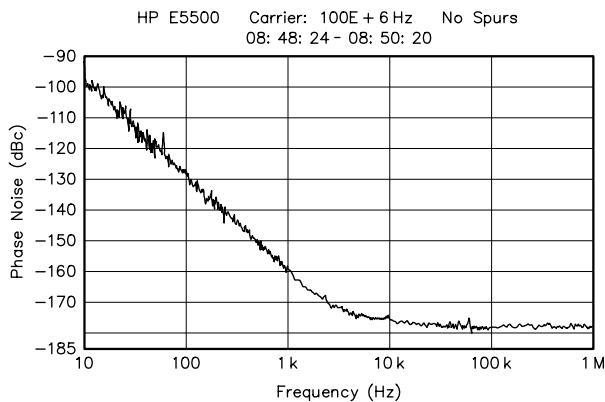


**Fig 8**—Phase-noise performance of a state-of-the-art 100-MHz crystal oscillator used as the reference clock in a high-performance DDS-driven PLL. The ultimate phase-noise performance of the synthesizer is affected by the master reference's phase-noise performance, but is limited by the DDS digital noise floor (typically  $-135$  dBc). Graphic courtesy of Techtrol Cyclonetics.

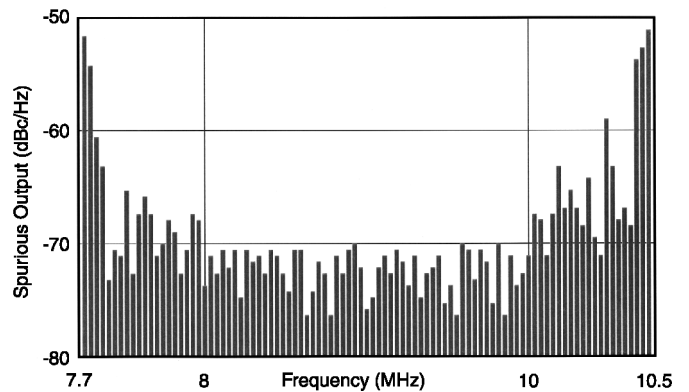


**Fig 9**—Best-case in-band spurious performance (actual) for an AD-9850 DDS using a reference at least eight times higher (84 MHz) than the highest output frequency. The DDS output frequency range is 7.7-10.5 MHz. Better spurious performance can be obtained with extreme care.

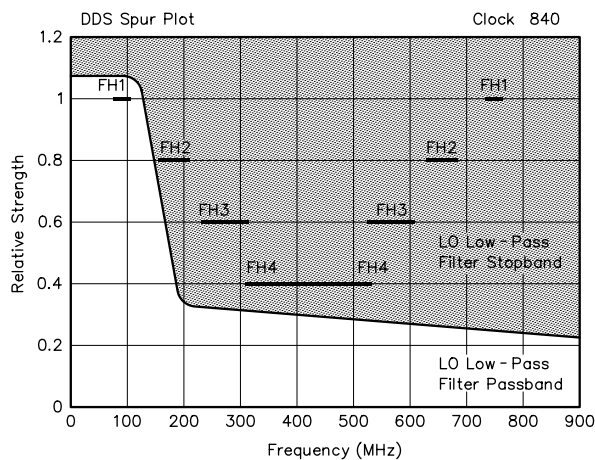


**Fig 10**—A simple Excel application determines phase-noise performance and reference oscillator frequency for a super-DDS that generates direct LO frequencies of 77-105 MHz in an HF transceiver. An 840-MHz reference is needed to minimize spurious products.

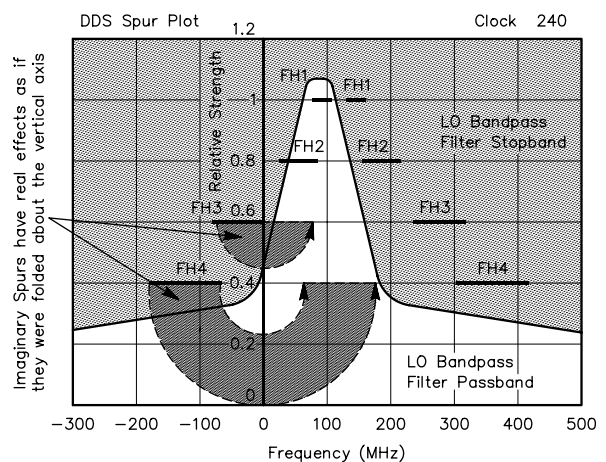


**Fig 11**—Obtaining good spurious performance from a DDS operating directly at frequencies compatible with up-converting HF radio LO requirements dictates reference frequencies above 800 MHz to produce a clean 77-105 MHz output. Using lower reference frequencies can cause alias frequencies that can fold back into the desired band of interest, degrading spurious performance (fold page along vertical axis to see in-band alias).

ited by the DDS technology itself. As discussed, this depends on many factors, particularly on the reference frequency choice as related to the output frequency.

In addition, spurious problems in DDS are created through several other mechanisms. First, intermodulation distortion is created just as in a mixer through various combinations of products of output-signal harmonics. These can be predicted largely using tools intended for predicting mixer products. Second, additional intermodulation products can be caused by mixing of the output and its harmonics with the clock itself. These spurious products can be predicted with less accuracy. Third, the glitch energy created by switching digital outputs in a stair-case like manner in D/As can cause unpredicted spikes that can only be cured through diligent work.

Best spurious performance of  $-70$  dBc is expected of today's low-cost DDS technology as shown in Fig 9. This implies a good DDS reference clock choice as shown in Fig 8. With extreme care in design and layout, better than  $-90$  dB spurious rejection can be achieved in a DDS-driven PLL synthesizer. This extraordinary performance is possible primarily because of a tight loop-filter realization in the PLL, which plays the role of removing unwanted spurious responses. This is also possible by observing careful power-supply isolation and using good power-line filtering, as enhanced by applying careful grounding techniques.

We have seen that the theoretical phase noise performance of a DDS output is proportional to the phase-noise performance of its reference oscillator and limited by the DDS's division number and by the noise floor of the DDS itself. We have also seen that the spurious performance of a DDS is determined by several other factors, including a strategically calculated reference frequency choice. (See Fig 10.) Although a super-DDS that accepts an 840-MHz reference frequency can be purchased commercially today, it is not within the reach of amateurs, or even equipment manufacturers. On the other hand, low-cost equivalents are now on the drawing board, and they should be available in the near future.

The above exercise clearly shows why the super-DDS cannot yet be used economically in an up-converting HF radio: It is a matter of cost versus performance. Ignoring the requirement for a high reference frequency can produce

alias frequencies that can fold back into the desired spectrum, spoiling the spurious response of the synthesizer, as shown in Fig 11. High Nyquist rates can be obtained only with higher reference frequencies. That requires a much more expensive technology to be used in the DDS, making it prohibitive for ham applications.

### Summary

The above discussion shows that the DDS-driven PLL remains a valuable LO solution, and the DDS used directly as an LO remains an expensive solution, at least for the time being. Nonetheless, the DDS-multiplier could be a more-economical solution because of its easier implementation (no tweaking in manufacturing required), even at the cost of reduced spurious performance.

Part 2 of this article will present the actual implementation of a microwave DDS-driven PLL, previously shown as Fig 6B.

### Notes

<sup>1</sup>An exception to this rule is in second- or third-conversion LOs, which are low enough in frequency to be implemented directly with DDS technology.

<sup>2</sup>Harmonic mixers are special mixers that embed multipliers in their construction. They are optimized for specific frequency plans.

<sup>3</sup>An octave is the frequency span between a fundamental frequency and its first harmonic.

<sup>4</sup>Initial publication of the DDS-driven-PLL concept is noted by Rockwell Collins in Reference 14, p 350 (1987). Actual implementation of the DDS-driven PLL was published by the author while at Honeywell in 1988 at RF-Expo (Reference 1). Additional work was later reported by others. The author has been developing practical high performance DDS-driven PLLs since 1981.

<sup>5</sup>This is because the Nyquist rate imposes a reference frequency of at least twice the highest output frequency.

<sup>6</sup>An improvement of 20 dB— $20 \log(10)$ —is realized by dividing the frequency by 10. However, the improvement is limited by the noise floor of the dividers used. Digital dividers, in general, have a noise floor limitation of  $-135$  dBc.

<sup>7</sup>This analysis considers the phase noise caused by the first LO at the output of the first mixer as it mixes with the MDS for a given SNR, and the first-IF bandwidth of say, 10 kHz (the roofing filter). These numbers are derived from computing the close-in noise spreading signal outside the bandwidth as well as the broadband LO noise convoluting with the receiver thermal noise, thereby raising the noise floor at the mixer's output.

### References

1. C. Drentea, "Designing Frequency Synthesizers," *Proceedings RF-EXPO 88*, Frequency Synthesis Session, Anaheim, California February 1988.

2. W. Egan, *Frequency Synthesis by Phase Lock*, (New York: John Wiley, 1981).
3. C. Drentea, *Radio Communications Receivers*, (New York: McGraw Hill, 1982).
4. A. Spooner, B. Lao, D. Rowe, *Superconductor Frequency Synthesizer*, TRW-Space and Electronics Group, Redondo Beach, California, internal paper.
5. A. Spooner, B. Lao, D. Rowe, "Superconducting Direct Digital Synthesizer," *IEEE Transactions on Applied Superconductivity*, Vol 7, No2, June-1997.
6. V. Manassewitsch, *Frequency Synthesizers Theory and Design*, (New York: John Wiley & Sons, 1980).
7. B. Bergeron, "Direct Digital Synthesis," *Communications Quarterly*, Summer 1993.
8. A. Blanchard, *Phase-Locked Loops Applications to Coherent Receiver Design*, (John Wiley & Sons, 1976).
9. R. Best, *Phase-Locked-Loops: Theory, Design, and Applications*, (New York: McGraw Hill, 1984).
10. D. Wolaver, *Phase-Locked Loop Circuit Design*, (Upper Saddle River, New Jersey: Prentice Hall, 1991).
11. P. Brennan, *Phase-Locked Loops: Principles and Practice*, (MacMillan Press, 1996; MacMillan is now part of Palgrave, with offices in New York).
12. F. Gardner, *Phase-Lock Techniques*, (John Wiley & Sons, 1966).
13. H. Berlin, *Design of Phase-Locked Loop Circuits*, (Indianapolis, Indiana: Howard W. Sams, 1980).
14. W. Sabin and E. Schoenike, *Single-Sideband Systems and Circuits*, (McGraw Hill, 1987).
15. R. Gilmore, and Qualcomm Inc, Patent 4,965,533—October, 1990: Direct Digital Synthesizer Driven Phase Locked Loop Frequency Synthesizer.

*Cornell Drentea was born in Bucharest, Romania. He studied electrical engineering there and in the United States, and he has been at the forefront of developing state-of-the-art RF products for over 40 years. These include receivers, synthesizers, transmitters and transceivers at frequencies up to 100 GHz.*

*During his career, Cornell has worked for several companies, including Honeywell and Hughes Aircraft. He is currently a Senior Principal Engineer in the Transmitters, Receivers and Exciters Group of Raytheon Electronic Systems, where he leads design and development of ultra wide-band receivers, synthesizers and ultra-high-frequency digital signal processors (DSP).*

*Cornell has published over sixty technical articles and papers in various trade and ham magazines. He is also the Author of the book Radio Communications Receivers. Cornell has been a ham for over 40 years and holds Amateur Extra class license, KW7CD. He lives in Tucson, Arizona.* □□

# *A Compensated, Modular RF Voltmeter*

---

*Build this voltmeter—it measures voltages from 100 mV to 300 V, from 30 MHz down to audio, on chassis or in coax, accurate to  $\pm 0.5$  dB, with built-in meter or with your DVM. It's portable, simple and inexpensive.*

---

By Sid Cooper, K2QHE

**T**his project was started to replace a reconditioned commercial RF voltmeter that required calibration every six months. It was quite accurate when it was in calibration, but was expensive to recalibrate. The idea then was to build a stable, solid-state RF voltmeter in less than six months so that the commercial one could then calibrate the homebrew unit, but—it has long been known what happens to your best-laid plans.

The requirements for my RF voltmeter (RFVM, Fig 1) are many:

- Provide accurate, stable measurements
- Measure voltage at frequencies from audio through HF

- Measure voltage levels from QRP to QRO
- Measure voltages inside equipment or in coax
- Operate portably or from ac lines
- Be flexible: work with digital voltmeters already in the shack, or independently
- Be inexpensive

This last goal is an old fashioned idea; most equipment today is not in that category.

## **Design Approach**

To achieve stability, the RFVM uses op amps and any drift in the probe's diode detector is compensated by a matched diode in the RF op amp. This stretches the sensitivity to QRP levels. The dynamic range extends linearly from 0.1 V to 300 V (RMS) by

using a series of compensated voltage multipliers.

The frequency response was flattened by using Schottky diodes, which easily reach from 60 Hz to 30 MHz. Both the basic probe and the multipliers very simply adapt to function as a probe, clip to various measurement points on chassis or to screw onto UHF connectors. The active devices are only two op amps. They draw 800  $\mu$ A of resting current and a maximum of 4.0 mA during operation from a 9-V battery, which is disconnected when a 9-V wall unit is plugged into a jack on the back panel. As designed, the RFVM has a small sloping panel cabinet with a microammeter display. A pair of front-panel banana **OUTPUT** jacks can be used with a DVM; this eliminates one op amp, the meter and

a multiposition switch. Since the meter and switch are the most expensive parts (when they are not bought at a hamfest), how low-cost can this RF voltmeter get?

### The Probe

The low-voltage probe is a detector circuit that uses a Schottky diode and a high-impedance filter circuit (Fig 2). The diode is matched with the one in the feedback circuit of the CA3160 shown in Fig 20. This match reduces the diode's threshold voltage from about 0.34 V to less than 0.1 V, making the voltage drop comparable to that of a germanium diode. Since I think 0.1 V adequately covers QRP requirements, I made no further tests with germanium diodes to determine how much lower in voltage we could go.<sup>1</sup>

Use the low voltage probe and the output of the CA3160 in the meter unit (Fig 20) to find a matched diode pair. Build the CA3160 circuit first for this purpose. Select a diode and place it in the feedback loop of the CA3160, then test each of the remaining diodes in the probe with the three pots set about midrange. Test each diode, first at probe inputs of 100 mV, then at 3.00 V, at 400 Hz. Record the dc output from the CA3160, using the **OUTPUT** terminals. A bag of 20 diodes from Mouser Electronics<sup>2</sup> contained seven matched pairs, with identical readings at both low and high voltages. My tests used the ac scale (good to 500 Hz) of a Heath 2372 DVM to read the input voltage, and its dc scale to read the output. The number of matched pairs is surprising, but the diodes in the bag may all be from the same production run.

<sup>1</sup>Notes appear on page 34.



Fig 1—The RF voltmeter with meter unit, RF probe and voltage multipliers.

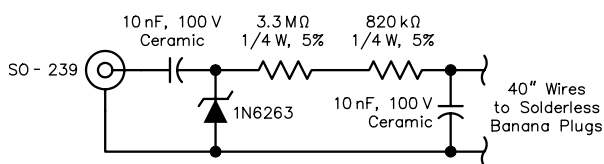


Fig 2—A schematic diagram of the RF probe.

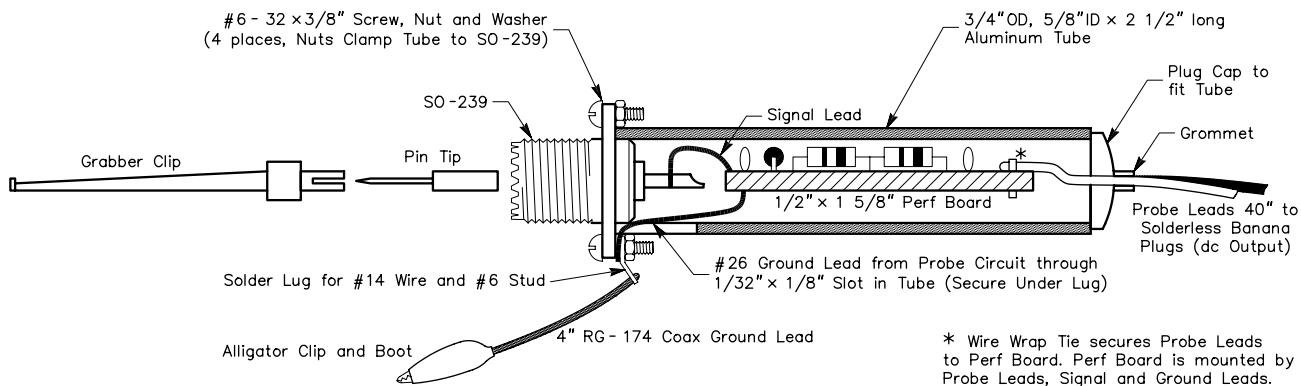


Fig 3—RF probe construction showing the grabber clip (RS 270-334), pin tip (Mouser 534-1600), lug (Mouser 571-34120, for #14-#16 wire and a #6 stud), alligator clip (RS 270-1545), plug cap (Mouser 534-7604), grommet (Mouser 5167-208) and four-inch ground lead made from shield of RG-174.



## RF Probe Assembly

After selecting matched diodes, all components of the RF probe are mounted on a piece of perf board that is inserted in an aluminum tube (Fig 3). Since the circuit board is very light, it is supported on each end only by its input and output wires. The input RF wire is soldered to the center pin of the SO-239 connector. The two dc-output wires are held to the board by a small tie wrap, consisting of a piece of the #26 insulated wire, after having been passed through the plug cap and grommet. Cut a slit in the aluminum tube, perpendicular to its end. Make it at least  $\frac{1}{8}$ -inch long and  $\frac{1}{32}$ -inch wide to allow a bare #26 ground wire to pass through it.

Let's look at how the probe is assembled. The aluminum tube just fits around the back end of the SO-239 connector. When the four #6-32 screws, nuts and washers are installed in the four holes of the SO-239 connector, the flat face of the nut bears down strongly on the aluminum tube and rigidly holds it in place. Most standard SO-239 connector holes easily accept #6-32 screws; if yours do not, enlarge them with a #27 bit. The slit cut in the aluminum tube allows the bare ground wire from the perf board to pass from inside the tube to the outside and around the screw that secures the ground lead of the probe. As can be seen in Fig 3, the threaded part of the SO-239 connector faces away from the aluminum tube.

This probe allows easy voltage measurements in a coaxial cable when the probe SO-239 is secured to a mating T connector. To make a probe reading at any point on a chassis or PC board with this connector, simply insert the larger end of a nicely mating pin tip into the SO-239. The pin tip's diameter is 0.08 inches at the small end and—fittingly—0.14 inches at the mating end. I made this purely fortu-

itous discovery while rummaging through a very ancient junk box. Further, to make measurements with the probe clipped to a part or test point on a PC board or chassis, a clip or grabber can be mated to the pin tip that protrudes from the SO-239. This is shown in Figs 3 and 4. This was another lucky strike. All this may have been known to people in the connector industry, but it appears not to have been known or used elsewhere. Fig 5 shows the grabber connected to the RF probe using the pin tip to join the two.



Fig 4—A photo of the grabber clip, pin tip and RF probe.

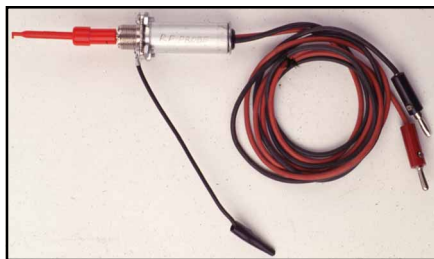


Fig 5—The RF probe with the pin tip and grabber clip in place. The pin tip is not visible, but it provides the physical bridge and electrical connection between the clip and SO-239 of the RF probe.

## Probe Measurements

The probe can accept RF signals up to 20 V (RMS) when there is no dc voltage or a combination of dc voltage and peak ac of about 28 V without exceeding the reverse-voltage rating of the diode. I made linearity measurements of the RF probe from 100 mV to 8.0 V at 400 Hz. (The range was limited by my available signal generator.) Fig 6 is a plot of the error at the probe output versus the input amplitude. This was measured using a digital voltmeter with a 10-M $\Omega$  input resistance. This input resistance and the 4.1-M $\Omega$  resistor in the probe converts the peak voltage of a sine wave signal to the RMS reading of the DVM. The error is -44% at 100 mV, then 10% (0.9 dB) at 1.0 V and finally 2.9% at 8.0 V. The RF probe and DVM are obviously intended for higher voltage readings where the diode voltage drop doesn't affect the accuracy significantly.

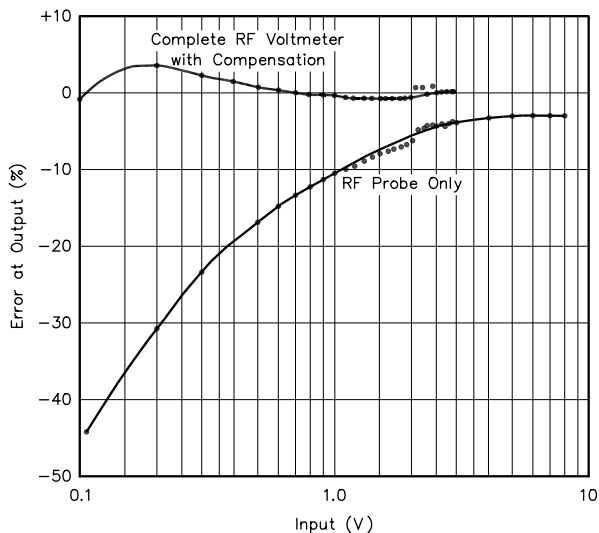


Fig 6—Amplitude linearity of the RF probe alone and in combination with the RF voltmeter.

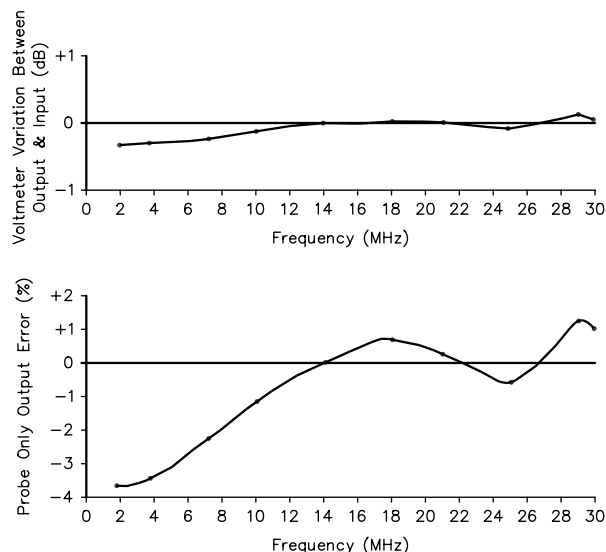


Fig 7—A frequency-response plot for the RF voltmeter. The response of the probe determines the overall system response.

The frequency response of the probe was measured at the midpoint of each ham band from 1.9 to 30 MHz with 650 mV input (see Fig 7). This time, because the input voltage was low and the absolute error would have been high, the probe was connected to the meter unit, which will be described later. The compensating diode loop of the meter unit reduces the error that would otherwise be read by the DVM from 90 mV (14%) to 4 mV (0.6%). The frequency response, however, is controlled by the probe. Use of the meter unit—which operates entirely on the dc signal—does not affect the frequency response, but it does improve the sensitivity of the readings. The measured response shown goes from -3.6% (-0.32 dB) to +1.2% (+0.1 dB).

### Multipliers

To extend the voltage range of the RF probe, use a 10× multiplier, which is a compensated divider, shown in Fig 8. The electrical design is straightforward and includes a small trimmer capacitor to adjust for a flat frequency response. These components are very lightweight, so they require no perf board and are easily supported by their leads, which are anchored at the two SO-239 connectors. To make measurements, the input connector can be mated to connectors in a coaxial cable, a pin tip can be inserted for probing PC boards or a grabber can be added for connections to components on a chassis. The multiplier can connect to the RF probe either through a male-to-male UHF fitting or by a piece of coax with a UHF male connector at each end.

The typical way to adjust the trimmer requires a square-wave input and



Fig 10—A view showing the 10× multiplier with grabber, pin tip and a male UHF coupler that connects the multiplier to the RF probe.

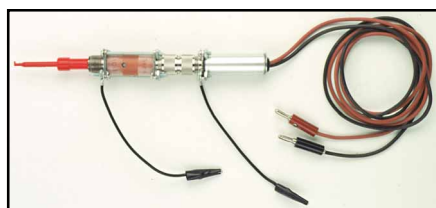


Fig 11—The complete RF probe and 10× multiplier assembly.

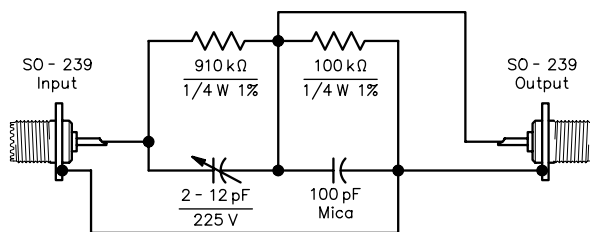


Fig 8—A schematic of the 10× multiplier. The trimmer capacitor is from Ocean State Electronics (see Note 10).

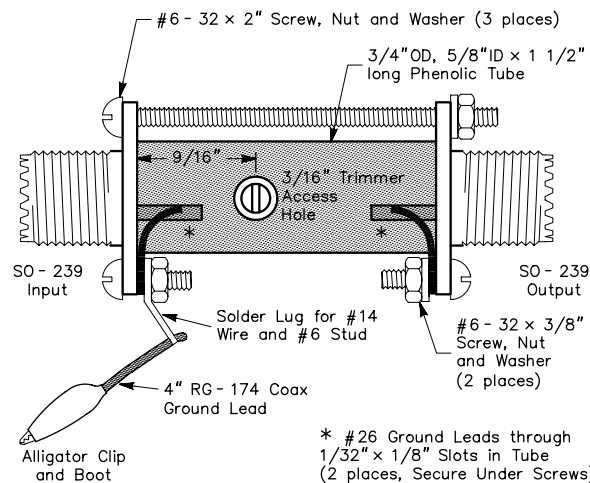


Fig 9—Construction of the 10× multiplier. The phenolic tube is US Plastics #47081, see Note 3. The lug is Mouser 571-34120.

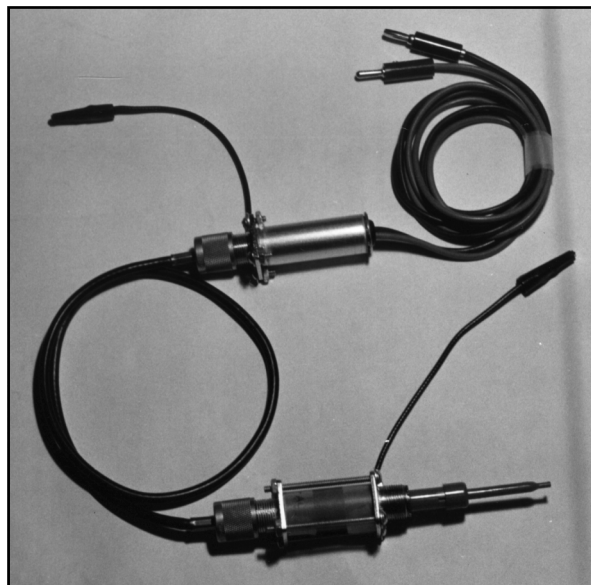


Fig 12—The RF probe and multiplier can be separated by a piece of coax less than 12 inches long if it makes measurements more convenient.

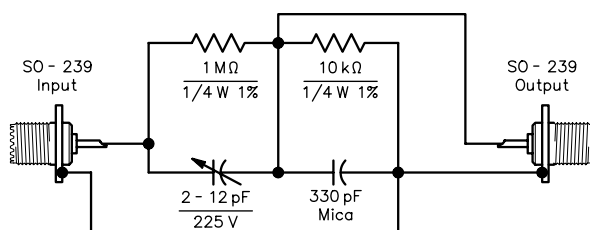


Fig 13—Schematic of the 100× multiplier (maximum allowable input is 150 V RMS). The trimmer capacitor is from Ocean State Electronics (see Note 10).

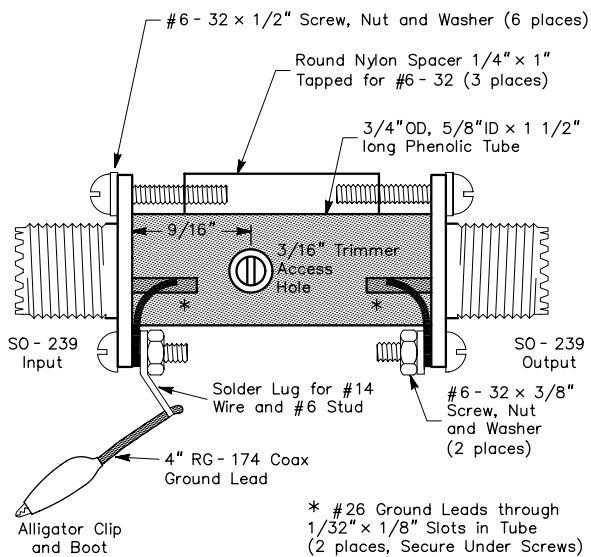


Fig 14—100× multiplier assembly showing the round Nylon spacer (Mouser 561-TSP10), phenolic tube (US Plastics #47081, see Note 3). The lug is Mouser 571-34120.

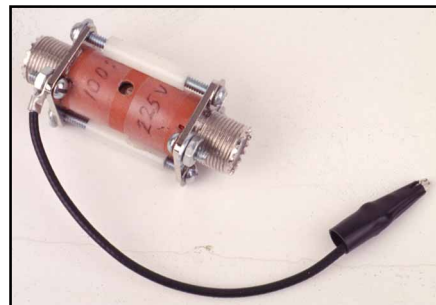


Fig 15—The assembled 100× multiplier.

that in the RF probe with #6-32 screws to hold it all together, but the frequency response began to drop off at 21 MHz. By replacing the aluminum tube with a phenolic tube<sup>3</sup> having the same dimensions, the response is adequate to 30 MHz.

Fig 9 shows construction methods. Two slits at the ends of the tube allow the ground wires at the input and output ends to exit and wrap around the screws of each connector. A hole in the phenolic tube allows adjustment of the trimmer capacitor.

Fig 10 shows the exploded view of the pin tip and grabbers at the input end of the multiplier and a UHF male-to-male connector on the output side to mate with the RF probe. The assembled multiplier and probe are shown in Fig 11. The whole assembly is only 3 1/2 inches long and is comfortable in the hand. If more flexibility is desired, the two pieces may be separated by as much as one foot of coax (Fig 12) without doing too much damage to the accuracy of the measurement.

The 100× multiplier follows the same design concepts as the 10× multiplier including the obligatory trimmer capacitor, as in Fig 13. Here too, the 225 V dc rating of the trimmer limits the maximum RF to 150 V RMS. So, this is not useful should it be used only with the probe and your DVM because the 10× multiplier already covers this range. Later, we will see how it is useful with the RF probe and the meter unit.

The 100× unit also uses a phenolic-tube housing with a hole to adjust the trimmer and a slit at each end to bring out the ground wires, which then wrap around screws in the connectors. In order to reach at least 30 MHz, however, the two-inch steel screws between the two SO-239 connectors must be insulated. Using plastic washers at the connector holes could do this job but would have required #4-40x2-inch-long screws. After a long search at the biggest hardware stores and catalogs,

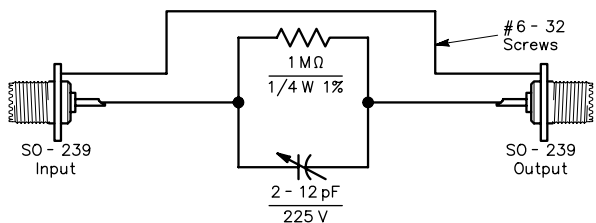


Fig 16—A schematic diagram of the 2× multiplier. Its output connects to the input of the 100× multiplier for 200× measurements up to 300 V RMS. This multiplier is used *only* with the 100× multiplier.

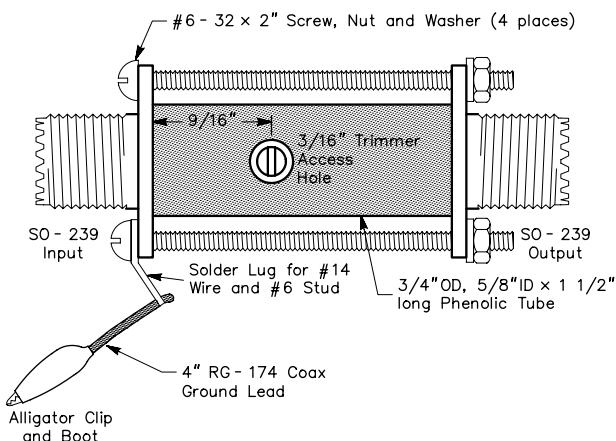


Fig 17—2× multiplier assembly showing the phenolic tube (US Plastics #47081, see Note 3). The lug is 16-14 #6 stud (Mouser 571-34120).

an oscilloscope on the output. The trimmer is then set to produce a flat square-wave output with no overshoots on the leading edges and no droop across the top. An RF signal generator that covers 1.9 MHz to 30 MHz can be used instead, if a square wave generator is not available. Since this is a 10× multiplier, it is reasonable to expect the input to handle up to 200 V

(RMS), but the limit is 150 V because the trimmer capacitor is rated at 225 V dc. You may be able to find small trimmers with higher voltage ratings that will take the multiplier to 200 V and still fit inside the tube housing.

Multiplier construction follows the same methods used for the RF probe but with a few differences. My first model used an aluminum tube like



I found nothing longer than 1½ inches. That's the best way to assemble this multiplier, if you can find the screws. Otherwise, use nylon spacers and shorter screws as shown in Figs 14 and 15. The pin tip and grabber at the input and UHF male-to-male connector or coaxial cable at the output are used as with the 10× multiplier.

The only purpose of the 2× multiplier is to create a 200× multiplier when used with the 100× multiplier in series, so as to extend the voltage range from 150 V to 300 V (1800 W at 50 Ω only under matched conditions<sup>4</sup>). The trimmer in each multiplier now divides in half the input voltage. Fig 16 shows the 2× multiplier with only one RC section since it relies on the RC sections in the 100× multiplier to complete the division (multiplication).

The construction, Fig 17, returns to the tubular format as before, but this time there are no slots to pass the ground wires; the four screws are able to do the job. The two multipliers are shown in series in Fig 18.

The input capacitance for each multiplier is shown in Table 1.

When measurements are made on a load resistance of 50 Ω, the input capacitance of the multipliers has no effect on readings below 30 MHz. When the impedance of the load resistance is larger, consider any error it introduces. To get a sense of the affects of the load resistance, use the equation below. It shows the relationship between the resistance, capacitance and frequency when the measured voltage is 3 dB down from what it would be if it were read by a meter with no input capacity:

$$f = \frac{1}{2\pi R_L C_p} \quad (\text{Eq 1})$$

where

$R_L$  = load resistance

$C_p$  = probe capacitance

For example, at a load of 1 kΩ and a probe capacity of 13.3 pF, the 3 dB down frequency is about 12 MHz, where the error is 30%. If an attenuator were used instead of the multiplier, it would not have this problem because it works with either a fixed 50-Ω load at high frequencies or a 600-Ω at low frequencies. Probes cannot select their frequency or load impedance and are thereby more flexible in use, so measurements must

be made with consideration, but these multipliers would not have a problem at 50 Ω or 600 Ω either.

Table 2 summarizes the voltage ranges using only the multiplier with the RF probe and a DVM that has a 10-MΩ input resistance that's available in the shack.

The multipliers are intended for use at high voltages where safety precautions are a primary consideration to avoid personal injury. *The ARRL Handbook* has an entire chapter devoted to safety, for good reason. In Tektronix' *ABC's of Probes*,<sup>5</sup> an entire section thoroughly covers the hazards and necessary precautions when making measurements with probes. It is worth the little effort to get a copy of it and also the Pomona Catalog,<sup>6</sup> which has some good information on probe use.

The multipliers have panel connectors at both ends and the RF probe has one at one end. Their grounds are connected and brought to the meter unit. This unit is grounded only when the ac-powered 9-V power supply that may be used with it, is grounded. When it is battery operated, the meter unit relies on the ground-clip connection to the ground of the equipment under test. This is satisfactory if there is no unknown break in the chain of ground connections that would make the panel connector hot. Furthermore, as insurance, it is well to wrap these connectors with vinyl tape or to cover the multiplier with a plastic boot to prevent contact with either hands or equipment under test. This is not shown in any photographs because it would have

obscured the appearance and construction of the probe and multipliers.

The frequency responses of the multipliers were determined using an RF signal generator set at the midpoint of each ham band from 160 to 10 meters, including 30 MHz. An error of 5.42% (0.46 dB) was measured from 160 to 17 meters, which then decreased to 4.13% (0.35 dB) at 15 meters and then to zero through 30 MHz. The constant error from 160 to 17 meters is probably due to the inherent errors in the test equipment. The oscilloscope has a 60 MHz bandwidth, an input impedance of 1 MΩ and 30 pF, which introduces a load effect on the multiplier outputs. It also has a reading accuracy of ±3%. When the multiplier-components accuracy of 1% is included, it is not surprising to find the overall inaccuracy to be at most 5.42%.<sup>7</sup> The error of the multiplier itself could be inherently less than this. Before the overall frequency response was measured, the trimmer capacitor was adjusted with the input frequency set mid-frequency at 15 MHz. If your interest in RF probes and multipliers has been raised and you have more questions, see the references in Notes 5 and 6.

### The Meter Unit

The meter unit serves several purposes when used with the RF probe. It increases the accuracy of the probe and DVM from -45% to -3.5% at a voltage of 100 mV RF. At higher voltages, it maintains a minimum advantage of 5:1 in reducing the error, when the probe is used with a DVM. This is an increase in both sensitivity and accuracy. The usual non-linearity caused by the diode in the probe is reduced when used with the meter unit. The technique also incidentally provides temperature compensation for diode drift. The meter unit has a ±5% panel meter to display measurements, but it also contains a pair of OUTPUT terminals for a DVM. Add a DVM when more accuracy is desired

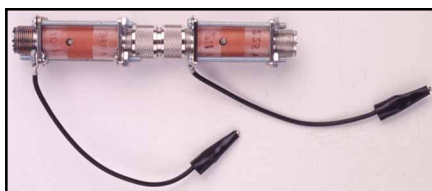


Fig 18—The 2× and 100× multipliers are joined by a male UHF coupler for readings up to 300 V (RMS, 1800 W, see Note 4).

Table 2—Multiplier versus Voltage Range

Probe Configuration	Range (V)	Maximum Voltage
Probe Alone*	1.0-20 V ac	20 V ac
With 10× Multiplier*	10-150 V ac	225 V (ac + dc)
With 100× and 2× Multiplier†	150-200 V ac	450 V (ac + dc)
With 100× and 2× Multiplier††	200-300 V ac	450 V (ac + dc)

\*error less than -10% or -0.83 dB

†with error of -45% to -10% or less than 3.2 dB. A trimmer capacitor with a rating of 300 V dc increases the 10× range to 200 V ac and reduces the error from 45% to 10%. The RF probe and meter unit reduces the error to less than -3.5% or less than -0.3 dB.

††with error less than -6% or -0.54 dB

Table 1—Multiplier Range versus Capacitance

Multiplier	10×	100×	200×
Input Cap (pF)	13.3	10.9	13.5



at the low end of the range or when you want a bit more resolution. Finally, since the meter unit is fully portable, low-level field-strength measurements are possible with a whip antenna at the probe input connector. Due to its sensitivity and accuracy, the probe can be adapted for use in many places around the shack.

The non-linear response of the probe diode is compensated (improved) by a circuit in the meter unit. The feedback loop of a CA3160 op amp contains a diode matched to the one in the probe (see Note 1). Fig 19 and its sequence of equations present a very simple sketch of how matched diodes do this when dc is applied through a diode. The final equation shows that any difference between the op amp input and output is due to a difference in voltage drops across the two diodes. When the diodes are matched, the error disappears. When RF is applied, the average currents through the diodes must be equal to keep the voltage drops

equal. Articles by Kuzdrall (Note 1) Grebenkemper<sup>8</sup> and Lewallen<sup>9</sup> are first-class descriptions of the principles used in this RF voltmeter.

Fig 20 shows three pots for calibrating the meter unit. This should be performed at 400 Hz to avoid any effects due to RF. The 100-kΩ pot is typi-

$$e_s - e_{d1} = e_p$$

$$e_o - e_{d2} = e_n$$

$$e_i = e_p - e_n = e_s - e_{d1} - e_o + e_{d2}$$

$$e_i = \frac{e_o}{G} \approx 0$$

$$e_s - e_o = e_{d1} - e_{d2}$$

$e_s$  represents the input of the RF probe as a dc signal.  
 $e_o$  represents the output from the high-gain CA3160 op amp.  
 $e_{d1}$  is the voltage drop across the diode in the RF probe.  
 $e_{d2}$  the voltage drop across the diode in the feedback loop.  
 $G = 320,000$  for the CA3160  
 The last equation shows that any difference between the signal and output results from unequal diode drops when the diodes are not matched.

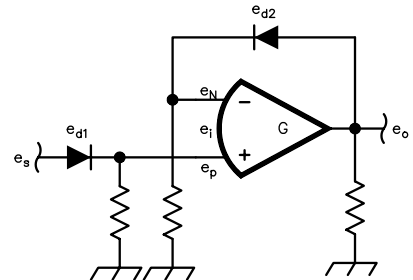
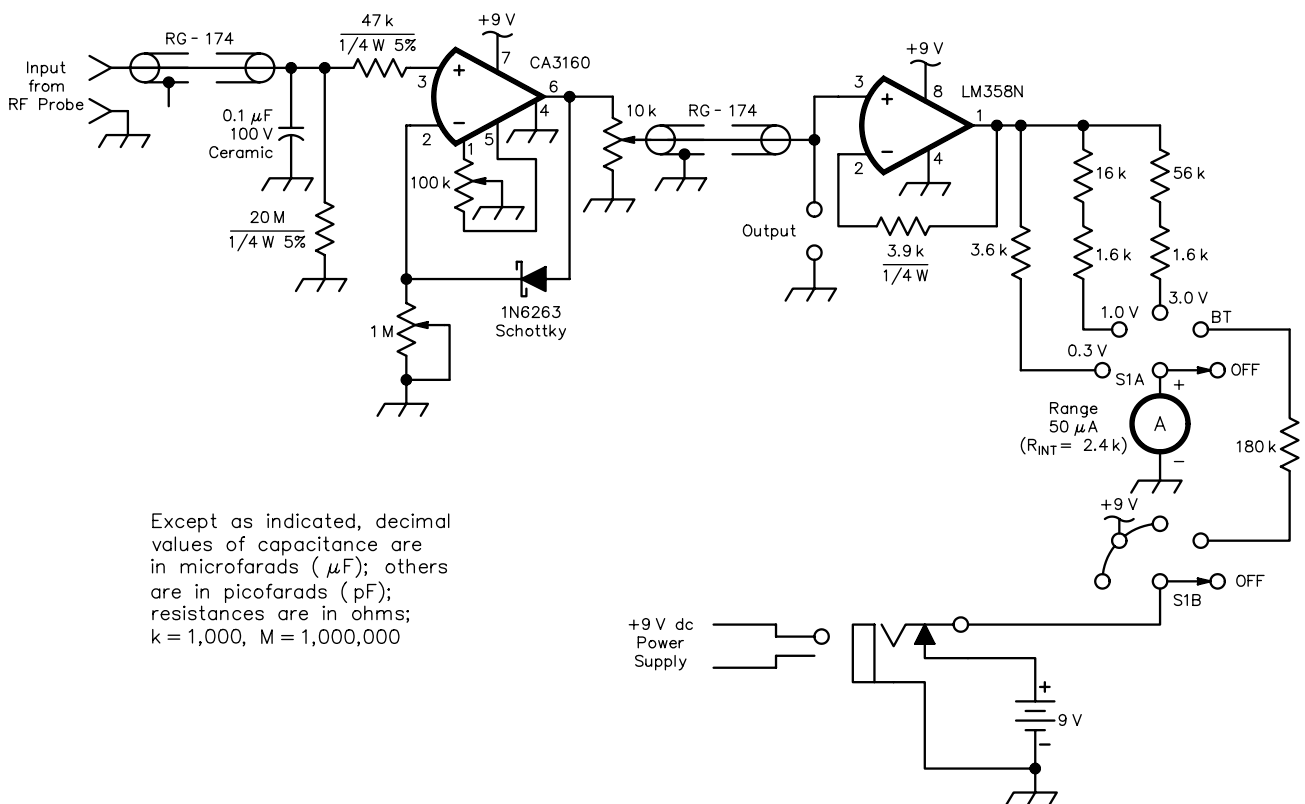


Fig 19—Basics of the diode-compensation method to improve measurement accuracy at low input voltages. It also provides a measure of temperature compensation and drift reduction. See Fig 6.



Except as indicated, decimal values of capacitance are in microfarads ( $\mu\text{F}$ ); others are in picofarads (pF); resistances are in ohms; k = 1,000, M = 1,000,000

Fig 20—Schematic of the RF voltmeter. The DVM adds resolution to the panel-meter reading. When the panel meter reads full scale with S1 in the B+ position, the battery is at 9V.

S1—2P5T non-shorting rotary switch, one-inch diameter. A one-lug tie strip is mounted on the negative-terminal screw of the meter to provide a mounting point for the meter resistors.

The following resistors are all carbon-composition or metal-film components ( $1/4\text{W}$ ,  $\pm 1\%$ ): 1.6 k, 3.6 k, 16 k, 56 k. The three pots are cermet 12-turn components adjustable from the top. The input connector for the RF probe and the output connector for the optional DVM

are double banana connectors. The resistors, capacitors, ICs diodes and pots are mounted on RadioShack multipurpose PC board #276-150. The meter, two banana plugs and switch are mounted on the front of the case, the phone jack on the back.

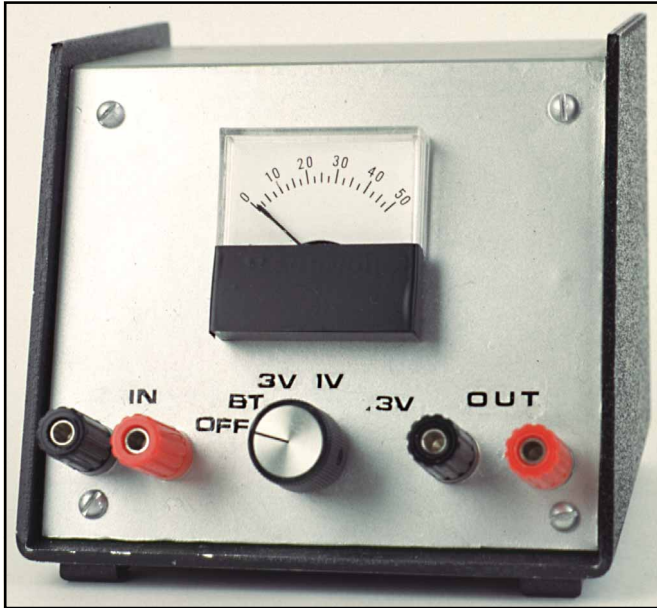
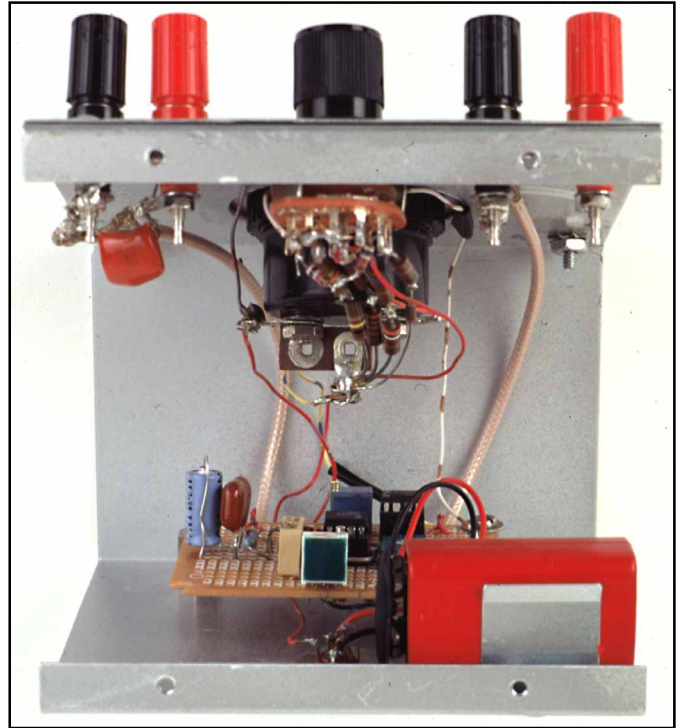


Fig 21(above)—The assembled meter unit.  
Fig 22(right)—Inside view of the meter unit. RG-174 connects the INPUT and OUTPUT banana binding posts to the circuit board. The rotary switch, one-lug tie strip and battery are also visible.



cally used to null the offset of the CA3160, but is used here to initially set the offset to about 0.5 mV to 1.0 mV with no input. Then the 1-M $\Omega$  pot sets the output to 100 mV with no input, and the 10 k $\Omega$  pot sets the output to 3.0 V when the input is 3.0 V. Finally, the three pots are alternately adjusted until the 100 mV and 3.0 V set points occur together. The 100-k $\Omega$  pot is helpful in fine tuning the 100-mV point. A DVM was used at the optional OUTPUT sockets during calibration.

A CA3160 was selected for the input op amp because of its high input impedance of 1.5 T $\Omega$  and high gain of 320,000. Although it has diodes that provide protection, I think it could be sensitive to electrostatic discharge, so handle it carefully. Use IC sockets to permit easy replacement of the ICs in case of damage. An LM358N IC follows the CA3160 (see Fig 20), primarily to drive the panel meter. If you use a DVM as the display, you can omit the LM358N circuit, meter and multi-position switch. The only functions lost are the battery-voltage check and power on/off switch. Add a on/off switch to the circuit when the multi-position switch is omitted. The CA3160 op amp circuit easily spans the range from 100 mV to 3.0 V without the need for a range switch.

### Construction

A 5 $\times$ 5 $\times$ 4 $\frac{1}{2}$ -inch sloping-front instru-



Fig 23—The meter unit with RF probes and a DVM connected to the OUTPUT jacks.

ment case was used to house the components of the meter unit (see Fig 21). The meter on the front panel has a 2 $\times$ 2-inch face and requires a 1 $\frac{1}{2}$ -inch hole in the panel. Although a 50- $\mu$ A meter from the junk box is used here, a 1-mA movement will work as well, provided the series resistors are changed accordingly.

The rotary switch has two poles and five positions for changing the meter range, testing the battery condition and switching the power off. Two sets of double banana binding posts are used, the INPUT pair accepts the dc signal from the RF probe. The OUTPUT pair provides a voltage for a DVM dis-

play, whether the panel meter is used or not. On the rear of the case, a miniature phone jack accepts 9-V power from either a battery or a 9-V dc supply. The ICs and other parts are mounted on a RadioShack multipurpose PC board that has very convenient holes and traces. The board is bolted to the back of the case via stand-off insulators and wired to the front panel components (see Fig 22). The assembly of the meter unit, RF probe and DVM are shown in Fig 23.

### Acknowledgement

The original goal of the design was a linear scale with an accuracy of 5%,



from 100 mV to 3 V (RMS) for frequencies from audio through HF. When I discussed it with *QEX* Managing Editor Robert Schetgen, KU7G, he thought the utility of the meter could be much improved if the voltage range were increased. That set off a chain reaction of improvements, beginning with the compensated multipliers for the RF probe input. The early probe design had a pin at its input, however, which does not easily connect to a divider with an SO-239 connector at its output. Part of the answer is a SO-239 panel connector at the probe input for measurements in coaxial terminations. This was a new voltmeter application, but it seemed to defeat the meter's original purpose: troubleshooting on a chassis.

Rummaging through an ancient parts box provided the link: a probe pin tip with a shank that fits perfectly into the female center pin of the SO-239 connectors on the probe and multipliers. This pin tip is still available in catalogs, surprisingly, but as a standard pin tip it also fits into available alligator clips. This single pin is used for probing

or for adding alligator clips or probe adapters to either the RF probe or multipliers. The tip can be removed anytime and the SO-239 used for cable measurements. Bob's outstanding suggestion was taken seriously. The result is an inexpensive, wide-range, RF voltmeter that should not require calibration every six months.

#### Notes

- <sup>1</sup>J. A. Kuzdrall, "Linearized RF Detector Spans 50-to-1 Range," Analog Applications Issue *Electronic Design*, June 27, 1994.
- <sup>2</sup>Mouser Electronics, 2401 Hwy 287 N, Mansfield, TX 76063; tel 800-346-6873, fax 817-483-0931; E-mail [sales@mouser.com](mailto:sales@mouser.com); [www.mouser.com](http://www.mouser.com).
- <sup>3</sup>United States Plastics Corp, 1390 Neubrecht Road, Lima, OH 45801-3196, tel 419-228-2242, fax 419-228-5034.
- <sup>4</sup>If the power remains constant, load mismatch multiplies the voltage by the SWR. A 2:1 SWR would produce 600 V, 3:1 900 V and so on.—Ed
- <sup>5</sup>*ABCs of Probes*, Tektronix Inc, Literature number 60W-6053-7, July 1998. Tektronix, Inc. Export Sales, PO Box 500 M/S 50-255 Beaverton, OR 97707-0001; 503-627-6877. Johnny Parham, "How to Select the Proper Probe," *Electronic Products*, July 1997.

- <sup>6</sup>Pomona Test and Measurement Accessories catalog. ITT Pomona Electronics, 1500 E Ninth St, Pomona, CA 91766-3835.
- <sup>7</sup>A. Frost, "Are You Measuring Your Circuit or Your Scope Probe?" *EDN*, July 22, 1999. E. Feign, "High-Frequency Probes Drive 50-Ω Measurements," *RF Design*, Oct 1998.
- <sup>8</sup>J. Grebenkemper, KI6WX, "The Tandem Match—An Accurate Directional Wattmeter," *QST*, Jan 1987, pp 18-26; and "Tandem Match Corrections," *QST*, Jan 1988, p. 49.
- <sup>9</sup>R. Lewallen, W7EL, "A Simplified and Accurate QRP Directional Wattmeter," *QST*, Feb 1990, pp 19-23, 36.
- <sup>10</sup>Ocean State Electronics, 6 Industrial Dr, PO Box 1458, Westerly, RI 02891; tel 800-866-6626, fax 401-596-3590.

*Sid Cooper, K2QHE, received his license 45 years ago, although he claims he was genetically programmed by his brother, Bert, WA0BHE (SK), for electronics long before that. He worked on radar and computer design programs as an electronics engineer and manager, then retired from RCA after 20 years. He is fairly active at the IRAC ham club in Roseland, New Jersey, and is a fairly regular participant on the Northeast Corridor Net on Monday nights.* □□

## EZNEC 3.0

### All New Windows Antenna Software by W7EL

*EZNEC 3.0* is an all-new antenna analysis program for Windows 95/98/NT/2000. It incorporates all the features that have made *EZNEC* the standard program for antenna modeling, plus the power and convenience of a full Windows interface.

*EZNEC 3.0* can analyze most types of antennas in a realistic operating environment. You describe the antenna to the program, and with the click of a mouse, *EZNEC 3.0* shows you the antenna pattern, front/back ratio, input impedance, SWR, and much more. Use *EZNEC 3.0* to analyze antenna interactions as well as any changes you want to try. *EZNEC 3.0* also includes near field analysis for FCC RF exposure analysis.

**See for yourself**

The *EZNEC 3.0* demo is the complete program, with on-line manual and all features, just limited in antenna complexity. It's free, and there's no time limit. Download it from the web site below.

**Prices** - Web site download only: \$89. CD-ROM \$99 (+ \$3 outside U.S./Canada). VISA, MasterCard, and American Express accepted.

Roy Lewallen, W7EL phone 503-646-2885  
P.O. Box 6658 fax 503-671-9046  
Beaverton, OR 97007 email w7el@eznec.com

**<http://eznec.com>**

## 800-522-2253

### This Number May Not Save Your Life...

But it could make it a lot easier!  
Especially when it comes to  
ordering non-standard connectors.


#### RF/MICROWAVE CONNECTORS

- Specials our specialty virtually any SMA, N, TNC, BNC, SMB, or SMC delivered in 2-4 weeks
- Cross reference library to all major manufacturers.
- Large inventory of piece parts for all types of coaxial connectors.
- Experts in supplying "hard to get" RF connectors.
- Connectors supplied to your drawings and specs.
- Our 56 Standard adapters can satisfy virtually any combination of requirements, between SMA, TNC, N, 7mm, BNC and others.
- Extensive inventory of passive RF/Microwave components including attenuators, terminations and dividers.

**NEMAL**  
Cable & Connectors  
for the Electronics Industry


NEMAL ELECTRONICS INTERNATIONAL, INC.

12240 N.E. 14TH AVENUE  
NORTH MIAMI, FL 33161  
TEL: 305-899-0900 • FAX: 305-895-8178  
E-MAIL: [INFO@NEMAL.COM](mailto:INFO@NEMAL.COM)  
URL: [WWW.NEMAL.COM](http://WWW.NEMAL.COM)




**ICOM IC-756 PRO**

The impressive **IC-756 Pro** covers HF plus 6 meters. The high resolution 5 inch TFT color display provides more operating information than ever, including a spectrum scope. The 32 bit floating point DSP provides crisp, clear reception with 41 built-in filters. The "Pro" is the choice for serious DXers and contesters.



**IC-746** ✓ 160 to 2 Meters!

The **IC-746** covers 160-10 meters plus 6 and 2 meters with 100 watts on all bands. Call or visit our website for further details and pricing on this and other ICOM radios.



**Universal Radio**  
6830 Americana Pkwy.  
Reynoldsburg, OH 43068  
♦ Orders: 800 431-3939  
♦ Info: 614 866-4267  
[www.universal-radio.com](http://www.universal-radio.com)

# *The Rectangle Family of Antennas, Part 1: The Not-So-Simple Rectangle*

---

*Loops are popular antennas. Here's a discussion of four-sided loops. It considers their resistance, gain and bandwidth as affected by their operating frequency, shape and conductor losses.*

---

By Dan Handelsman, N2DT

In this series of articles, we shall study the rectangular loop antenna and all the others that derive from it. This first article will concern itself with the behavior of the simple rectangle, shown in Fig 1A. We need to understand this basis before we consider more-complex antennas that use a rectangle as an element. Among these are the asymmetrical double rectangle (ADR), one variant of which is the Hentenna (Fig 1B); the symmetrical double rectangle (SDR, Fig 1C); and the multiple-loops, parasitic rectangles and large multi-element rectangular arrays.

The genre of rectangular antennas

includes not only closed loops, such as the quad and the simple rectangle, but also open loops such as the half-square and bobtail that—on initial impression—don't appear to be loops at all. Vertically polarized rectangles have been called “self-contained verticals” (or SCVs) and have been extensively investigated by L. B. Cebik, W4RNL.<sup>1</sup> In this series, I intend to add to what is known about these antennas and their horizontally polarized kin.

Practically speaking, a rectangle antenna can be thought of as encompassing two types of antenna. One is horizontally polarized with relatively thick conductors; it is useful from 30 meters up into the UHF range. The other is vertically polarized with rela-

tively thin wires (Fig 1D); it is useful as a gain antenna from 40-160 meters.

Why are there such differences that render antennas of the same shape so qualitatively different? Because, with thicker wires—relative to wavelength ( $\lambda$ )—on the higher frequencies the limiting factors in antenna performance are low radiation resistance and narrow SWR bandwidth (BW). On the low bands with relatively thin wires, the limiting factor is antenna loss, which, at some dimensional point, offsets any gain increase.

I propose to discuss the following:

1. The gain of a rectangular antenna increases as you shorten its radiators because of the compensatory increase in the distance between them; or, its shape affects the gain of a rectangle.<sup>2</sup>

<sup>1</sup>Notes appear on [page 45](#).



2. The performance of the rectangle can be derived from both field and transmission-line theory.
3. Resistive loop losses, on the lower HF bands, limit the gain of the antenna. The antenna length at which the gain reaches its maximum can be determined from the formulas found later in the text. This will be useful in designing these antennas for 40-160 meters, where the loop perimeters are large and the wire losses are a major factor affecting their performance.
4. The loop perimeter is predictable. Formulas later in the text enable designers to determine the loop circumference of any rectangle if the frequency and the wire diameter are known.

### Rectangles: An Overview

A rectangle is a four-sided loop that can be fed at any of its sides. This so-called full-wavelength loop can range in shape from that of a folded dipole (FD), where the radiators are almost  $0.5\lambda$  long and are separated by a small fraction of a wavelength, to a transmission line, terminated at both ends, where the radiators are *isotropic hertzian dipoles* (see the “[What is a Hertzian Dipole?](#)” sidebar for an explanation of this term—*Ed*) separated from each other by  $0.5\lambda$ . Lying between these two extremes is the square, with all sides equal in length. The reasons for the existence and popularity of such loop antennas are their increased gain and an increased radiation resistance relative to simple dipole antennas.

The theoretical and unattainable endpoint in gain of such an antenna is the “limit rectangle” with hertzian dipoles separated by  $0.5\lambda$ . As we approach these limit dimensions in the loss-less case, the radiation resistance approaches  $0\ \Omega$ , the current magnitudes approach infinity and the gain approaches a figure slightly in excess of 6 dBi. Since the major focus of this article is on gain, we may note that this limit rectangle can theoretically deliver about 4 dB more gain than a dipole and almost twice the gain of a square loop. Our goal will be to see if we can design antennas for any band that come close to this limit while still being easily fed and having useful bandwidths.

It may seem that throwing a loop together would be a simple exercise, but many of us who have tried to construct simple quads have found it frequently turns out to be the opposite. It is difficult to predict the circumference of a resonant quad loop. We all know that in reality it is somewhat greater than  $1\lambda$  at the operating frequency. How much greater depends on variables that have been discussed by Haviland<sup>3</sup> and Cebik.<sup>4</sup> We shall get into that from a different perspective. We start by examining the performance of the rectangle from the perspective of both field and transmission line theory.

### Theoretical Basis for Rectangle Performance

Jim Lawson, W2PV,<sup>5</sup> derived the properties of the rectangle from field

theory. To summarize his findings, the antenna can be thought of as two truncated dipoles that are separated by a length of transmission line and fed in phase. Fig 2 illustrates how the truncated dipoles— $0.5\lambda$  dipoles that have a short radiator with folded end wires—are joined to form a rectangle. The antenna can be imagined in this way, or as two short radiators connected together by a transmission line at their ends. The square is a special case, being equilateral and having, a set of  $0.25\lambda$  radiators and an equal sized set of transmission-line wires.

Fig 3 describes the direction of the antenna currents. Notice that in this horizontally polarized example, the radiator currents are co-directional. They are also in phase and equal in magnitude. This results in far-field, broadside gain analogous to that of two “stacked” dipoles, fed in phase and separated by a distance equal to that between the rectangle’s radiators. The currents along the vertical connecting wires are anti-phase and their radiation cancels in the broadside direction.

The gain of such an antenna is related to how far apart you can practically space its radiators. The stacking gain of a pair of the rectangle’s truncated radiators, under loss-less conditions, is related to how close you can come to the maximum element separation of  $0.5\lambda$ . We will get into this later under “[A Dipole Model of Loop Antennas.](#)”

### Radiation Resistance (Radiation Induction)

The radiation resistance at a feed

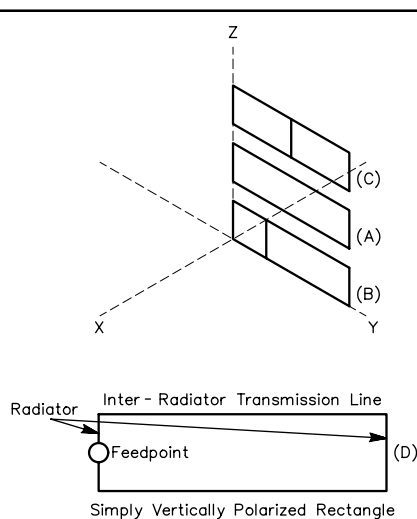


Fig 1—Rectangular-loop antennas: a simple rectangular loop (A), asymmetrical double rectangle (B) and symmetrical double rectangle (C). (D) Shows a vertically polarized loop.

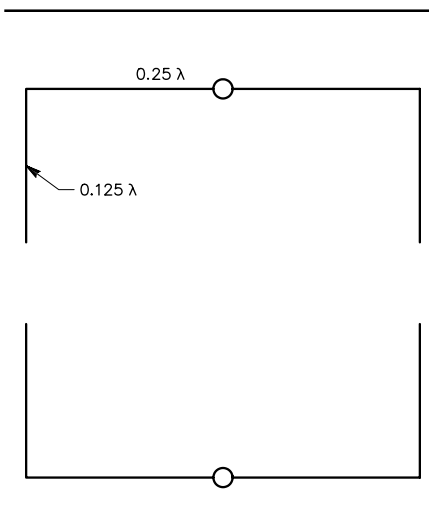


Fig 2—A square loop composed of two truncated dipoles.

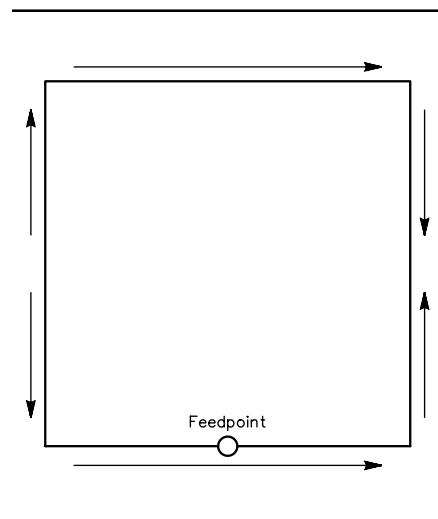


Fig 3—Current directions in a square loop.

point in the center of one of the antenna's sides is a function of the self resistance ( $R_{\text{self}}$ ) of the parallel radiating elements and the mutual resistance ( $R_m$ ) related to the distance separating them. Lawson's calculations for  $R_{\text{self}}$  require modification; they were derived over 25 years ago, before the advent of sophisticated antenna-modeling programs such as *NEC*. In fact, all of the modeling data you see in this article was done with different versions of *NEC-2*.<sup>6</sup> The figures for  $R_m$  and  $X_m$ <sup>7</sup> (mutual reactance) as functions of element separation can be found in many sources: Kraus, Lawson and the *ARRL Antenna Book*.<sup>8</sup> My numbers vary slightly from Lawson's calculations because the radiation resistance of loops varies with wire thickness, and I have no idea what he assumed for this variable.

With extremely thin wires ( $10^{-5}\lambda$  diameter),  $Z_{\text{self}} = 40.2 - j3.5 \Omega$  for each of the two component truncated  $0.25\lambda$  dipoles with folded ends of  $0.125\lambda$ . When these dipoles are joined at the tips of the bent wires to form a rectangle and we feed one port,  $Z_{\text{in}} = 112 - j147 \Omega$ . If we feed two ports, the  $Z_{\text{in}} = 56.2 - j73.7 \Omega$  at each one. The large change in  $X_{\text{in}}$  is related to the proximity of the high-voltage points at each dipole's end. This negative  $X$  is also the reason that, in order to make these antennas resonant, we must increase the loop perimeter beyond  $1\lambda$ .

If we look at the rectangle model solely from the radiation point of view, the feed-point resistance—from FD, to squares, to rectangles with narrow radiators and ending with the  $0.5\lambda$  transmission-line model—is simply:

$$R_{\text{in}} = R11 + R22 + R12 + R21 = 2(R_{\text{self}} + R_m) \quad (\text{Eq 1})$$

In analyzing simple loops of  $1-\lambda$  perimeter, we can think of  $R_{\text{self}}$  and  $R_m$  as sources in the center of each radiator. There is always, nominally,  $0.5\lambda$  of transmission line separating them.<sup>9</sup> Therefore, there is no impedance transformation looking into either end of the transmission line and the  $R_{\text{self}}$ s and the  $R_m$ s are simply in series with each other. For these loops, we may simply neglect the intermediate transmission line connecting the ends of the radiators. A source then sees its own  $R_{\text{self}}$  plus  $R_m$  and those of its twin opposite it. Therefore, with one port fed, the net feed-point resistance is twice their sum.

### Radiation Resistance (Transmission-Line Theory)

Although we can simplistically and accurately use the above analogy, in real life the current and phase relationships are somewhat more complicated. From a transmission-line point of view, we see the following: Because of their co-directional currents, the fed wires are radiating transmission lines that are in phase with each other and exhibit little phase variation along their entire length. If resonant at their central feed points, their end impedances are almost purely resistive. There is a phase inversion of  $180^\circ$  at the current minima or high-voltage points at the midpoint of the  $90^\circ$  interconnecting transmission lines. This, in turn, results in a  $180^\circ$  phase shift along a transmission line of  $90^\circ$  physical length. The result is exactly as above: There is a net  $180^\circ$  phase shift between the radiators that allows each to see the  $R_m$  from its opposite. In a single-port system, the  $R_{\text{in}}$  is somewhat under  $120 \Omega$ .

### Must We Connect the Ends of the Truncated Dipoles?

The answer is “yes” and “no.” “Yes” if we feed one port and “no” if we feed both in phase. If we feed both ports and open the vertical transmission lines at the current nulls/voltage maxima at their midpoints, the  $Z_{\text{in}}$  at either port remains unchanged. However, if we feed only one port and interrupt the conductive pathway at the center of the transmission line, we see a significant change in the feed-point impedance to  $Z_{\text{in}} = 99.4 + j54 \Omega$ . In addition to this, the gain drops dramatically.

Because of the interruption of the conductive pathway in the one-port system and alteration of the impedance to differential-mode currents, we observe the following: The currents along the two radiators become anti-directional and their magnitudes and phases along the parasitic element are significantly different from that of the driven. The conclusion is that the continuity of the transmission lines is necessary if you feed only one port to maintain the proper current relationships among the two elements. This cannot be attained by parasitic mutual coupling alone.

The “non-radiating” transmission-line wires separating the radiators in a rectangle serve three functions. They complete the dipole radiator in order to maintain resonance as the radiator size changes. They maintain the currents

oppositely directed along the transmission line wires between the radiators at a net phase shift of close to  $180^\circ$  and provide the radiators with currents that are co-directional and in phase. These wires do radiate but, since their currents are out of phase, their radiation cancels—for the most part.

### Practical Examples

As examples, let us examine three types of rectangles: the FD, the square and a tall narrow rectangle. The folded dipole consists of two parallel, nominally  $0.5-\lambda$ , rods separated by a small distance and shorted at their ends. The center of one of the rods is fed. Let us assume that the  $R_{\text{self}}$  of such rods is  $72 \Omega$ . If we look up the numbers, we find that  $R_m$  for  $0.5-\lambda$  rod elements, at such narrow separations, is also about  $72 \Omega$ . Therefore  $R_{\text{in}} = 2(72 + 72) = 288 \Omega$ .

A square has approximately  $0.25-\lambda$  truncated radiators separated by approximately  $0.25\lambda$ . This is never true because the actual perimeter of such an antenna is always greater than  $1\lambda$ ; but, assuming  $0.25\lambda$  per side, we can look up or calculate (after Lawson) that the  $R_{\text{self}}$  of such a radiator is about  $40 \Omega$ .  $R_m$  for  $0.5-\lambda$  dipoles separated by  $0.25\lambda$  is about  $40 \Omega$  also, but we are not dealing with full-sized dipoles, and this serves as an introduction to a concept that is critical in analyzing rectangles with even shorter radiators. *The  $R_m$  of a truncated element is proportional to its degree of shortening with respect to  $0.5\lambda$ .* Simply put,  $R_m(\text{truncated}) = \text{truncated dipole length in } \lambda / 0.5\lambda \times R_m(0.5\lambda)$ . Going back to the analysis of the square, we find that  $R_m(0.25\lambda) = 20$ . Therefore  $R_{\text{in}} = 2(40+20) = 120 \Omega$ .

Now for a tall, narrow rectangle with relatively short radiators: Let us assume a radiator width of  $0.15\lambda$  and a height of  $0.35\lambda$ . Lawson's numbers indicate that  $R_{\text{self}} = 16.3$  and  $R_m = 4.5 \Omega$  for each dipole.  $R_{\text{in}}$  therefore calculates out as  $41.6 \Omega$ . The *NEC* model that I used gave a result of  $36.7 \Omega$ .

### Dimensional Characteristics of Rectangles

Before going further, let's define some terms. The radiators in a rectangular antenna can be either horizontal or vertical. In free space, without the effects of ground, the antennas perform identically; however, confusion can result since the radiators can have a width dimension when horizontal and a height when vertical. The shape of the same antenna can therefore be characterized by a height-to-

width ratio in the first case and a length-to-height ratio in the second. I will try to make the orientation of any antenna we discuss explicitly clear.

### Rectangle's Parameters and Radiator Separation

Figs 4 through 6 show what happens to the impedance, free-space gain, loop size and currents of a rectangle as its length or inter-radiator distance is varied from that of a "near" folded dipole to a shorted  $0.5\lambda$  transmission line. In the model for these graphs, I have used *loss-less wires of #100 AWG* at 3.5 MHz. These were chosen to minimize the wire-thickness variable that, with loops, increases the loop size as the wire diameter increases. Also, the loss-less conditions enable us to see what I call the *potential gain* of the antenna would be at extreme dimensions when the radiator dimensions approach those of a hertzian dipole and the length between them

approaches  $0.5\lambda$ . As we will see later, in the real world, losses overcome the gains long before this extreme condition is reached. For reference,  $1\lambda$  at 3.5 MHz is about 281 feet and  $0.5\lambda$  is about 140.5 ft.

Fig 4 shows us that the radiation resistance of a resonant antenna falls sigmoidally—that is, in the shape of a "S"—if you look at the curve over the full range of antenna lengths. The gain increases sigmoidally over the same range as we go from the folded dipole to the square and then to the transmission-line model. The antenna currents increase exponentially and inversely with the radiation resistance as shown in Fig 5. The loop size, as seen in Fig 6, is a parabolic function. At one extreme, the folded dipole is somewhat under  $1\lambda$  in circumference. At the other extreme, the transmission-line model is exactly  $1\lambda$  in circumference. An antenna that is 26 feet or  $0.09\lambda$  long at 3.5 MHz also

has a loop circumference of exactly  $1\lambda$ . The peak circumference is reached at around 80 feet ( $0.28\lambda$ ) of length or radiator separation. Therefore, a  $1\lambda$  loop is actually  $1\lambda$  only when the radiators are separated by either  $0.09\lambda$  or  $0.5\lambda$ . These curves are replicable at all frequencies. In later approximations, I found it convenient to use  $0.1\lambda$  and  $0.5\lambda$  as the end or  $1\lambda$  loop perimeter limits and  $0.3\lambda$  as the loop perimeter maximum. Why is there such a large variation in loop perimeter?

### A Dipole Model of Loop Antennas

Darrel Emerson, AA7FV,<sup>10</sup> suggested that a rectangular loop could be modeled as two dipoles, fed in phase and exhibiting broadside gain. We have already seen that the rectangle can be envisioned (Fig 2) as two truncated dipoles of  $0.5\lambda$  length overall that are folded at the ends. Longer rectangles shorten the radiator and lengthen the folded or loading sec-

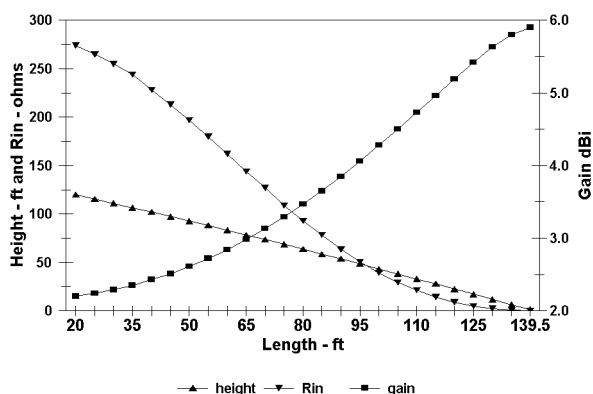


Fig 4—Relationships between height, impedance and gain in rectangles of #100 AWG *loss-less* wire at 3.5 MHz.

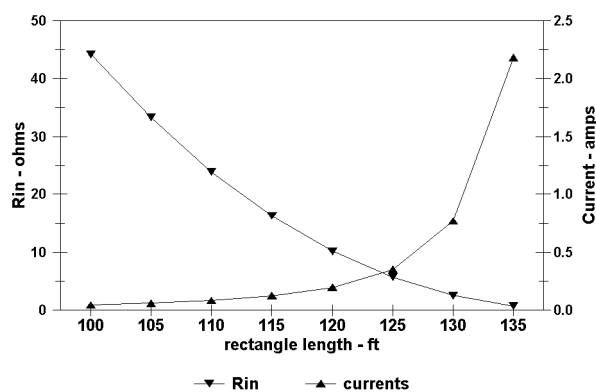


Fig 5—Relationships between impedance and current in rectangles of #100 AWG *loss-less* wire at 3.5 MHz.

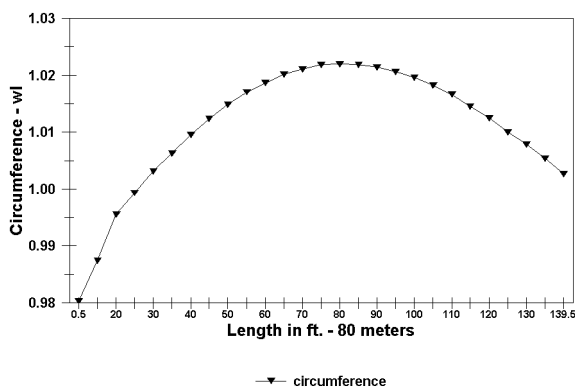


Fig 6—Variations in resonant loop circumference with rectangle shape ("Length" is width of rectangle).

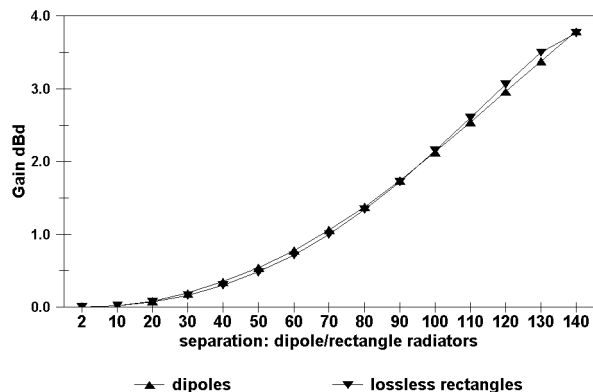


Fig 7—A gain comparison of loss-less rectangles to stacked, in-phase dipoles.

tions. The mutual impedances between the radiators affect their size at resonance, feed resistance and gain of the array. As you may notice in Fig 7, the dipole array and the *loss-less* loop have virtually identical gains, when at the same radiator separation (in feet). Interestingly, under *loss-less* conditions, the gain of a loop with hertzian-dipole radiators approaches that of two full-sized dipoles separated by  $0.5\lambda$ .

Fig 8 shows changes in reactance in the two-element dipole model compared with loop size in the rectangle model. The models show complementary points at  $0.09\lambda$  radiator separation where the phased dipole reactance is zero and the rectangle's loop size is exactly  $1\lambda$ .

Further along, there is more of a disparity in the curves since the mutual reactances are clearly different. The combined variation of  $X_m$  with element spacing and with radiator shortening results in the loop perimeter circumscribing a parabola as a function of radiator spacing over the gamut of rectangular shapes, from folded dipole to transmission line. Because of the highly inductive  $X_m$  at very narrow radiator separations, the folded-dipole variant of the rectangle has the smallest loop perimeter of the genre, going below  $1\lambda$ .<sup>11</sup>

In analyzing the data that provide the basis for the curves, I have concluded that the *single most important variable, as manifested in loop size, impedance and gain, is the distance separating the radiators of the rectangle.*

#### Shape Factor or Aspect Ratio

Two-dimensional ratios have been

used to describe the shape of rectangular antennas. Remember that the rectangle is a resonant loop antenna and the height must vary inversely with length to maintain resonance. Given an infinite number of possible resonant lengths and heights, it has been found that, assuming vertical polarization, the gain of a rectangle peaks at a specific length and associated height. Cebik has found  $L/H$  (length/height) ratio useful in predicting the dimensions associated with peak gain, for a given wire size. Haviland uses the term "shape factor" similarly.<sup>12</sup> For example, Cebik's  $L/H$  for a rectangle constructed #12 AWG wire is:<sup>13</sup>

$$\frac{L}{H} = \log(100f_{\text{MHz}}) \quad (\text{Eq 2})$$

On 80 meters, this is a rectangle with an  $L/H$  ratio of about 3.7 having a gain of 4.30 dBi. Note that this ratio varies with frequency and calculates out as 4.87 on 10 meters for an antenna having a gain of about 4.90 dBi. Haviland's shape factor is:

$$SF = \frac{2\text{Length}}{\text{Circumference}} \quad (\text{Eq 3})$$

where the length is the inter-radiator distance.

Since, as we have discussed earlier, the dimensions of rectangular loops may be characterized by different terms such as length, height and width depending on the polarization, another term must be used in place of the  $L/H$  ratio to denote the ratio between the long and short sides. The term *shape factor (SF)* has also been used by Cebik in this sense, but it is different from that used by Haviland. In order to eliminate this confusion I think it useful to find a substitute term for  $L/H$  ratio and *SF*. This term

is aspect ratio (*AR*), which may be familiar from television, where it characterizes the width/height ratio of a picture. For our purposes, I shall define it as the inter-radiator (long) dimension/radiator size (short). It doesn't matter how this concept is characterized, save for the fact that it illustrates the extreme changes in the shape of rectangular loops as the distance between radiators changes. The *AR* is zero in the case of the folded dipole, 1 for the square and infinite for the transmission-line model. The corresponding *SFs* are 0, 0.5 and 1, respectively.<sup>14</sup>

Having written that, *the AR is not a primary characteristic of a loop antenna. That one is loop size, which we have already seen, is dependent on the length of the antenna between radiators. The AR or the SF is simply a statistic that is derived from the loop size.* If one knows the length between radiators and can calculate the loop size, then the radiator size is simply a matter of subtraction. The formula for calculating loop circumference at any length between  $0.09$  and  $0.5\lambda$  for an extremely thin #100 AWG wire loop is:

$$\text{Circumference}(\#100\text{AWG}) = 1.021970 - 0.529\Delta L^2 \quad (\text{Eq 4})$$

where  $\Delta L = \text{Length}(\lambda) - 0.2961$

With this equation, you can determine the smallest possible loop size as a baseline. Note the correspondence between the modeled data and the calculated data in Fig 9. Given any length in this range and knowing the loop circumference the radiator size may be calculated by:

$$\text{Radiator size} = \frac{\text{Circumference}}{2 - \text{Length}} \quad (\text{Eq 5})$$

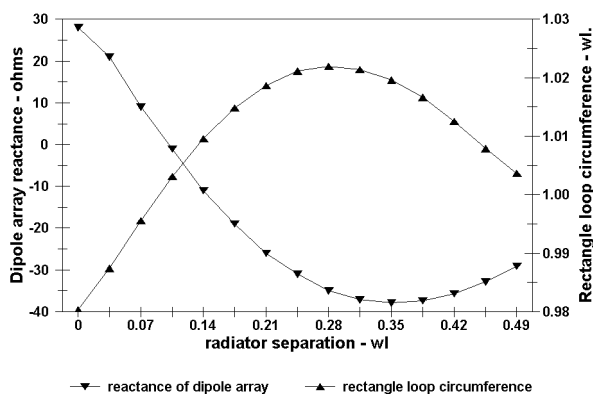


Fig 8—A comparison of reactance and loop circumference between rectangles and dipole arrays.

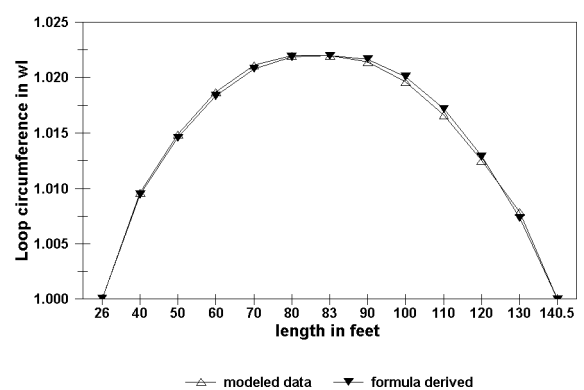


Fig 9—A comparison of modeled and calculated data for rectangles of #100 AWG *loss-less* wire at 3.5 MHz.



## Losses

Power loss is the limiting factor in the performance of high-gain rectangles on the lower HF bands. In square loops, gains with #10 or #20 (AWG) wire are within 0.2 dB of each other,<sup>15</sup> but a square's gain is not close to that of a maximum-gain rectangle and neither are its losses. Loss is not an issue in high-gain rectangles above 10 MHz, but it is the gain-limiting factor from 1.8-7 MHz. Three variables are associated with  $I^2R$  losses: wire resistivity, the length of wire in the antenna and the antenna current.<sup>16</sup>

Two questions arise: Why does gain peak at a specific AR, and why does the AR yielding peak gain change with frequency? For example, we know that the gain of a loss-less rectangle increases with length until the "limit" conditions are reached: length of  $0.5\lambda$ , height of zero, impedance of zero and currents of infinity (see Figs 4 and 5).

I noticed that the maximum gain curve shifts to peak at a lesser length when you introduce losses into a loop. Fig 10 compares the gain curves of 80-meter rectangles with slight resistivity against loss-less ones. It shows that an increase in resistivity (from  $10^{-20}$  to  $10^{-10}$ ) and the consequent increase in losses shifts the length at maximum gain from 140 feet or  $0.5\lambda$  to less than 130 feet or  $0.46\lambda$ . This was confirmed when I modeled rectangles on 80 meters with #10 and #6 (AWG) wire as shown in Fig 11. The latter has 2.5 times the cross-sectional area of the former and 40% of the dc resistance. The gain peak<sup>17</sup> occurs with a shorter (114-foot) antenna in the case of #10 AWG wire compared to 118 feet for the antenna constructed from #6 AWG wire.

The peak gain over a range of lengths is therefore a trade-off between the increasing potential gains—as the length increases—and the more rapidly increasing losses.<sup>18</sup> You can use a longer rectangle if you can reduce the resistive losses by decreasing the resistivity of the wire or by making it thicker. Efforts to reduce resistivity, such as substituting silver wire for copper, are too costly to be practical. It is comparatively easy, however, to do something detrimental, such as using aluminum or phosphor bronze conductors. (We will get into this shortly.) In the real world, the best option is to use a thicker conductor.<sup>19</sup> Nonetheless, I believe that we have reached the limit on 80 meters by using over 280 feet of

#6 AWG wire. So, the practical limit for the size of a rectangle on 80 meters is an inter-radiator length of slightly less than 120 feet or  $0.43\lambda$ . Notice also that the feedpoint resistance of a 120-foot antenna is about  $10\ \Omega$ .

Now why should the AR, using Cebik's formula, increase with frequency? Using 10 meters as an example,  $\lambda$  there is  $1/8$  as long as on 80 meters. A 10-meter loop made of #10 AWG wire therefore has  $1/8$  as

much dc resistance as does one for 80 meters. This enables a shift of the maximum-gain point to a longer antenna (in wavelengths) with a much higher AR. Fig 12 illustrates how the AR of peak gain changes with wire size at three frequencies:<sup>20</sup> 3.5, 35 and 350 MHz. On the higher frequencies, much larger wire sizes are practical. That is, we can use large-diameter aluminum tubing. With longer antennas having higher ARs, however, we

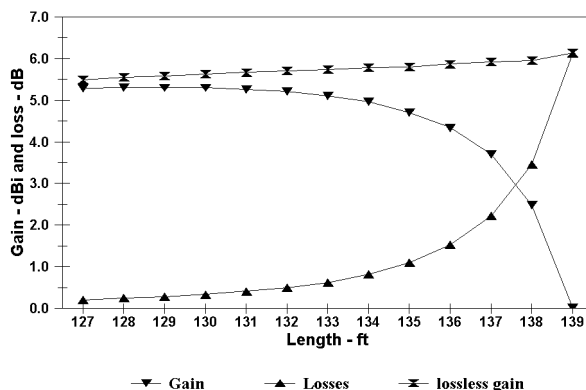


Fig 10—Plot of gains and wire losses against rectangle shape ("Length" is width of rectangle) for lossy wire ( $1 \times 10^{-10}\ \Omega/\text{meter}$ ).

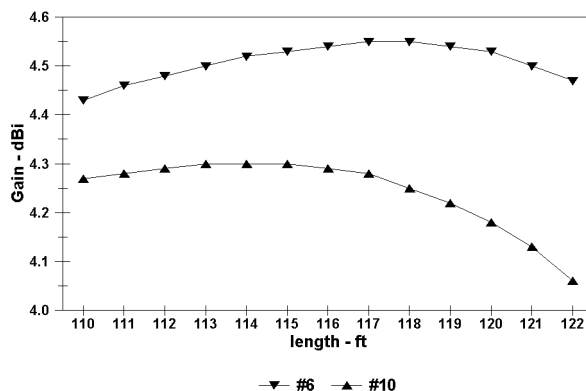


Fig 11—A comparison of gain against shape for rectangles of #6 and #10 AWG copper wire at 3.5 MHz.

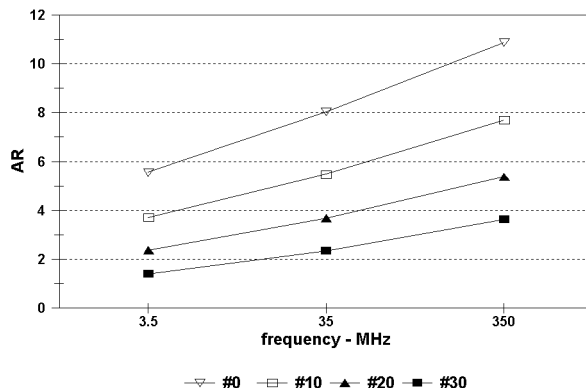


Fig 12—A plot of aspect ratio (width/height) versus frequency for rectangles of AWG #0, #10, #20 and #30 wire.

may easily overlook the fact that the feedpoint resistance is well below 10 Ω. Nonetheless, the gains are substantially higher when the losses are reduced.

### Resistivity

The gains of wire-loop antennas on the lower HF bands are loss-limited. As their lengths approach those with the greatest potential gains, losses increase more rapidly,<sup>21</sup> offsetting any gain increase. This happens because the radiators shorten as the antenna length increases, and this is associated with an exponential decrease of the feedpoint resistances and an exponential increase in currents (see Figs 4 and 5).

As I have mentioned, the wire resistance of a loop appears to limit how far apart one can space the rectangle's radiators—and thus, the gain. Wire resistance is a product of the wire resistivity ( $\rho$ ) and its diameter—or more exactly, its cross-sectional area. As an example, aluminum tubing (say 6061, T6 alloy) has a resistivity 2.8 times that of copper. For aluminum and copper wires of the same diameter, the aluminum wire's dc resistance per unit length is 2.8 times that of the copper wire.

### Skin Effect

At radio frequencies of 1 MHz or higher, another factor affects wire resistance and losses. This is the skin effect, which is the result of the fact that only a thin shell of the outer part of the wire effectively conducts RF. In essence, a solid conductor effectively becomes a hollow cylinder. The skin effect is inversely proportional to the square root of the frequency so that the skin depth is smaller the higher the frequency.

Antenna modeling programs such as *NEC* and *MININEC* account for skin effect when calculating antenna gain and losses. It is one purpose of this article to find appropriate correlating parameters that one may use to predict the losses. Some factors that we can use as correlates of antenna length at peak gain are the dc loop resistance and the RF loop resistance. To this end, let us first examine dc wire resistance.

### Calculation of DC Wire Resistance

$$R = \rho \frac{L}{A} \quad (\text{Eq 6})$$

where  $\rho$  is the resistivity of the wire material,  $L$  is the length of wire and  $A$

is the cross-sectional area of that wire. Resistivity is expressed in ohm-lengths. For copper wire, of the alloy used most commonly in household wiring, it is  $1.77 \times 10^{-8}$  ohm-meters or  $5.66 \times 10^{-8}$  ohm-feet. For 6061-T6 aluminum, it is  $4.1 \times 10^{-8}$  ohm-meters or  $1.345 \times 10^{-7}$  ohm-feet; for phosphor-bronze, it is  $1.1 \times 10^{-7}$  and  $3.61 \times 10^{-7}$ , respectively. The difference in resistivity/unit length is a function of the ratios between the cross-sectional areas of square meters to square feet. Please remember that you must be consistent; if you are calculating  $R/\text{foot}$  then you must use resistivity in ohm-feet, length in feet and wire area in square feet.<sup>22</sup>

Let us compare the dc loop resistances of two antennas, each at an optimum length for peak gain: one, an 80-meter rectangle of #10 AWG wire and the other, a 10-meter rectangle of 1-inch-diameter aluminum tubing. The 80-meter antenna's resistance/ $\lambda$  ( $R/\lambda$ ) is easy to calculate because you can look up the wire resistance/foot in the wire tables:  $R/\text{foot} = 0.001 \Omega$ .

If you want to calculate the wire resistance: #10 AWG wire diameter  $D \approx 0.1$  inches or, more accurately, 0.00849 feet. The cross-sectional area  $A = \pi (D/2)^2$  or  $5.66 \times 10^{-5}$  square feet;  $R/\text{foot} = \rho(\text{ohms-feet}) \times 1(\text{foot})/A$  (square feet) or  $5.66 \times 10^{-8} \times 1/5.66 \times 10^{-5} = 10^{-3} = 0.001 \Omega$ —the same as in the lookup table. At 3.5 MHz,  $\lambda \approx 281$  feet, so  $R/\lambda = 281 \text{ ft}/l \times 0.001 \Omega/\text{ft} = 0.281 \Omega/\lambda$ .

For the 10-meter antenna: wire  $D = 1$  inch or 0.0833 feet;  $A = 5.45 \times 10^{-3}$  square feet;  $R/\text{ft} = \rho \times 1/A$  or  $1.345 \times 10^{-7}/5.45 \times 10^{-3}$  or about  $2.5 \times 10^{-5} \Omega$ . At 28.5 MHz,  $\lambda = 34.53$  feet, so  $R/\lambda = 34.53 \times 2.5 \times 10^{-5} = 8.6 \times 10^{-4} \Omega/\lambda$ . The disparity in dc loop resistance between

the two antennas is a factor of 327 (0.281/0.00086).

### Calculation of RF Resistance

The skin effect reduces this disparity in dc loop resistance. The formula for skin depth is:<sup>23</sup>

$$\delta = \frac{1}{\sqrt{\pi f \mu \sigma}} \quad (\text{Eq 7})$$

where  $f$  is the frequency in Hertz,  $\delta$  is the skin depth,  $\mu$  is the permeability of free space or  $4\pi \times 10^{-7}$  and  $\sigma$  is the conductivity of the wire or  $1/\text{resistivity}$ .

The skin depth of the hollow cylinder is the effective conducting area and this is calculated by:

$$\text{Area} = \text{Circumference} \times \text{SkinDepth} = A = 2\pi R\delta \quad (\text{Eq 7A})$$

The RF resistance is calculated as in the section above by using this area in the denominator of the resistance-resistivity equation (Eq 6).

The result of this effect is that over the same range of wires as above, #10 AWG copper wire at 3.5 MHz to 1-inch-diameter aluminum tubing at 28.5 MHz, the range of RF resistance overall is only about 18:1.<sup>24</sup> Also, because of the cylindrical effect, the *RF resistance is proportional to the circumference* and not to the area of the wire (as with dc resistance).

The relationship between dc and RF resistance over the range of wire sizes we are using is shown in Fig 13. The wire sizes are multiples of the diameter of #10 AWG wire, which is 0.00849 feet or about 0.1 inches. The modeling was at 3.5 MHz with copper wire, but the RF resistance of the wire at a point corresponding to 20x on the X-axis is the normalized resistance of 1-inch-diameter aluminum tubing at 10 meters.

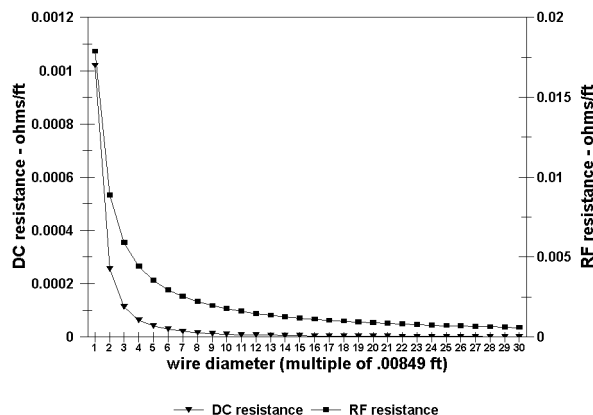


Fig 13—DC and RF resistances of various sizes of copper wire.

Because the modeled gains over any range of rectangle lengths have already accounted for skin depth, what we must find is an appropriate parameter that we can use to make predictions of the optimum lengths. Although we could use RF resistance and its correlates, the radius, diameter or circumference, I shall be using dc resistance and wire area since these are more easily calculated or looked up.

More exactly, the parameter on which the calculations in the section below are based is the *dc resistance of a 1-λ loop or  $R_{\lambda}$* , since this will account for frequency. It is also easier to use than the actual loop size, since, as we will see in the section entitled “[Loop Size and Wire Diameter](#),” the loop size will vary with both antenna length and wire diameter.

### Effect of Wire Resistance on the Optimum Size of the Rectangle

Table 1 shows how the reduced losses on 10 meters permit a longer antenna (in terms of wavelength) than on 80 meters (0.47λ versus 0.41λ), with a significantly higher realizable gain—if you can match the 1-Ω feed-point resis-

tance. It also summarizes the dimensions over the HF spectrum at which peak gains are attained. These are all vertically polarized models in free space, characterized by radiator height and inter-radiator length.

Clearly, by 10 MHz, the losses are not the limiting factor for rectangles. You can stretch the shape of even thin wire antennas to a point where the feedpoint resistance becomes low enough to make feeding them difficult. By the time you get to 10 meters and higher, losses are not a factor, and the only limit is the  $R_{in}$  that you can handle. The other limit on how far you would want to stretch a rectangle is bandwidth, which we will discuss later.

### Calculation of Length at Optimum Gain

It is important, especially on the low bands with large loops, thin wire and high loop resistance, to be able to predict the optimum length at which gain will peak. I have compared the lengths at peak gain with both the RF and dc resistance to show that either would be useful as a predictive variable. Fig 14 illustrates the relationship between

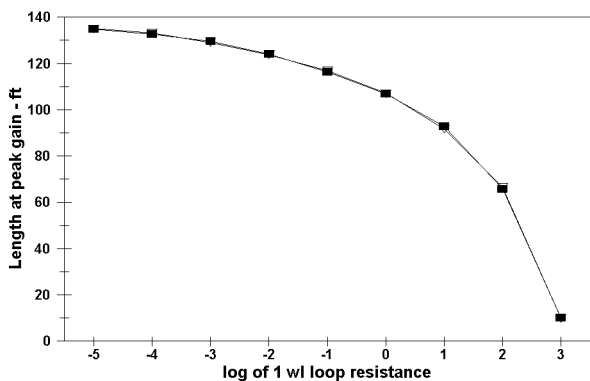
antenna length at peak gain versus the 1-λ loop dc resistance.<sup>25</sup> Figs 15, 16 and 17 show the relationships between gains, RF resistances, lengths at peak gain and losses with wire diameter (copper wire), which is a parameter of the RF resistance. Remember that the wire diameter multiple corresponding to 1-inch-diameter aluminum alloy tubing on 10 meters is 20 on the X-axis.

Fig 15 shows the relationship between the length at peak gain and the gain with the wire diameter. The gain and the length at peak gain vary similarly. Fig 16 shows you what happens to length at peak gain and the RF resistance with changes in the wire diameter. These also appear to be very similar but inverse functions. Next, Fig 17 is the relationship between gains and losses as a function of wire diameter. Again, there is a very similar but inverse relationship.

The curves for length versus the logarithm of dc loop resistance (Fig 14) and length versus wire diameter (Fig 15) appear to be similar. The equation for the curve in Fig 14 turns out to be a fifth-order polynomial<sup>26</sup> as you will see just below. The dc-resistance limits in Fig 14 correspond to a range of 10<sup>-5</sup> to

**Table 1 —Comparison of rectangles: lengths at peak gain over the HF bands**

frequency (MHz)	Wire Size	Length (ft)	Height (ft)	$R^{in}$ -ohms	Gain (dBi)	Loss (dB)	AR	Length (λ)
1.8	#10 Cu	210	72.1	30.5	4.10	0.58	2.91	0.384
3.5		115	29.8	18.5	4.30	0.66	3.86	0.409
7		58	14.5	17.2	4.54	0.51	4.00	0.413
10		41	9.78	15.7	4.63	0.47	4.19	0.417
14		29.8	6.45	13.1	4.73	0.46	4.62	0.424
21		20	4.3	12.2	4.83	0.41	4.65	0.427
28	1" Al	15.1	3.06	11.4	4.90	0.38	4.93	0.430
28		16.4	1.03	1.25	5.50	0.05	15.92	0.467



**Fig 14—Effects of dc resistance (in a 1λ circumference) on rectangle shape that yields maximum gain (“Length” is width of rectangle or inter-radiator distance).**

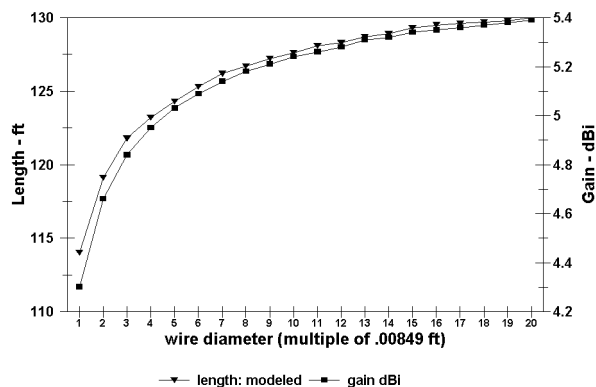


**Fig 15—The relationships of rectangle shape and maximum gain to wire diameter.**

$10^3 \Omega$ . That is far greater than the range of 327:1 ( $8.6 \times 10^{-4} - 2.8 \times 10^{-1} \Omega$ ) bounded by the #10 AWG copper antenna on 80 meters and the 1-inch-diameter aluminum antenna on 10 meters. I feel that, by extending the range, you can get a better idea of the effects of resistance on loop length.

A very close approximation of the ideal length of a rectangle can be made if you know the total dc resistance/ $\lambda$ .<sup>27</sup>  $X$  is the multiple of 0.00849 feet or the diameter of #10 AWG wire. These multiples are for copper wire at 3.5 MHz, but you can do what I did for 1-inch-diameter aluminum at 28.5 MHz. Simply determine the skin depth from the formula in the text, determine the conductive area from the next formula and use that area in the in the resistivity formula to give you the ohms/foot. Then determine the wire diameter from the copper wire tables that corresponds to that wire resistance. You now must determine the ratio of that wire diameter to that of #10 AWG wire and use that number as  $X$  in the formula above. Once you get the length, divide it by 281 to determine the length in terms of wavelength. Now, extrapolate the length to any band. The equation uses the log of the dc  $1-\lambda$  loop resistance or  $\log(R_\lambda)$ :

$$\begin{aligned} \text{Length at peak gain} = & 106.851 - 11.009\log(R_\lambda) - 2.07145\log(R_\lambda)^2 \\ & - 0.79807\log(R_\lambda)^3 - 0.2261\log(R_\lambda)^4 - 0.0213\log(R_\lambda)^5 \end{aligned} \quad (\text{Eq 8})$$

The formula gives the length in feet for 80 meters. You can extrapolate to any other band simply by dividing the length by the wavelength, 281.143 feet at 3.5 MHz. These gain peaks are for a range of lengths—on 80 meters—with a tolerance of about  $\pm 1$  foot. You need not be exact.

Look carefully again at Fig 14. You see only one curve, but there are really two. The curves for the modeled data and that calculated from the formula above are so close as to be one.

Given the resistivity of wire you may want to use—be it phosphor bronze at the seashore or aluminum fence wire—and its diameter you can calculate the resistance of one wavelength from the formula for dc wire resistance in the earlier section. Then calculate the optimum length of the rectangle from the formula immediately above or from Figs 14 or 15.

### Loop Size and Wire Diameter

As we mentioned earlier, the loop sizes we have been discussing at various lengths were predicated on using #100 AWG wire at 3.5 MHz to eliminate confusion caused by the effects of wire diameter. As we have seen, loop antennas have larger perimeters as the wire  $D/\lambda$  increases. For example a #10 AWG wire on 80 meters has about the same  $D/\lambda$  as a #30 AWG wire has on 10 meters. Using #10 AWG wire at 28 MHz will require a substantially larger loop (in wavelengths) than on 3.5 MHz.

Fig 18 gives you an idea of how loop size varies with wire  $D/\lambda$  over a range that is defined by the smallest practical wire to the largest, over about an 8:1 range of wavelengths (see below). I modeled the entire range on 80 meters, but the loop circumferences in wavelengths are applicable to any other band. There is certainly a very large variation in loop size as the  $D/\lambda$  is varied (the actual variable used for the X-axis of Fig 18 is  $\log(D/\lambda)$ ). The curves are a family of parabolas.

### Calculation of Loop Circumference

Fig 18 was generated with the formulas below. The curve corresponding to  $\log(D/\lambda) = -8$  is that of #100 AWG wire on 80 meters.

$$\text{Loop Circumference}(\lambda) \text{ or } C_\lambda = C_{\max} - k(\Delta L)^2 \quad (\text{Eq 9})$$

where  $\Delta L = \text{length}(\lambda) - 0.2846$

The 0.2846 corresponds to the length ( $\lambda$ ) at the peak loop size (80 feet at 3.5 MHz.).

$C_{\max}$  is the loop circumference maximum (occurring at a

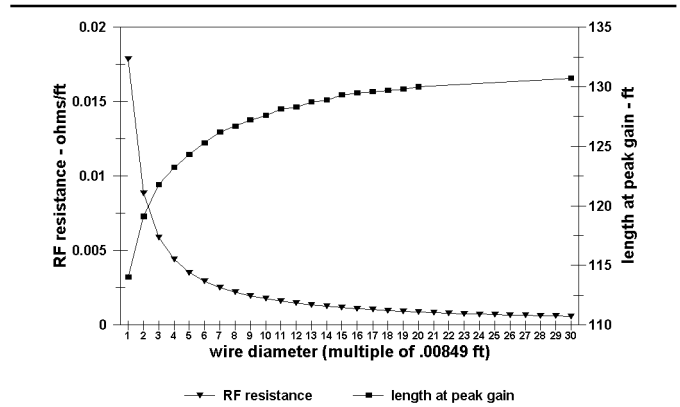


Fig 16—RF wire resistance and rectangle shape at maximum gain plotted against wire diameter.

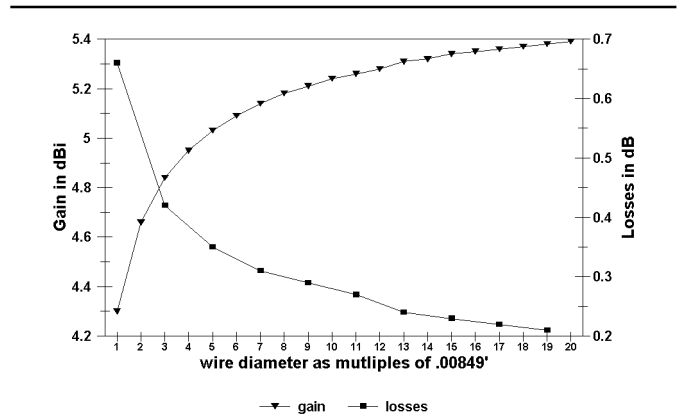


Fig 17—The influence of wire size on rectangle gains and losses.

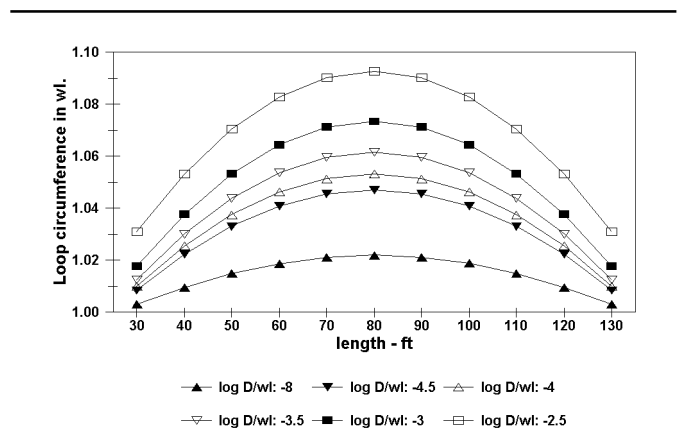


Fig 18—Effects of wire diameter ( $\log(D/\text{wavelength})$ ) and rectangle shape on resonant loop circumference.



length of  $0.2846\lambda$ ). This varies with wire thickness and  $\lambda$  or  $\log(D/\lambda)$  and is calculated by the formulas below:

$$\text{Log}\left(\frac{D}{\lambda}\right) - 4.5 \text{ to } -4 : C_{\max} = 1.1033 \cdot 1.0117^{\log\left(\frac{D}{\lambda}\right)} \quad (\text{Eq 10A})$$

$$\text{Log}\left(\frac{D}{\lambda}\right) - 4 \text{ to } -3.5 : C_{\max} = 1.1228 \cdot 1.0161^{\log\left(\frac{D}{\lambda}\right)} \quad (\text{Eq 10B})$$

$$\text{Log}\left(\frac{D}{\lambda}\right) - 3.5 \text{ to } -3 : C_{\max} = 1.1471 \cdot 1.0224^{\log\left(\frac{D}{\lambda}\right)} \quad (\text{Eq 10C})$$

$$\text{Log}\left(\frac{D}{\lambda}\right) - 3 \text{ to } -2.5 : C_{\max} = 1.1944 \cdot 1.0362^{\log\left(\frac{D}{\lambda}\right)} \quad (\text{Eq 10D})$$

$k$  = parabolic coefficient, which determines the loop-size minima at lengths of  $0.1067\lambda$  and  $0.4624\lambda$  (30 and 130 feet at 3.5 MHz).<sup>28</sup> " $k$ " varies with  $\log(D/\lambda)$  also:

$$\text{Log}\left(\frac{D}{\lambda}\right) - 4.5 \text{ to } -4 : k = 3.3595 \cdot 1.2523^{\log\left(\frac{D}{\lambda}\right)} \quad (\text{Eq 11A})$$

$$\text{Log}\left(\frac{D}{\lambda}\right) - 4 \text{ to } -3.5 : k = 3.804 \cdot 1.2919^{\log\left(\frac{D}{\lambda}\right)} \quad (\text{Eq 11B})$$

$$\text{Log}\left(\frac{D}{\lambda}\right) - 3.5 \text{ to } -3 : k = 3.7997 \cdot 1.2914^{\log\left(\frac{D}{\lambda}\right)} \quad (\text{Eq 11C})$$

$$\text{Log}\left(\frac{D}{\lambda}\right) - 3 \text{ to } -2.5 : k = 3.3222 \cdot 1.2224^{\log\left(\frac{D}{\lambda}\right)} \quad (\text{Eq 11D})$$

As examples of the range of  $D/\lambda$  used in the curves, lets look at #10 AWG wire on 80 meters and 1-inch-diameter tubing on 10 meters: #10 AWG wire has a  $D = 0.00849$  feet;  $\lambda = 281.143$  feet on 80 meters.  $D/\lambda = 3 \times 10^{-5}$ ;  $\log(D/\lambda) = -4.5$ . This is the thinnest extreme of the range. For 1-inch-diameter tubing,  $D = 0.0833$  feet;  $\lambda = 34.53$  feet at 28.5 MHz;  $D/\lambda = 2.4 \times 10^{-3}$ ;  $\log D/\lambda = -2.6$ . This is the thickest extreme.

With these formulas, you can get a very close approximation of the loop size at any rectangle inter-radiator length, with any wire thickness and at any wavelength in *free space*. The remaining variable relating to loop circumference is the effect of ground, and that is impossible to predetermine. The predicted loop sizes should put you close enough to minimize pruning.<sup>29</sup>

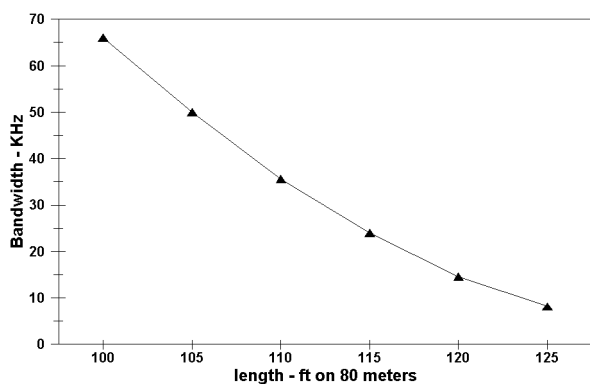


Fig 19—SWR bandwidth for various shapes of loss-less rectangle antennas.

## Bandwidth

In addition to losses, two other disadvantages of simple rectangular loops are related to the rapid decrease of feed resistance and radiator height. These are our ability to match the feed resistance and the Q as reflected by bandwidth where the operating SWR 2 or less.

Let's consider the feed resistance; look again at Table 1. On 10 meters, even with #10 AWG wire, a maximum-gain rectangle with 4.9 dBi of gain has a feed resistance of 11  $\Omega$ . This is probably as low as you can go and still get a relatively low-loss match. It is far better on this band to go with thicker aluminum tubing and a shorter antenna that has a higher feed-point resistance, lower losses and a wider bandwidth as we will see next.

Antennas with the shortest radiators exhibit the highest Q and the narrowest bandwidths. Fig 19 shows the bandwidths of loss-less rectangles and gives you the worst-case scenario since the bandwidth is not inflated by resistive losses.

There is no getting around the fact that a rectangle is a high-Q antenna. The good news is that a bandwidth of 30 kHz<sup>30</sup> for a 115-foot antenna on 80 meters is adequate to cover either the CW or SSB DX windows. There is no way to avoid using a tuner if you want to cover both ends of 80, but the same holds for a dipole or any other gain antenna.<sup>31</sup>

On 10 meters and higher bands, the story is different. We have already noted that the loop dc and RF resistance is significantly lower on this band for antennas constructed with 1-inch-diameter aluminum tubing. The Q (excursions of reactance with frequency) is inversely related to wire diameter/wavelength,<sup>32</sup> so we would expect a greater relative bandwidth on 10 meters, and this is exactly what we get. Fig 20 shows the relationship between bandwidth and the feedpoint resistance<sup>33</sup> as functions of the antenna length. A 13-foot- or  $0.38\lambda$ -long rectangle will have a bandwidth of almost 1 MHz and should be practical with a 40  $\Omega$  feedpoint resistance. Its gain of 4.49 dBi<sup>34</sup> is, however, less than you would get from a Hentenna, which is not much larger and has a greater bandwidth. We will discuss this in a later article about the asymmetrical double rectangle or ADR.

## Pattern Characteristics

The gain of these antennas comes from the narrowing of one of their radiation lobes. In the case of vertically polar-

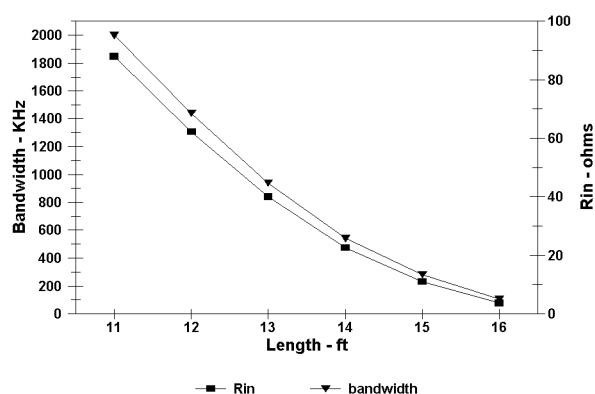


Fig 20—Bandwidth and  $R_{in}$  versus shape for 10-meter rectangles made of 1-inch-diameter aluminum tubing.

ized rectangles, there is a narrowing of their azimuthal beamwidth as their gain increases. For practical antennas in the lower-HF bands (40-160 meters) the beamwidth (-3 dB) is in the 60° range.

The radiation patterns are more advantageous on the higher bands, above 10 MHz.<sup>35</sup> At and above this frequency, horizontally polarized antennas are preferred and their gain comes from elevation-lobe compression. This is a huge advantage because the azimuthal coverage is about 90°, no matter how great the gain. The secondary elevation lobes are attenuated as gain increases, thus reducing high-angle QRM.

### Stretched “Diamond Loops”

It has been said that the diamond quad has the same performance as the square. The diamond is simply a square that has been rotated 90°. The major difference is that the diamond is fed at a corner, while the square is fed in the center of one side.

I will not get into actual numbers here about what happens when you stretch the diamond between a feedpoint and its opposite apex and simultaneously narrow it along the perpendicular axis. In essence, we are turning the diamond into the ARRL emblem. This is analogous to what we have done with rectangles by stretching the distance between the radiators and narrowing the radiators themselves.

To summarize the results, the gain increase is nowhere near that with the rectangles. The feedpoint resistance drops more precipitously and the losses increase more rapidly. The diamond and the square are two different antennas if one looks at their current distributions and the only time they are equal is at the precise point where they are equilateral. The diamond is truly not a square.

### Summary

The rectangle is simple to construct and provides the gain all DXers seek. As its dimensions are changed to increase its gain, however, it becomes loss-limited on the lower HF bands due to increasing resistive losses. This article enables a builder, by accounting for losses, to construct one of optimum gain for a given conductor material and size, while still subject to the constraints of impedance matching. It also provides a means, given the wire diameter and the distance between the antenna’s radiators, to predict the final loop perimeter.

### What is a Hertzian Dipole?

For the purposes of this article, a *hertzian dipole* is defined to be a dipole with extremely short elements. Perhaps the simplest example is a dipole consisting of two charged particles, each in uniform harmonic motion and moving alternately away from and toward each other. As element length is decreased from  $\lambda/4$  toward such a limit, a dipole’s radiation pattern does not change its shape much; its gain does decrease, though, from about 2.2 dBi to about 1.8 dBi.

Since it retains its linear shape, a hertzian dipole does not reach the 0 dBi performance of an isotropic source as one might be tempted to think. A cross-section of its radiation pattern still resembles a doughnut, with nulls along the axis of the dipole and maximum radiation in a plane at right angles to that axis. It thereby exhibits some gain over an isotropic radiator, which evenly illuminates a surrounding sphere. Consult Kraus (see [Note 7](#)) for more detail —*Doug Smith, QEX Editor.*

From the higher-HF bands into the UHF, rectangles with truly high gain are limited by low feedpoint resistance and by narrow bandwidth. These problems can be dealt with by limiting the distance between the radiators and thus reducing their gain slightly. A more elegant solution is available, however, that of tacking on an extra loop. This will be the focus of Part 2: the ADR or asymmetrical double rectangle.

These studies of the rectangle form the basis for studying all the other closed-loop antennas, which behave similarly. In addition to the next article, other articles in this series will show how multiloop antennas can be constructed by joining rectangles and the excellent characteristics rectangle-based antennas have in parasitic arrays. We will also delve into parasitic combinations of multiloop antennas to show how one can construct very high gain three-dimensionally compact arrays.

### Acknowledgements

I am heavily indebted to L. B. Cebik, W4RNL, for his kindness, patience and the inordinate amount of time that he spent in teaching me about antenna modeling and in advising me. I am thankful also to Darrel Emerson, AA7FV, for his advice on the theoretical basis of the rectangle, the “Dipole-Array Analogy” and “Resistivity” sections. I also thank David Jefferies, G6GPR, for giving me a better understanding of how loops perform. Lastly, I am also grateful to Dean Straw, N6BV, for his editorial advice and comments.

### Notes

<sup>1</sup>L. B. Cebik, W4RNL, “SCV’s: A Family Album; Part 1: The Group Picture,” *National Contest Journal*, Sep/Oct 1998, pp 12-16. The rectangle is discussed in Part 3 of the *NCJ* series and at his Web site. The con-

tents of the *NCJ* series and additional information are available at [www.cebik.com/radio.html](http://www.cebik.com/radio.html) under “Self-Contained Vertically Polarized Wire Antennas: A Family Album, Parts 1-5.”

<sup>2</sup>Loops are seldom discussed in terms of “radiators” this way. Current is distributed in a sine wave around a resonant  $1-\lambda$  loop. When a  $1-\lambda$  loop is driven by a low-impedance feed, there will be a current maximum (which is confusingly called a “current loop”) at the feedpoint and  $\lambda/2$  away from the feed point on the opposite side (see [Fig 3](#)). Halfway between these current maxima are current minima, sometimes called “nodes.” Antennas can be modeled and understood by considering them as an assembly of small segments, each segment having a current magnitude and phase. Segments on either side of a current loop are in phase, and segments on either side of a node are of opposite phase. Thus, fields (radiation) from segments surrounding a current loop reinforce each other, while fields from segments surrounding a current node cancel. Consequently a loop’s radiation and polarization are determined by the location of its feedpoint: A loop will be horizontally polarized if fed at the center top or bottom, vertically polarized if fed at center left or right. The author is considering the side containing the feedpoint (and its parallel, opposite side) to be “radiators.” Want a puzzle? Consider a corner-fed loop.—*Ed.*

<sup>3</sup>R. Haviland, “The Quad Antenna Revisited,” *Communications Quarterly*, Summer 1999, p 43.

<sup>4</sup>L. Cebik, “2 Element Quads as a Function of Wire Diameter, Part 3 Fatter Elements from Mere Wire”, *AntenneX* ([www.antennex.com/](http://www.antennex.com/)), Dec 2000.

<sup>5</sup>J. Lawson, W2PV, *Yagi Antenna Design*, (Newington: ARRL, 1980). This book was compiled by the ARRL staff, shortly before Lawson’s death, from a series of articles in *ham radio* magazine. See Chapter 4.

<sup>6</sup>These were initially K6STI’s *NEC/Wires*, and at present *NEC-Win Plus+* from Nittany Scientific, [www.nittany-scientific.com/](http://www.nittany-scientific.com/).

<sup>7</sup>The  $R_m$  function is a decaying sine wave generated by  $\int \frac{\sin(x)}{x}$ .  $X_m$  is a function of  $\int \frac{\cos(x)}{x}$ .

<sup>8</sup>See J. Kraus, *Antennas*, second edition

(New York: McGraw-Hill, 1988), Fig 10-12, p 426; *The ARRL Antenna Book*, 16th edition (Newington: ARRL, 1991), Fig 19, p 8-15; and J. Lawson, W2PV, *Yagi Antenna Design*, Chapter 4, 1982.

- <sup>9</sup>I am indebted to Darrel Emerson, AA7FV for suggesting this approach using transmission-line theory. He also suggested the formula for  $R_{in}$  as a function of  $R_{self}$  and  $R_m$  before I found it in Lawson's book.
- <sup>10</sup>I cannot thank Darrel Emerson enough for indicating some earlier modeling errors and for pointing me in the right direction to find the correct phased-dipole analogies for the entire class of loops.
- <sup>11</sup>My modeling of FDs over a range of rod separations from 0.01 through  $0.1\lambda$  shows that the loop perimeter is strictly a function of  $X_m$ . These are closed rectangular loops and there is no basis for the concept of shortening due to "end effects" as with rod elements.
- <sup>12</sup>See Haviland, Note 6, p 67.
- <sup>13</sup>See Cebik, Note 1, above.
- <sup>14</sup>The shape factor at the gain peak has been known for a while, since Haviland (personal communication) mentions the rectangle called the "skeleton slot" with an SF of 0.8 as the one with most gain. This corresponds perfectly with the AR of 3.7 for a #10 AWG wire antenna whose gain is 4.30 dBi.
- <sup>15</sup>This is a worst-case scenario on 80 meters. The gain/loss of a square of #10 AWG wire (sides of 73.5 feet) is 3.15 dB/0.09 dB. The same for a #20 AWG wire (sides of 73.16 feet) square is 2.95 dB/0.29 dB. Any real difference in performance is more likely to be reflected in bandwidth than in gain. See Haviland, above.
- <sup>16</sup>The fact that wire resistance causes excessive power loss has been known by antenna designers. Brian Beezley, K6STI, in a comment on one of his models included with his *AO MININEC* program states re the rectangle that a large conductor should be used to minimize conductivity losses.
- <sup>17</sup>This is not a sharp peak. *There is always a RANGE of dimensions at peak gain.* For a rectangle constructed of #10 AWG wire the gain peak is  $\pm 1$  foot. Notice that, because of the losses that increase exponentially, the gain drops off more rapidly as the antenna is made longer. There are minuscule gain decrements for shorter antennas. Always err on the short side.
- <sup>18</sup>That is why gain rises slowly and falls rapidly as you approach and then pass the gain peak. The increase in gain with length is a slowly rising function while the increase in losses rises at a much higher exponential rate.
- <sup>19</sup>A thicker conductor, alone, is sufficient to increase gain significantly.
- <sup>20</sup>If you look closely you will see a correspondence in the ARs related to wire gauge and frequency. A rectangle of #10 AWG wire at 3.5 MHz has close to the same overall resistance as one of #20 AWG wire at 35 MHz. Even without accounting for the variable of wire diameter/wavelength, the ARs are reasonably close.
- <sup>21</sup>This is not a problem with squares—see Note 12, above. As Haviland states, p 58 above, #12-14 AWG wire is perfectly fine at HF. Due to the low currents involved, the losses amount to less than 0.1 dB. The major problem with squares appears in arrays. The thin wire significantly reduces the front-to-back ratio bandwidth as compared to Yagis.
- <sup>22</sup>The wire diameters in the tables are in inches—divide that by 12 to get the appropriate diameter in feet, and then calculate the wire area from that. If you calculate R in meters, be aware that the metric wire

tables are in millimeters and the diameters must be converted into meters in order to calculate the wire area.

- <sup>23</sup>Kraus, see Note 8, above, page 426.
- <sup>24</sup>This range also considers that skin depth is greater in materials of greater resistivity. This is the reason that the RF-resistance difference between aluminum and copper is not so great as their resistivities would imply.
- <sup>25</sup>If you want to extrapolate to any other band just divide the length by the 80-meter wavelength (281.143) to get the length in wavelengths.
- <sup>26</sup>Again, I must thank Darrel Emerson, AA7FV. He used a more sophisticated curve-fitting program than mine to fit my data points and generate the formulae I use.
- <sup>27</sup>You can narrow the range to more-practical loop lengths. The curve in Fig 14 can be generated by a sixth-order polynomial function:

$$L = 106.585 + 9.40213 \log(X) - 2.09287(X)^2 + 0.260087 \log(X)^3 - 0.0176426(X)^4 + 6.11288 \times 10^{-4} \log(X)^5 - 8.46216 \times 10^{-6} \log(X)^6$$

- <sup>28</sup>I chose these extremes because: the 30-foot end was very close to 26 feet (0.09 $\lambda$ ), where the loop was expected to be exactly  $1\lambda$  long with an infinitely thin wire. The other point where the loop is expected to be  $1\lambda$  is at a length of  $0.5\lambda$  but, because the radiator height becomes extremely small beyond 130 feet (0.46 $\lambda$ ), modeling errors increase. Besides, no one is ever going to build a rectangle with a length greater than 130 feet. See Table 1 for the 10-meter equivalent.
- <sup>29</sup>There are two other effects of loop size. A larger loop at any given length yields more gain and longer radiators. This in turn increases the feedpoint resistance. See Haviland, above, at pp 58-59. An antenna with a greater diameter/wavelength at any given frequency will potentially have more gain—beyond merely decreasing the losses.
- <sup>30</sup>This is for a lossy antenna of #10 AWG wire.
- <sup>31</sup>Later in this series, I will show that one can construct an antenna that allows for instant change between two resonant frequencies, to QSY over large band segments.
- <sup>32</sup>See Haviland, above, p 59 and Fig 16, where he shows the square's reactive excursions on either side of the design frequency relative to the wire size being used.
- <sup>33</sup>There is an almost direct correspondence between the feedpoint resistance and the bandwidth of loop antennas. We will examine this in more detail later in this series with the asymmetrical double rectangle.
- <sup>34</sup>Although I do not find this rectangle's gain impressive, especially in light of what I know about the ADR, we can notice that it is equivalent in size to a 107-foot rectangle on 80 meters. A 105-foot rectangle has a gain of 4.18 dBi with losses of 0.34 dB. The 10-meter antenna has losses of only 0.02 dB, and this accounts for its significantly greater gain.
- <sup>35</sup>D. Handelsman, N2DT, "The Double Loop on 30 Meters," *AntenneX*, Feb 2000. This band is the point in the HF spectrum where, at attainable antenna heights, a horizontally polarized loop will outperform a vertically polarized one. □□




**TOROID CORES**

Ferrite and iron powder cores. Free catalog and RFI Tip Sheet. Our RFI kit gets RFI out of TV's, telephones, stereos, etc.

**Model RFI-4 ..... \$25.00**  
+ \$6 S&H U.S./Canada. Tax in Calif.  
Use MASTERCARD or VISA

 **PALOMAR**

BOX 462222, ESCONDIDO, CA 92046  
TEL: 760-747-3343 FAX: 760-747-3346  
e-mail: Palomar@compuserve.com  
www.Palomar-Engineers.com



**American Radio Relay League**  
225 Main Street  
Newington, CT 06111-1494 USA  
For one year (6 bi-monthly issues) of QEX:  
In the US

ARRL Member \$22.00  
 Non-Member \$34.00

In Canada, Mexico and US by First Class mail

ARRL Member \$35.00  
 Non-Member \$47.00

Elsewhere by Surface Mail (4-6 week delivery)

ARRL Member \$27.00  
 Non-Member \$39.00

Elsewhere by Airmail

ARRL Member \$55.00  
 Non-Member \$67.00

**QEX Subscription Order Card**

QEX, the Forum for Communications Experimenters is available at the rates shown at left. Maximum term is 6 issues, and because of the uncertainty of postal rates, prices are subject to change without notice.

Subscribe toll-free with your credit card 1-866-277-5289

Renewal     New Subscription





Name \_\_\_\_\_ Call \_\_\_\_\_

Address \_\_\_\_\_

City \_\_\_\_\_ State or Province \_\_\_\_\_ Postal Code \_\_\_\_\_

Payment Enclosed

Charge:

Account # \_\_\_\_\_ Good thru \_\_\_\_\_

Signature \_\_\_\_\_ Date \_\_\_\_\_

Remittance must be in US funds and checks must be drawn on a bank in the US.  
Prices subject to change without notice.

11/88



# The Quad Antenna Revisited, Part 4: Effects of Ground on Quad Loops

---

*You want to build a killer quad, but how high must it be to provide the desired DX fireworks?*

---

By R. P. Haviland, W4MB

## Characteristics of the Earth Pertinent to Antennas

The characteristics of the ground under an antenna or at a point of impingement of radiated energy on the earth can be described adequately by two quantities, at least in most practical situations. The first of these is the relative dielectric constant,  $\epsilon_r$ , since most types of soil act as dielectrics, actually of rather poor quality. The second may be described as a resistance, the same type found in a poor capacitor; however, usual practice is to describe this by a derived quantity: the loss factor,  $\delta$ . For a discussion of

the effects of these, see Kraus<sup>1</sup> and for information on measured values, the next two references.<sup>2, 3</sup> Note that the actual ground is probably complex, occurring in layers, with some water present, or is even mineralized; so the data presented must be considered as representative of typical conditions, rather than being all-inclusive.

For this work, four types of ground

<sup>1</sup>Notes appear on [page 54](#).

---

**Table 1—Ground Characteristics**

Medium	$\epsilon$	$\delta$
Seawater	80	5.0
Average Soil	13	0.005
Poor Soil	5	0.0002

---

are used. One is the ideal ground, which acts as a sheet of perfectly conducting metal. The properties of the others are shown in Table 1. Here, average soil is typically found in pastures, poor soil in deserts and cities.

Some studies were made with fresh water ( $\epsilon_r = 80$ ,  $\delta = 0.008$ ), and good soil ( $\epsilon_r = 30$ ,  $\delta = 0.008$ ); good soil is typically found in river deltas. These studies are not covered in detail here because the difference between these and sea water does not seem to be very significant.

## Ground Effects on Antenna Gain

In the following material, heights are given with respect to the center of the loop, in wavelengths at the operating frequency, unless otherwise stated. Calculations are made with nine segments per loop side, which is



ample for reasonable accuracy except in a few notable cases. Designs are scaled from the prototype 8-meter-perimeter loops of earlier article segments.<sup>4</sup>

Since the ground is “lossy,” we may expect it to reduce antenna gain, partly because of losses in the ground directly underneath the antenna, partly because of losses at the point

where energy is reflected from the earth. Because of interference between the direct ray and the ray reflected from the earth, however, the reflections increase energy at some

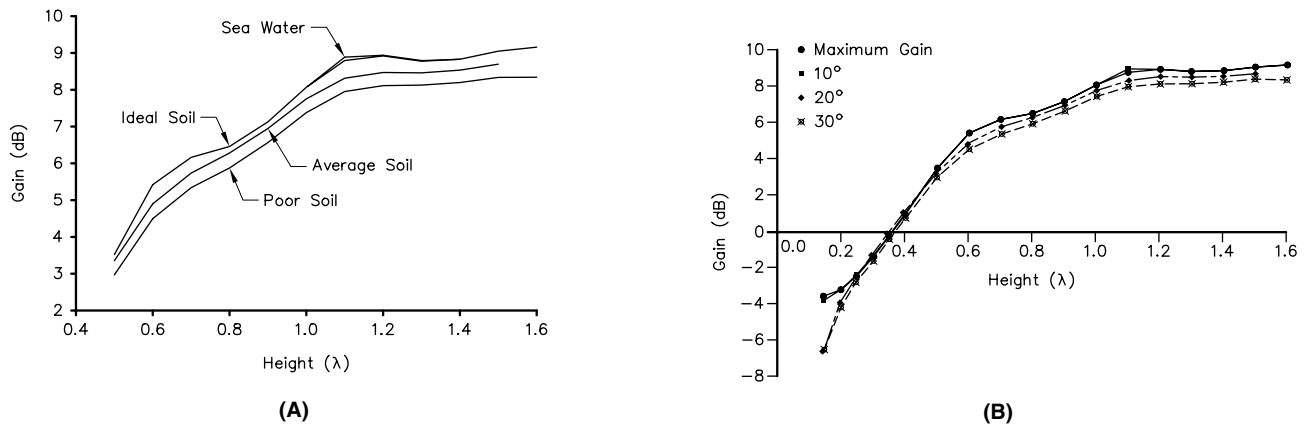


**Fig 1—Gain (10° elevation) versus center height of a 14-MHz loop (no wire loss). At (A), the effects of soil; at (B), the pattern variation for average soil at various elevation angles.**

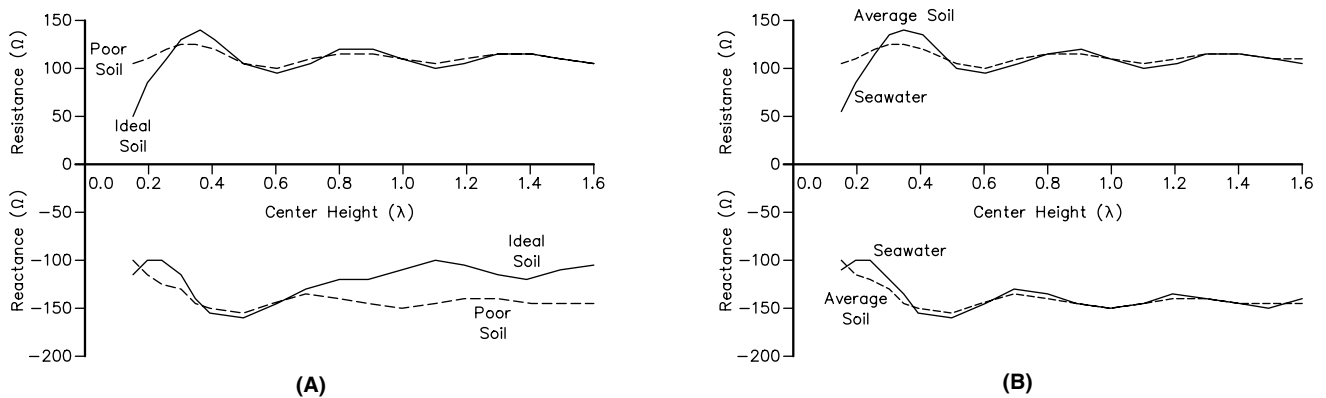


**Fig 2—Drive impedance versus height of a 14-MHz loop (no wire loss). At (A) are resistance and reactance curves for ideal and poor soils, at (B), resistance and reactance for seawater and average soils.**

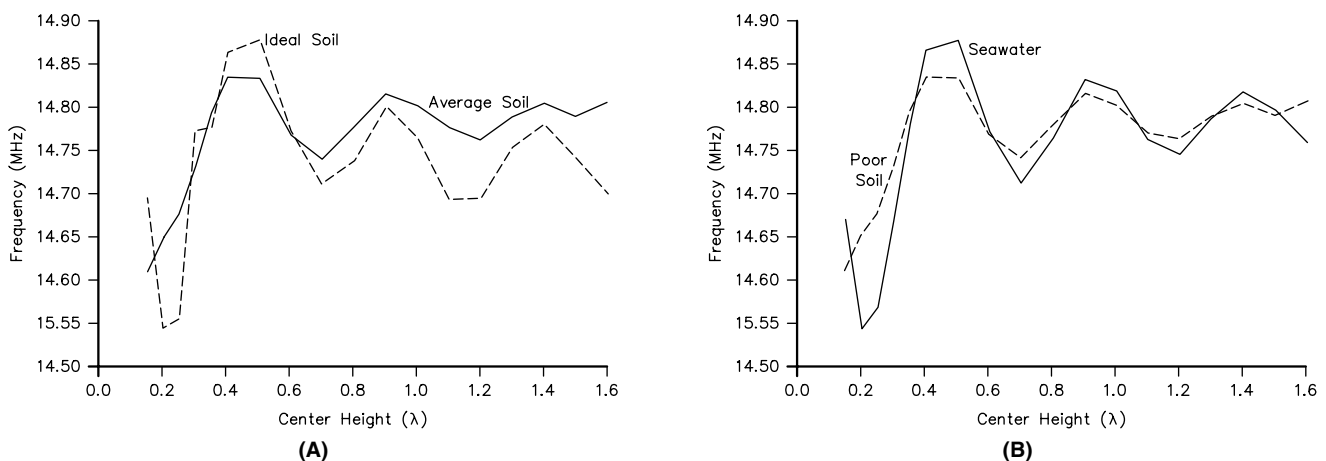


**Fig 3—Resonant frequency versus height of a 14-MHz loop (no wire loss). At (A), ideal and average soils, at (B), seawater and poor soils.**

elevation angles and reduce it at others; the effects change with the angle of incidence of the signal. Thus, changes in antenna gain and in pattern shape are evident as height changes. Drive characteristics also change because of interaction between the physical antenna and the “image” antenna, located about as far below the surface as the antenna is high. As noted in Part 1 of this series, several methods of ground-impact analysis are available; for this study, the high-accuracy method of Sommerfield is used, as included in the *NEC* program and its derivatives.

Fig 1 summarizes ground effects on antenna gain, showing gain change at 10° elevation angle as a function of height (Fig 1A), for four soil conditions. Horizontally polarized antennas over earth, such as a bottom-fed quad, have no signal at 0° elevation angle. Note that the seawater and ideal-soil curves are almost identical. The variation in height is largely due to the way lobes change with height, as shown later. Fig 1B shows the gain change with height at 10°, 20° and 30° elevation angles. Again, the variation is largely because of pattern changes.

Note the suggestion that there is a cyclic component of gain change with height. It is not very large, but it helps explain why small changes in height may not give increases in signal levels.

### Impedance Changes With Height

Fig 2 shows the change in drive impedance with height. The curves in Fig 2B are for seawater and average soil; those in Fig 2A are for ideal and poor soil. The differences are not great except for heights below about 0.3  $\lambda$ . To a reasonable approximation, ideal soil and seawater act as short circuits to currents flowing on a wire very close to the ground. For a dipole, the drive resistance goes nearly to zero, but this does not happen with quads having their lower sides close to the ground. The current around the loop does change appreciably, but the upper side—typically near  $\lambda/4$  above ground—remains a good radiator.

Note that the cyclic behavior is more marked in the impedance curves. It disappears completely at greater heights as the impedance converges to the free-space value. Since the reactance changes with height, the resonant frequency also varies. Fig 3 shows the pattern of this, with (B) being for seawater or poor soil and (A) for ideal and average soil. The fre-

quency scale is expanded, which emphasizes the cyclic behavior.

Variation of drive resistance with height is covered in some texts, with analysis of the causes: See Reference 1, for example. However, all texts I have seen ignore the changes in drive reactance and resonant frequency. They make an assumption—usually unstated—that the antenna is operated at resonance.

These changes appear to have practical importance in only two situations. One occurs in designs for maximum front-to-back ratio at a given frequency, which changes with height: The change in gain is negligible. The second situation occurs in antenna measurements. For accuracy, the measurement must be at design height, or a correction determined.

### A Comparison: Quad Loops and Dipoles

The dipole change mentioned above is shown in Fig 4, for average soil. As shown in Reference 1, both resistance and reactance approach zero for a dipole almost touching ideal soil, and a low value over saltwater. Reference 2 gives a method of analysis for any soil. This shows, for example, that impedance can increase markedly for antennas at low heights over poor soil. A form of subsurface mapping has developed from these findings.

Practically, quads and dipoles behave alike in two respects. As noted for greater heights above ground, the impedance tends toward the free-space value. In addition, the change can usually be neglected for antennas that are not too low—above about

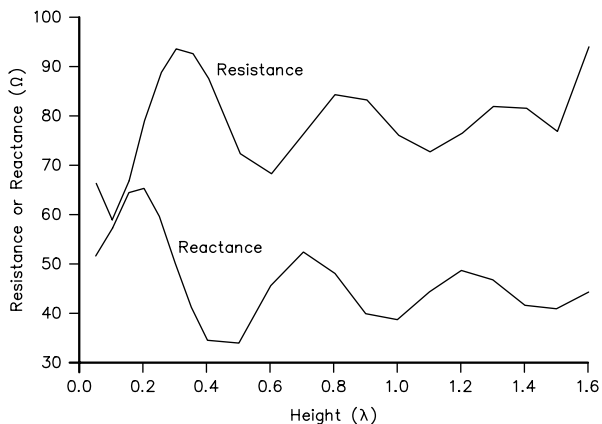


Fig 4—Impedance of a 14-MHz  $\lambda/2$  dipole over average soil.

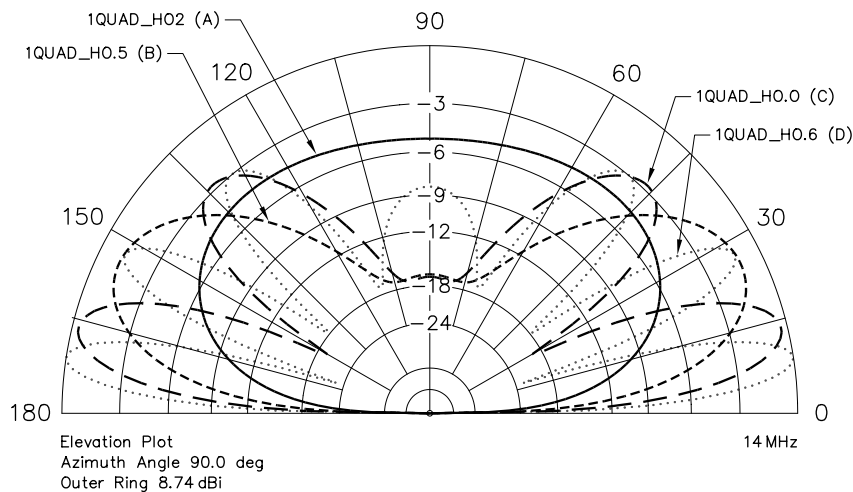


Fig 5—Effect of height on a 14-MHz quad loop over average soil. Vertical-plane patterns are for antenna center heights of: (A) 0.2  $\lambda$ =14 feet, (B) 0.5  $\lambda$ =35 feet, (C) 1.0  $\lambda$ = 70 feet and (D) 1.6  $\lambda$ =112 feet.

0.2  $\lambda$  for dipoles and 0.3  $\lambda$  center height for typical quads.

### Effects of Height on Radiation Patterns

Fig 5 shows typical changes in vertical-plane patterns of a bottom-fed quad as height changes; (A), (B), (C) and (D) are for center heights of 0.2, 0.5, 1.0 and 1.6  $\lambda$  (14, 35, 70 and 112 feet), respectively. All are for 14 MHz over average soil. By far, the most apparent change is in lobe pattern due to radiation interference between the direct and reflected signal components. See, for example, *The ARRL Antenna Book*<sup>5</sup> for details of this effect.

A secondary effect is the “fill-in” of lobe minima, which are around 20 dB below the lobe maxima in this example. The amount of change varies with ground losses. Maximum gain also changes with antenna height, as is evident on comparison of the gains tabulated on each plot, and as covered in discussing Fig 1.

### Vertically Polarized Quad Loops

Drive impedance and pattern changes are quite different when a loop is side fed to give vertical polarization. Fig 6A shows impedance variation with height for average soil. Rather than decreasing at very low heights, both components increase. The cyclic pattern is present, but small.

Fig 6B shows the gain variation with antenna height. Virtually all values are lower than the gains with horizontal polarization (see Fig 1). The dips in the 30° elevation curve are caused by lobe changes with antenna height. Unlike a horizontally polarized antenna, a vertically polarized antenna may have a signal component at essentially 0° elevation angle.

For comparison, the antenna characteristics for three vertically polarized conditions are shown in Table 2. This table shows why quad antennas are nearly always fed at the bottom to produce horizontal polarization. For most soil types, signal strengths from vertically polarized quads are nearly an S-unit weaker than those from horizontally polarized quads. The expense and work of construction is nearly wasted if vertical polarization is used.

The situation is different, however, when seawater is present. At low antenna heights, vertical polarization may give the strongest signal, especially for DX where the lower radiation angles are so important. This is one reason for strong signals from island

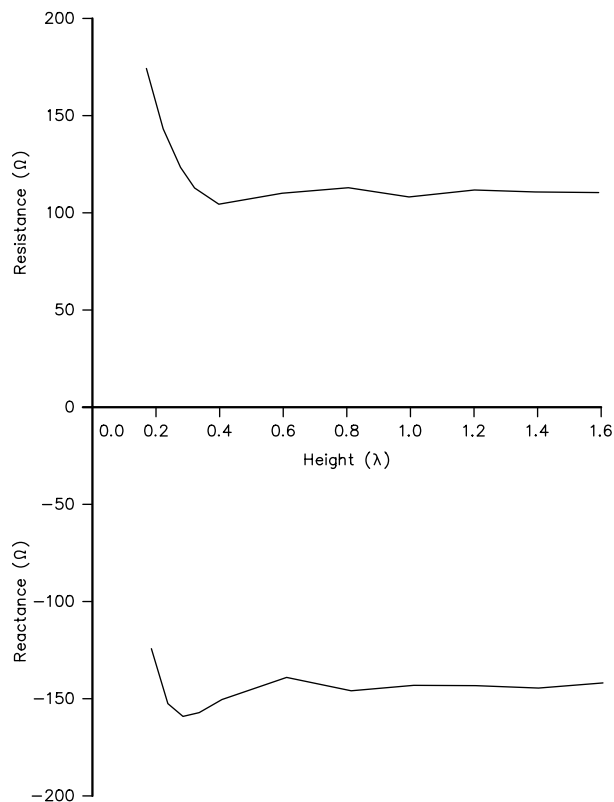
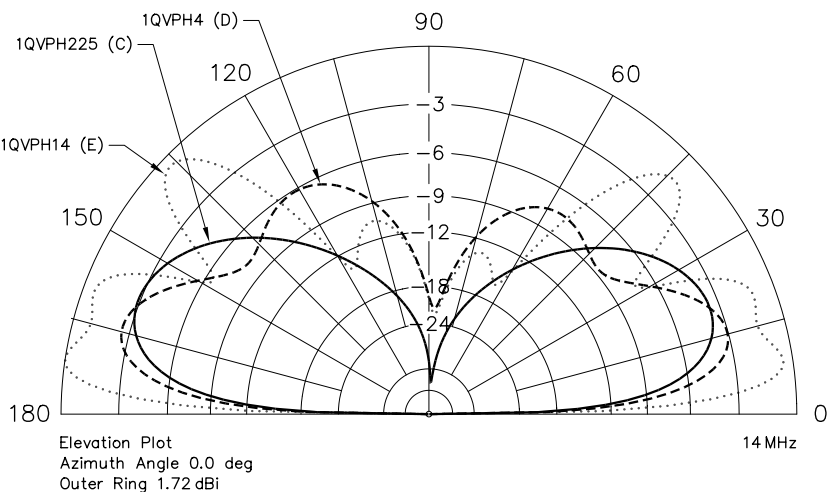
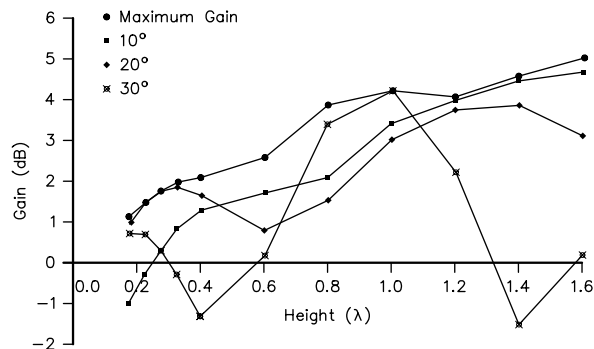


**Fig 6—Effects of antenna height on a vertically polarized loop. At (A), drive impedance, (B) gain at several elevation angles. C through E are vertical-plane patterns with antenna heights of (C) 0.225  $\lambda$ , (D) 0.4  $\lambda$ , (E) 1.4  $\lambda$  (18, 28 and 98 feet, respectively).**



locations and the reason that many such stations use vertical polarization.

Continuing with Fig 6, parts C, D and E show vertically polarized elevation plots for heights of 0.225, 0.4 and 1.4  $\lambda$  (16, 28 and 98 feet, respectively). Note the excellent radiation at very low angles and that the nulls between lobes are much smaller than for horizontal polarization. Vertical polarization may be good for some sites.

### Very Low Antennas and Height Restrictions

The quad has a reputation for good performance at low heights. As an exploration of this, Fig 7 shows some characteristics of a quad loop with its lower arm at 2 meters (just over 6 feet) above average soil. This height was chosen to give reasonable clearance for movement underneath. Fig 7A shows drive impedance over the range of 5-30 MHz, which is reasonably constant.

Figs 7B and C show the vertical-plane (elevation) plots at the extremes of this frequency range, 5 and 30 MHz. Because of the low height, the angles of maximum radiation are quite high: 52° and 30°, respectively; but appreciable radiation occurs at DX angles. At 5 MHz, angles around 20° are useful for F-layer propagation, with signals being about 6 dB or just over one S unit below the maximum gain. At 30 MHz, the 6-dB-down point is at 10°, so DX performance is not bad. The antennas are very good performers for intermediate distances, such as are involved in E-layer propagation. If height is a problem, try a quad.

To explore these height effects further, Fig 8 gives patterns for a two-element, 14-MHz quad at heights of 30, 60 and 90 feet. These correspond, respectively, very nearly to common, small-lot installations, to US average beam-antenna heights, and to many "super-station" heights.

At 30 feet, pattern (A) has its maximum radiation at 27°, with the 1-S-unit-down elevation angle at 10°. Day-time E layer, 14-MHz signals will be excellent; working DX will be chancy. If no one else is calling the DX, the station will likely get through. Long-path DX, which depends on low-angle radiation, will be scarce.

At 60 feet, maximum radiation has increased by over 1 dB and has moved to 16°. The signal is only 6 dB lower at 5°. It usually won't be possible to crack a pile-up on one call, but working DX won't be too difficult, even on the long path. A moderately strong lobe ap-

pears at 55°, so the antenna is a good performer for E-layer propagation.

At 90 feet, the maximum radiation has increased a little more and has moved to 11°; it is only 4 dB down at 5°. DXing starts to get easy; the two higher lobes give good E-layer performance.

These patterns include both horizontally and vertically polarized components; that is, the total patterns. As noted in earlier series segments, the

vertically polarized component of a bottom-fed quad is typically 20-30 dB below the main lobe. Even if not specifically shown, its intensity can be seen in the horizontal-pattern plots as the signal level in the plane of the loop, at 0° and 180°, as used here. For example, in the pattern of Fig 8D, the vertically polarized component is 35 dB below the main lobe, both for elevation angles of 10°.

**Fig 7—Impedances of two-element frequency-scaled quad loops, each with its lower-element side at 3 meters above average soil. (A) shows drive impedances for frequencies from 5 to 30 MHz. (B) and (C) show elevation patterns for 5 MHz (B) and 30 MHz (C).**

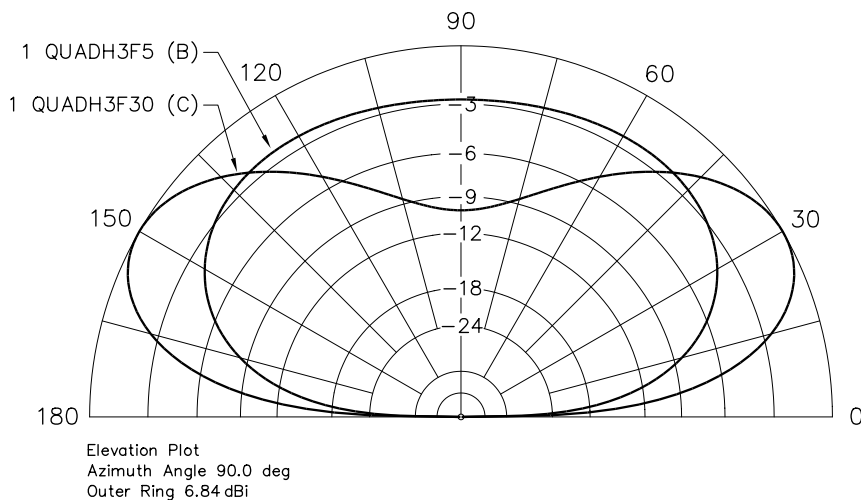
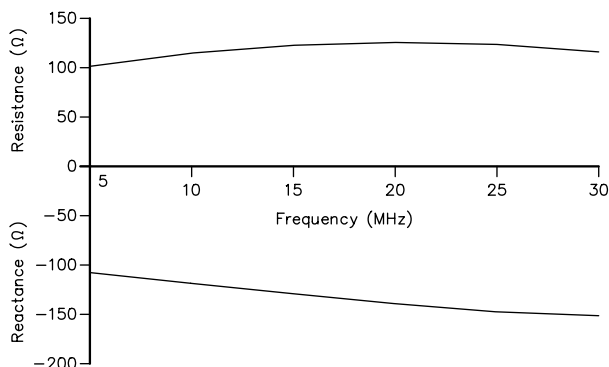


**Table 2—Vertically versus Horizontally Polarized Quads**

Condition	R ( $\Omega$ )	X ( $\Omega$ )	Gain at 10° (dB)
Free space	111	-144	2.97
Seawater	105	-156	8.11
Average Soil	105	-151	2.10

**as compared to horizontal polarization:**

Condition	R ( $\Omega$ )	X ( $\Omega$ )	Gain at 10° (dB)
Free space	111	-144	3.01
Seawater	133	-155	7.41
Average Soil	123	-152	6.69

where the height for sea water and average soil is 0.4  $\lambda$ .



The patterns for a four-element quad, Fig 9A, B and C show the same general characteristics, with more gain and slightly lower radiation angles. There won't be too many signals at the same antenna heights that are better. The 90-foot installation will start to be a "band opener" and "closer," giving acceptable signals appreciably before others find an opening to their areas. The good performance for E-layer propagation continues. The lobes in the plane of the loop are satisfactorily small, as shown at

(D). E-layer signals from the side will be about 3-4 S units below main-lobe signals of the same field strength.

These three antennas were designed to produce good front-to-back-ratio performance, as shown by the relatively weak back lobes. This "anti-QRM" measure is important in DX work and makes it possible to "dig for DX" when others are working E-layer or even first-hop F-layer signals.

To conclude this examination of height effects, Fig 10 shows two patterns for a 12-element quad on

144 MHz. Fig 10A is for an antenna height of 10 feet, B for 30 feet. Both give good performance for meteor-scatter and sporadic-E propagation, with the 30-foot height giving outstanding signals. The 30-footer will have the edge, especially for extended ground-wave propagation.

### Two Horizontal Quads

Various conditions at many locations prevent installation of antennas at an appreciable height. At least for suburban lots, a horizontal loop is one

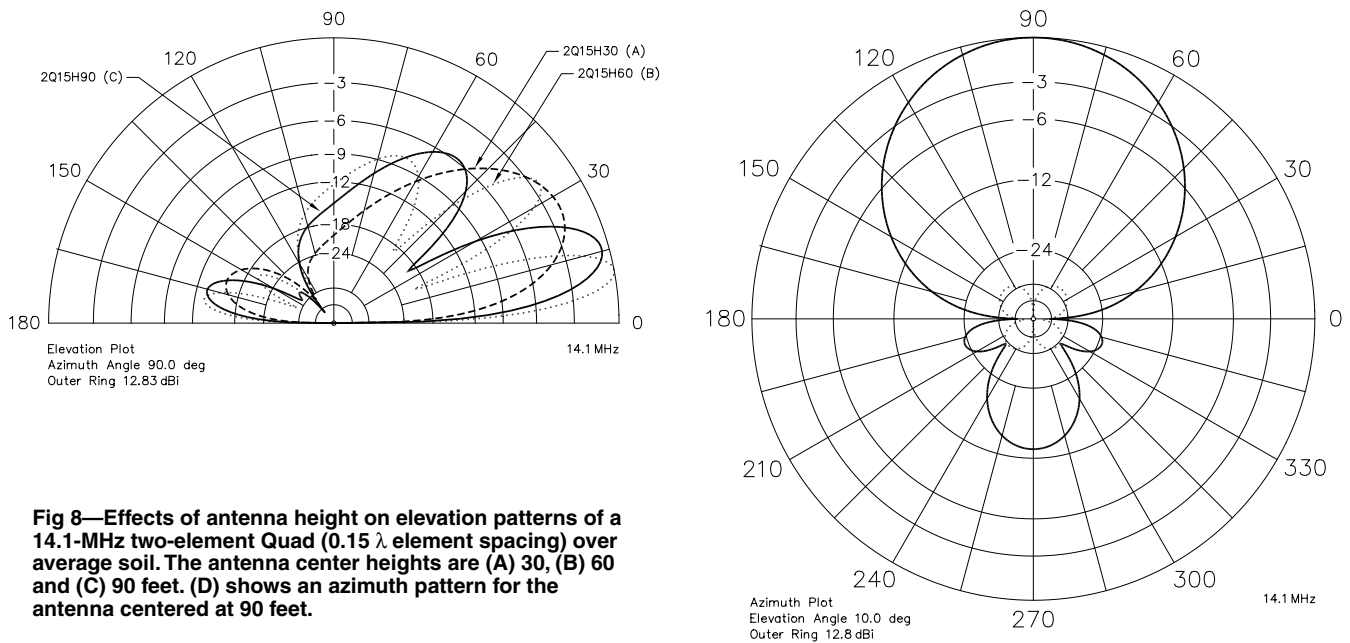


Fig 8—Effects of antenna height on elevation patterns of a 14.1-MHz two-element Quad (0.15 λ element spacing) over average soil. The antenna center heights are (A) 30, (B) 60 and (C) 90 feet. (D) shows an azimuth pattern for the antenna centered at 90 feet.

Table 3—Horizontal Quad Characteristics

30 meters per side, 3 meters high over average soil with no wire losses and nine segments per side

Frequency (MHz)	R (Ω)	X (Ω)	30° Gain	Gain at Azimuth	Number of Lobes	Maximum Gain	at Elevation (°)
1.8	8084	12800	-15.4	0	2	-12.3	90
3.6	83	-114	-6.1	0	2	-0.2	90
7	205	-370	-1.9	0	2	-0.7	51
10.5	302	-700	0.9	40	4	2.1	45
14	608	-1009	1.7	41	6	4.6	90
17.5	1214	-663	4.4	50	8	6.1	45
21	1509	-96	6.9	59	6	7.6	38
24.5	1420	278	7.6	64	8	7.9	36
28	1007	402	6.8	68	12	6.89	32
30	256	-115	9.2	70	10	9.2	31
50	397	468	9.6	20	18	9.7	28
144	419	887	5.1	281	48	7.7	10

way around this. **Table 3** summarizes two wide-band possibilities of a reasonably small antenna of this type: One has 30-meter (100 feet) sides and is 3 meters (10 feet) high. Except on 1.8 MHz, the signal produced is as good as isotropic, with appreciable gain at 14 MHz and higher. While there are large variations in drive impedance, a ladder-line feed and matchbox easily handle this. Note: With only nine segments per side, higher-frequency results are only approximate.

The patterns of such an antenna are not wonderful, but they are useful. **Fig 11A, B and C** show the vertical-plane patterns at 14 and 24.5 MHz and the 50-MHz horizontal-plane pattern for 30° elevation. F-layer propagation won't be great, but performance will be good for daytime E-layer and short-skip propagation.

It should be noted that such an antenna need not be square, or even any regular shape; it may even have sections folded back at acute angles (a form of loading). The wire size may be small; losses do increase, but #26 AWG copper wire twisted around nylon fishing line, makes a nearly invisible antenna, even from 10 feet away. This particular size example is probably good only for reception on 1.8 MHz, but a trial would be worthwhile. Even better would be to increase the length of one or more sides, if possible.

My point here is that we should not give up on antennas just because it isn't feasible to erect a big beam at 60 feet. Assess your own size and height constraints and create an antenna to fit the space with a computer program or with a full-size trial. If you put up an antenna and it doesn't work

well, quietly take it down and put up another one. When you get one that works, tell all your friends and brag on the air. Before long, you will be known as an antenna expert!

### Testing a Beam

A standard method of testing a beam antenna before erection is to aim it vertically, with the reflector element fairly close to the ground. **Fig 12** shows results for a typical two-element quad. Drive impedances at 12A nearly equal the free-space values for reflector heights greater than  $0.2 \lambda$ , and are roughly equal for heights greater than  $0.1 \lambda$  (about 6 feet) for the 20-meter band. The pattern at 12B is typical of such an antenna, but there should be good signals for E-layer propagation. These two factors provide a good indication that the antenna is working as designed.

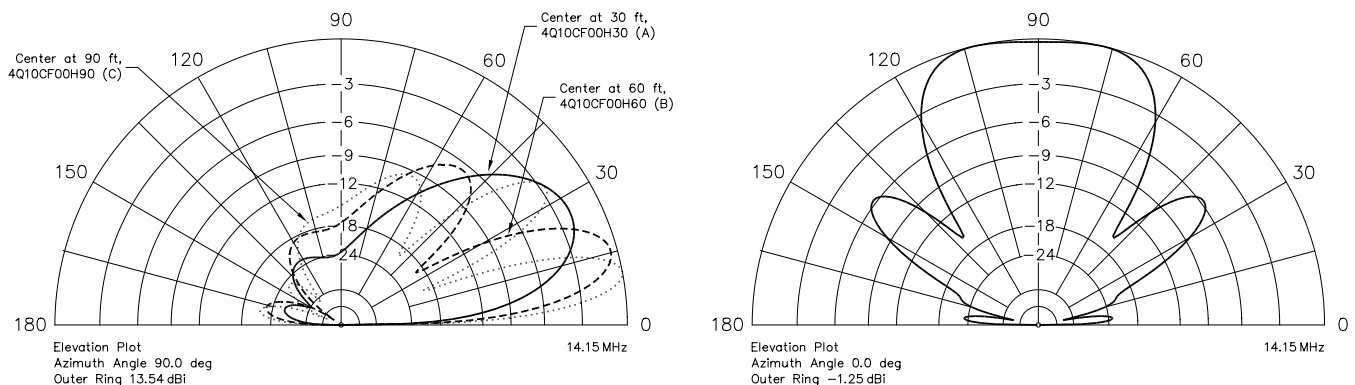


**Fig 9—Effects of antenna height on elevation patterns of a 14.1-MHz four-element Quad ( $0.2 \lambda$  element spacing) over average soil. At (A), the antenna center is at 30, (B) 60 and (C) 90 feet. At (D) is the elevation pattern in the plane of the driven element centered at 90 feet.**

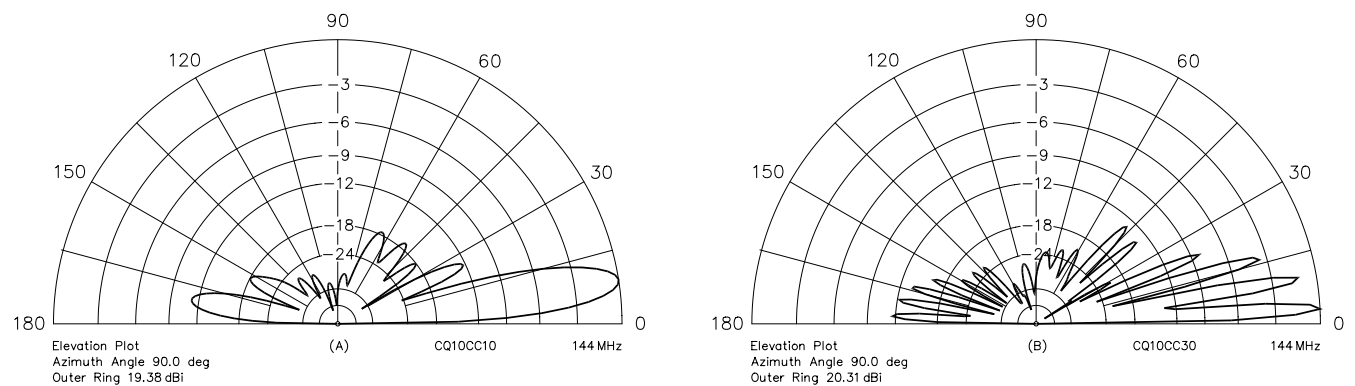


**Fig 10—Effects of antenna height on vertical-plane patterns of a 144 MHz 12Quad over average soil with the antenna centered at (A) 10 and (B) 30 feet.**

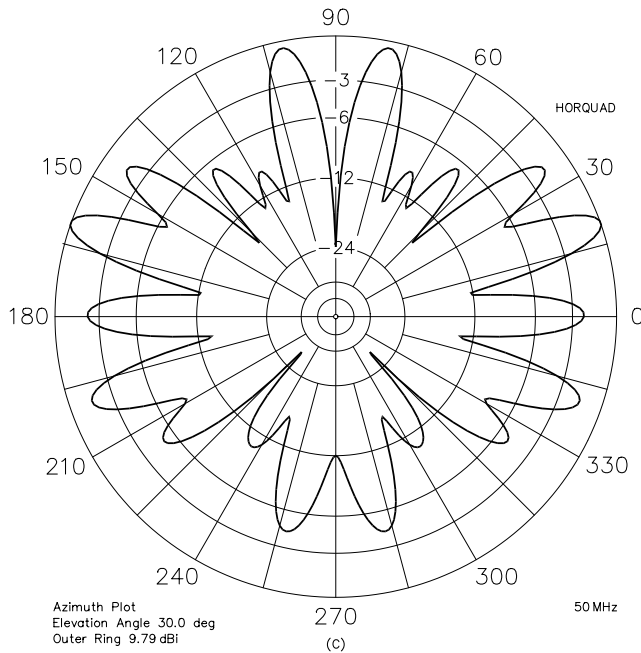
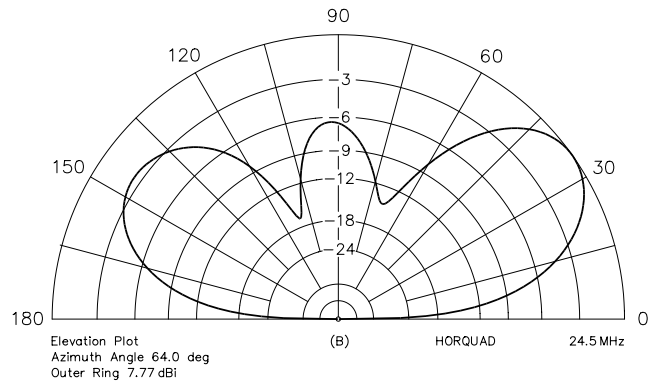
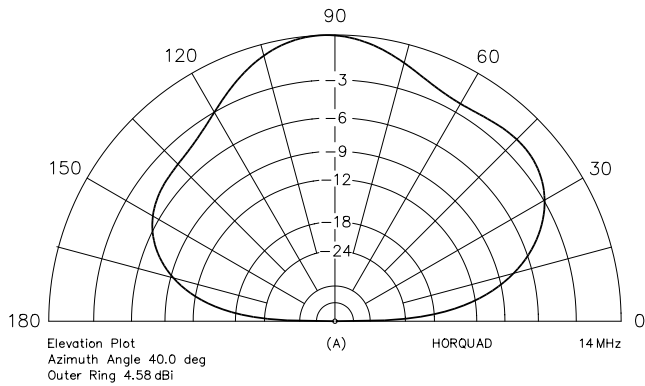


**Fig 11—A 20-meter horizontally oriented square loop mounted 2 meters above average soil. At (A) and (B) vertical-plane patterns at 14 MHz and 24.5 MHz (91 segments). At (C), a horizontal-plane pattern for 50 MHz (91 segments).**

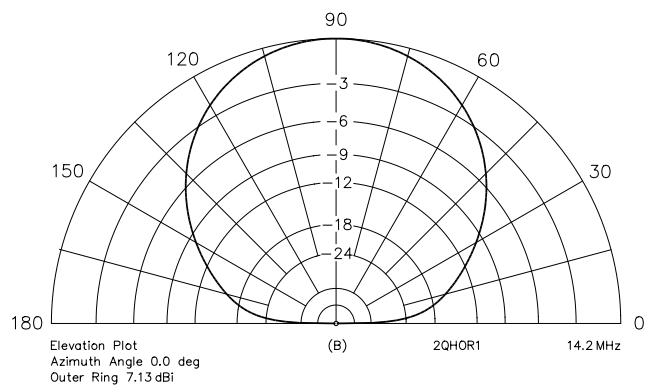


**Fig 12—Test results from a two-element 14-MHz quad mounted with the boom pointed at the zenith (loop elements in horizontal planes) over average soil. At (A), drive impedance versus reflector-to-ground spacing. At (B), a vertical-plane radiation pattern for a 0.1  $\lambda$  height.**

You can always impress the neighbors by taping a 2- or 3-foot-long fluorescent tube to a stick and placing it near the high-voltage points. This is another useful check: The brightest points should be 90° from the radiator centers, at the ends of  $\lambda/2$  Yagi elements and on the sides of full-wave loops.

#### Notes

- <sup>1</sup>J. Kraus, *Antennas*, (New York, McGraw-Hill, 1988).
- <sup>2</sup>R. Haviland, "Ground Parameters for Antenna Analysis," *The ARRL Antenna Compendium, Vol. 5*, (Newington: ARRL, 1996).
- <sup>3</sup>G. Hagn, "HF Ground Measurements at the Lawrence Livermore National Laboratory Field Site," *Applied Computational Electromagnetics Society Journal and Newsletter*, Vol. 3, No. 2, 1988.
- <sup>4</sup>R. Haviland, "The Quad Antenna Revisited," *Communications Quarterly*, Pt 1, Summer 1999, pp 43-73; Pt 2, Fall 1999, pp 65-85; Pt 3, QEX/Communications Quarterly, Nov/Dec 2000, pp 10-19. A multitude of EZNEC2 description files used in this series are available for download from the ARRL Web [www.arrl.org/files/qex/](http://www.arrl.org/files/qex/). Look for QUADS.ZIP.
- <sup>5</sup>G. Hall, K1TD, Editor, *The ARRL Antenna Book*, 16th edition, (Newington: ARRL, 1991).

---

# RF

---

By Zack Lau, W1VT

## Making Off-Center Fed Dipoles Work

Many amateurs would like a simple coax fed antenna that works reasonably well on many, if not all bands. A center-fed dipole antenna typically suffers from excessive feed-line loss on some bands, unless the characteristic feed-line loss is very low. This is due to the harmonic relationship of many amateur bands that makes high impedances inevitable—I am sure that many hams have unsuccessfully looked for a “magic” design. A line loss of 10 dB is not unusual for 100 feet of flexible coaxial feed line.<sup>1</sup> Despite the

<sup>1</sup>Notes appear on [page 58](#).

---

225 Main St  
Newington, CT 06111-1494  
[zlau@arrl.org](mailto:zlau@arrl.org)

touted low losses of open-wire fed antennas, many hams prefer the convenience of coaxial feed line. Not only is it tolerant of proximity to metal masts, but the effect of weather on performance is minimal. In contrast, commonly used window ladder line is significantly affected by water.<sup>2</sup>

An attractive candidate for such an antenna is the off-center-fed dipole, or OCFD: each side of the antenna has a different length.<sup>3, 4, 5, 6</sup> By making the lengths unequal, we can obtain feed-point impedances that match 200  $\Omega$  fairly well on four amateur bands. A 200- $\Omega$  impedance is convenient—I find it easy to design an efficient 50:200  $\Omega$  broadband transformer. Other values, such as 300  $\Omega$ , are much tougher to design. A typical OCFD design is shown in [Fig 1A](#). I was able to improve SWR performance by mod-

eling it over real ground at a height of 46 feet, as shown.<sup>7</sup> The SWR is under 2.1:1 at 7, 14, 21 and 28 MHz. This isn't surprising if you study the chapter of *The ARRL Antenna Book* that discusses effects of ground on antennas. At a height of  $0.35 \lambda$ , the impedance of a horizontal  $\lambda/2$  antenna is maximized. This is precisely what this antenna needs, since the input impedance on 40 meters is less than 200  $\Omega$ , and needs to be increased for better SWR performance.

Unlike a center-fed dipole, the feed line of an OCFD may significantly interact with the antenna. This is true because the longer wire couples more strongly to the feed line than does the shorter wire. This is easily shown through computer modeling—placing an unconnected  $\lambda/2$  of wire perpendicular to the antenna feedpoint will



raise the 20-meter SWR from 1.6 to 4.0:1.

I modeled all these antenna situations with *EZNEC* and a *NEC4* engine. In all cases, I modeled the rig end of the feed line as an open circuit. A 1:1 line isolator at the rig end looks like a good idea, since the feed-line shield is likely to pick up RF. It could also be grounded, but an open circuit is easier to duplicate with *Mininec* based modeling programs. I modeled the antennas with copper loss, as well as the zero-conductor-loss case. The difference in impedance is small.

Connecting the 45-foot feed-line shield directly to the shorter wire reveals a significant problem. While the 7-MHz SWR drops to 1.3:1, the 14-MHz SWR skyrockets to 13.1:1. The 21- and 28-MHz ratios are also a bit worse. This antenna is shown in Fig 1C.

A line isolator can reduce this problem. This antenna is shown in Fig 1D. A line isolator is designed to block shield currents on a coaxial transmission line. It is often suggested that a 4:1 balun or current balun be used as a line isolator with OCFDs. Fig 1D shows the model of an OCFD with a current balun. The current balun is designed with the popular "4× rule," in which the impedance is four times the impedance being transformed. I modeled it as a pure resistance of 800 Ω. There is a noticeable mismatch on 20 and 15 meters. Increasing the impedance to 2400 Ω is better, and the SWR performance is quite good at 8000 Ω. Unfortunately, 8000 Ω of isolation is a bit much to achieve in a single isolator—one wonders whether a line isolator in the center of the feed line would help? Surprisingly, a second

isolator of 1600 Ω actually degrades performance. The SWR on 20 meters actually increases from 2.7 to 3.1.

It should be obvious why Amateur Radio operators have had mixed results with OCFD antennas. Typical designs have no line isolator or feed-line length specification, although these elements are critical for obtaining optimum SWR performance. This isn't like a  $\lambda/2$  dipole, which often works well despite little or no feed-line decoupling. Similarly, RF pickup by the shield is typically negligible if the coax is routed perpendicular to the dipole wires.

This investigation has just scratched the surface. I expect that many "optimum" designs can be developed if someone were to devote enough and time and effort to find them. Not only can we develop OCFDs for different overall lengths, but one might also

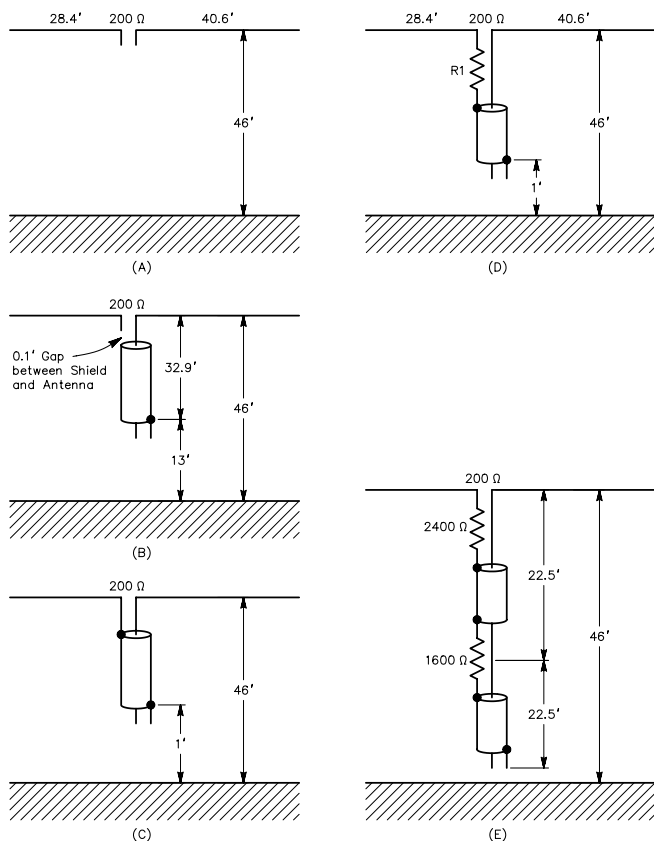


**Fig 1—The antenna test conditions. The dipole is made of #12 AWG wire. Antennas modeled with ground are all 46 feet (optimum height) above real ground. Coax is RG-58 (0.15-inch shield OD). R1 decouples the coax shield from the antenna; its value varies as indicated in Table 1. In C, D and E, the total feed-line length is 45 feet.**

**Table 1—EZNEC/NEC4 Results**

**Free-Space Off-Center-Fed Dipole (file *ocfd.ez*, Fig 1A).**

Band (MHz)	7	14	21	28
SWR	2.5	1.7	1.4	1.7
Z (Ω)	80+j16	330-j21	208-j65	140-j65
Z (Ω, copper)	81+j17	335-j16	213-j62	143-j62

**OCFD 46 feet above Real Ground (file *ocfdg.ez*, Fig 1A).**

Band (MHz)	7	14	21	28
SWR	2.1	1.6	1.4	1.6
Z (Ω)	98+j16	306-j26	211-j67	143-j63
Z (Ω, copper)	99+j17	311-j21	215-j64	146-j20

**OCFD with Perpendicular 20-Meter  $\lambda/2$  Wire next to Feed (file *ocfdres.ez*, Fig 1B).**

Band (MHz)	7	14	21	28
SWR	2.1	4.0	1.4	1.3
Z (Ω)	98+j15	796-j14	183-j62	166-j42
Z (Ω, copper)	99+j16	800-j13	187-j59	169-j39

**OCFD with RG-58 Shield Connected to Shorter Antenna Wire (file *ocfdfs.ez*, Fig 1C).**

Band (MHz)	7	14	21	28
SWR	1.3	13.1	2.9	3.1
Z (Ω)	233-j44	478-j995	517-j179	152-j201
Z (Ω, copper)	233-j41	477-j990	516-j173	153-j199

**OCFD with 800-Ω Feedpoint Isolator (R1) (file *ocfd800.ez*, Fig 1D).**

Band (MHz)	7	14	21	28
SWR	1.7	4.2	2.1	1.7
Z (Ω)	120+j24	609-j362	384-j95	180-j103
Z (Ω, copper)	121+j25	613-j361	386-j92	183-j100

**OCFD with 2400-Ω Feedpoint Isolator (R1) (file *ocfd2400.ez*, Fig 1D).**

Band (MHz)	7	14	21	28
SWR	1.9	2.7	1.6	1.6
Z (Ω)	105+j21	483-j154	306-j55	168-j82
Z (Ω, copper)	106+j22	489-j151	308-j52	171-j79

**OCFD with 8000-Ω Feedpoint Isolator (R1) (file *ocfd8000.ez*, Fig 1D).**

Band (MHz)	7	14	21	28
SWR	2.0	2.0	1.3	1.6
Z (Ω)	100+j19	392-j73	251-j31	161-j74
Z (Ω, copper)	101+j20	398-j68	254-j28	164-j71

**OCFD with 2400-Ω Feedpoint Isolator and 1600-Ω Isolator at Center of Feed Line (file *ocfdmc.ez*, Fig 1E).**

Band (MHz)	7	14	21	28
SWR	2.0	3.1	1.7	1.6
Z (Ω)	102+j21	523-j217	304-j77	166-j83
Z (Ω, copper)	104+j22	528-j214	307-j74	169-j80

experiment with inverted-V variations. One commercial vendor sells an OCFD variation that utilizes part of the feed line as a vertical radiating element.<sup>8</sup> He claims this modification improves low-angle performance.

### Homebrew 1:1 and 4:1 Line Isolators

I decided to break up the task of designing the 4:1 isolator into two parts—designing a 1:1 isolation transformer and a 4:1 impedance transformer. The 1:1 isolation transformer is also useful for blocking RF at the rig. Choke baluns wound with coax make excellent isolation transformers, so I performed some experiments using a spectrum analyzer and a tracking generator. It should be possible to make similar measurements with a QRP transmitter, a power attenuator and a sensitive power meter as shown in Fig 2. A 6- to 10-dB attenuator will provide a good impedance match to the transmitter, regardless of load. It is possible to damage some transmitters with a poor load. A spectrum analyzer isn't required if you have a signal source with spurious signals and harmonics well attenuated. The power meter should be able to detect signals 30 dB weaker than the output of the attenuator. A 50-Ω load and a simple 1N34A diode detector driving a high-impedance voltmeter should be adequate with 1 W of available power.

I chose a size 140 core, as it appeared

to the smallest core in which I could wind a relatively large number of turns, using RG-58C coax as the conductor. I chose a 50-Ω cable with a stranded center conductor, since it is more flexible and easier to wrap around the toroid than one with a solid-copper center conductor. I found that an isolation choke formed with 8 turns of RG-58C shield on a FT140-77 core had just 17 dB of isolation, while the same winding had 30 dB of isolation at 30 MHz on an FT140-43 core. Adding three more turns to the type-43 core lowered the parallel resonant frequency, so 30 dB of isolation was obtained between 10 and 30 MHz.

I think the type-77 material is too lossy to make a good isolation choke, as the frequency response was quite flat. Normally, I start with the most permeable materials first, since fewer turns are required for a given inductance. Next, I add enough turns to obtain good performance at low frequencies, since low-frequency performance is typically determined by the inductive reactance. While I am doing this, I watch the high-frequency performance by frequency-sweep testing the choke. As more and more turns are added stray capacitance increases, and that degrades the high frequency performance. Thus, with a typical design, one more turn improves the low-frequency performance just a little bit at the expense of the performance at the high end.

I didn't worry as much about isola-

tor performance at 7 MHz, as computer modeling indicated that excellent isolation wasn't as important. In fact, the SWR actually improved as the isolation worsened.

I decided to use the impedance transformer on page 56 of *Solid State Design for the Radio Amateur*.<sup>9</sup> It is described more fully as the Guanella 1:4 in Section 1.3 of *Transmission Line Transformers*, by Jerry Sevick, W2FMI.<sup>10</sup> It was originally designed for balanced to balanced work. Fortunately, the isolation choke provides the necessary equal and opposite currents needed to drive it properly. It has very little loss—the maximum loss between 3.5 and 30 MHz is just 0.11 dB. Just as with the choke, you can experiment with different materials and windings to optimize performance for a particular frequency range. The complete 50:200-Ω line isolator is shown in Fig 3.

It is important, but difficult, to assess the power-handling ability of the transformer. Two FT82-61 cores have a surface area of 22 square centimeters. To obtain a 25° temperature rise, 1.0 W of heat dissipation is required.<sup>11</sup> With a loss of just 0.11 dB, 97.5% of the power gets to the load. Thus, the cores will handle 40 W with the rated 200-Ω load. It's more difficult to measure the loss with non-ideal loads. I've looked at this problem but have not found any simple solutions. This looks like a challenge for an advanced amateur to solve! However, based on my experience with ferrite transformers, I'd expect this

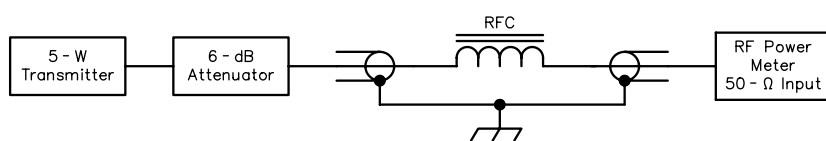


Fig 2—Test setup for measuring RF choke isolators.

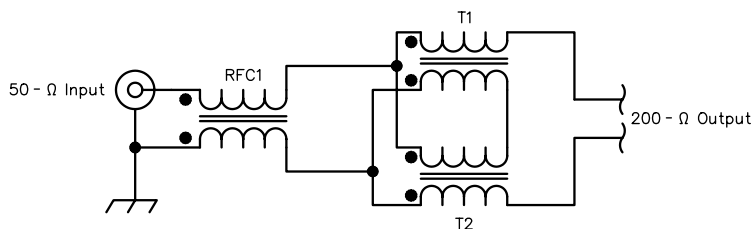


Fig 3—50:200-Ω line isolator optimized to cover 10 to 30 MHz.

RFC1—11 turns of RG-58C on FT140-43 ferrite core.

T1, T2—8 turns #20 AWG enameled wire bifilar wound on FT82-61 ferrite toroids.

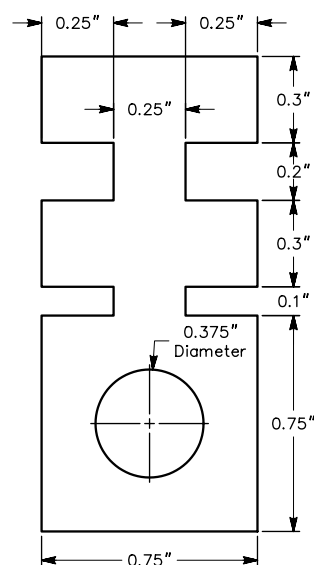


Fig 4—Shop made solder lug for attaching coax shield to  $\frac{3}{8}$ ×32 threaded BNC jacks. Use 0.020-inch-thick copper sheet.

transformer to handle typical QRP levels of 5-W CW and 10-W PEP sideband.

The last step is packaging the isolation choke and transformer in a rugged enclosure. I described how to do this in detail in my Nov/Dec 2000 RF column, packaging a tiny balun in 1/2-inch PVC pipe. I found there was just enough room inside a 3-inch length of Schedule 40, 1.5-inch diameter PVC tubing. End caps were attached with #2-56 screws. I tapped the plastic to hold the screws in place. On the top of the 1.5-inch PVC cap, I mounted an inverted 3/4-inch pipe cap with holes in it for attaching support ropes. You might want to use a more standard eyebolt, as I have not extensively tested the plastic cap for ruggedness. Use #10-32 stainless steel hardware to provide convenient connections to antenna wires.

I found it easiest to connect the transformer first to the screws mounted on the top end cap. Then, the isolation choke was added. Finally, the coax was attached to the bottom end cap with a large copper solder lug. Fig 4 shows how to make your own solder lugs out of 0.020-inch-thick copper sheet. Solder lugs that fit around 3/8-inch-threaded connectors are also available from Amphenol.

### System Considerations

It is a reality that efficient antennas are sensitive to their environment. Changes in height or proximity to metal objects change SWR performance of the antenna. This is particularly true of temporary antennas, which are typically installed close to the ground. In quickly installed portable installa-

tions, it may be wise to sacrifice some theoretical performance, perhaps utilizing an automatic antenna tuner for quick band changes, instead of looking for a efficient broadband design that will work anywhere.


The feed-line loss is an important variable. Instead of spending a lot of time trimming an antenna for best performance, it may actually make more sense to optimize a coaxial feed line for the shortest length. For instance, one might bring 30 feet of feed line, 5 and 10 foot extension cables. Thus, depending on antenna height, feed-line lengths of 30, 35, 40 and 45 feet can be selected, minimizing the amount of unused feed line. This can be done quite quickly with BNC or C connectors.


### Summary

An off-center-fed dipole can be an excellent choice for multiband operation in portable installations, if installed by a perceptive ham using an antenna tuner. I think it is unreasonable to expect quick installations with very low SWR on all bands—there are just too many variables involved. However, the SWR is typically low enough to work well with automatic antenna tuners. A perceptive ham won't apply the antenna casually; using a junk-box balun as the isolator and an excessive length of lossy coax can easily result in poor system performance. Nor will he unwisely trade antenna height for a better SWR. For beginners, an OCFD cannot compare with the simplicity of a  $\lambda/2$  40-meter dipole that will work well with a tuner on 15 meters, or single-band 20- or 10-meter center-fed dipoles.

### Notes

- <sup>1</sup>D. Straw, N6BV, *The 2000 ARRL Handbook*, Table 10.3, "Modeled Data for a 100-ft Flat-Top Antenna," p 19.7.
- <sup>2</sup>W. Stuart, N7WS, "Balanced Transmission Lines in Current Amateur Practice," *The ARRL Antenna Compendium Vol 6*, pp 174-178.
- <sup>3</sup>W. Wright, G0FAH, "Four Bands, Off Center," *QST*, Feb 1996, p 65.
- <sup>4</sup>R. Formato, K1POO, "Improved Feed for the Off-Center-Fed Dipole," Technical Correspondence, *QST*, May 1996, p 76.
- <sup>5</sup>R. Formato, K1POO, "Off-Center-Fed Dipole Comments, Part 2," Technical Correspondence, *QST*, Oct 1996, pp 72-73.
- <sup>6</sup>R. Formato, K1POO, "Feedback to Off-Center-Fed Dipole Comments, Part 2," clarifies the wire diameter as 0.2053 cm, #12 AWG, *QST*, Dec 1996, p 71.
- <sup>7</sup>You can download the EZNEC description files from the ARRL Web [www.arrl.org/qexfiles/](http://www.arrl.org/qexfiles/). Look for OCFDEZ.ZIP.
- <sup>8</sup>The Radio Works, Box 6159, Portsmouth, VA 23703; tel 757-484-0140; [www.radioworks.com](http://www.radioworks.com).
- <sup>9</sup>W. Hayward, W7ZOI, and D. DeMaw, W1FB (SK), *Solid State Design for the Radio Amateur*, (Newington: ARRL, 1977) p 56.
- <sup>10</sup>J. Sevick, *Transmission Line Transformers*, (Newington: ARRL, 1990), pp 1-5 to 1-7.
- <sup>11</sup>Z. Lau, W1VT, "Calculating the Power Limit of Circuits with Toroids," *QEX*, Mar 1995, pp 24-25. □□





## VARI-NOTCH® DUPLEXERS

### FOR 2 METERS

The TX RX Systems Inc. patented Vari-Notch filter circuit, a pseudo-bandpass design, provides low loss, high TX to RX, and between-channel isolation, excellent for amateur band applications. TX RX Systems Inc. has been manufacturing multicoupling systems since 1976. Other models available for 220 and 440 MHz, UHF ATV and 1.2 GHz.

**MODEL 28-37-02A**

144-174 MHz

92 dB ISOLATION AT 0.6 MHz SEPARATION


400 WATT POWER RATING

**TX RX SYSTEMS INC.**

8625 INDUSTRIAL PARKWAY, ANGOLA, NY 14006

TELEPHONE 716-549-4700 FAX 716-549-4772 (24 HRS.) e-mail: [sales@trrx.com](mailto:sales@trrx.com)

A MEMBER OF THE BIRD TECHNOLOGIES GROUP



19" RACK MOUNT

## A Family Affair

### The R.L. Drake Story



By John Loughmiller, KB9AT

- Brand new!
- Printed October 2000
- 23 Chapters
- 300 Pages
- 150 Photos
- Glossy four color cover
- Over 150 pages of radio mods.
- \$29.95 (+\$4.95 ship)

John Loughmiller KB9AT reveals the behind-the-scenes history of the famous R.L. Drake Company, focusing on the glory days, when Drake was king in amateur radio. Every ham and SWL knew R.L. Drake from the outside, but now the inside story of this incredibly interesting company is told. This book also includes 150 pages of useful circuits and modifications for many Drake amateur radios. An entertaining read and a great technical reference for every Drake owner.



**Universal Radio**

6830 Americana Pkwy.

Reynoldsburg, OH 43068

◆ Orders: 800 431-3939

◆ Info: 614 866-4267

[www.universal-radio.com](http://www.universal-radio.com)



# Upcoming Conferences

## Southeastern VHF Society, April 20-21, 2001

The Southeastern VHF Society will host its fifth annual conference at the Holiday Inn Brentwood in Nashville, Tennessee. The program will include presentations by antenna specialist L. B. Cebik, W4RNL, EME enthusiast Bob McGraw, K4TAX, and many other VHF+ operators.

In addition to the technical program/presentations and conference proceedings, there will be pre-amp noise figure testing (50-1296 MHz), antenna-gain measurements (144-2304 MHz), a family program, flea market, vendor sales displays, the SVHFS auction, annual business meeting, Saturday night banquet with a guest speaker, K4UHF-award presentation and many door prizes.

Attending this conference will be some of the most capable amateurs in the world, with respect to both operations and technical aspects. In addition to weak-signal VHF enthusiasts, we want to reach Skywarn/ARES/RACES and the general population in surrounding states near Nashville. Many VHF specialty areas are directly related to emergency management, but no one has yet made a formal connection between the two areas. SVHFS wishes to introduce area Skywarn/ARES/RACES personnel to VHFers and vice-versa. Both organizations could benefit directly in both personnel and technical assistance.

Reservations for the Holiday Inn Brentwood may be made by contacting the hotel at 615-373-2600. The hotel Web site is [www.hotel-nashville.com/holidayinn/](http://www.hotel-nashville.com/holidayinn/). Mention the SVHFS 2001 Conference to get the group rate of \$80/night; the cut-off date for the group rate is March 2, 2001.

You can pre-register for the conference by completing the form on the SVHFS Web site at [www.svhfs.org](http://www.svhfs.org). To be added to the SVHFS mailing list, contact Robin Midgett, KB4IDC, via e-mail at [KB4IDC@arrl.net](mailto:KB4IDC@arrl.net). The SVHFS mailing address is SVHFS Inc, PO Box 1255, Cornelia, GA 30531. You can find more information about the conference at [www.svhfs.org](http://www.svhfs.org) or [www.ETDXA.org/svhfs.pdf](http://www.ETDXA.org/svhfs.pdf).

## SETI League Technical Symposium

The SETI League Inc, nonprofit leader in the privatized Search for Extra-Terrestrial Intelligence, will be holding its first Technical Symposium the weekend of April 28 and 29, 2001, in Trenton, New Jersey. SETI League members from around the world will present papers about radio astronomy, microwave communications, and the hardware, software and search strategies being used to seek scientific evi-

dence of other intelligent civilizations in the cosmos. The Symposium is being hosted by the Engineering Department of The College of New Jersey (formerly Trenton State College). In attendance will be a respectable sampling of the SETI League's 1200 members from 60 countries, including many of the over 100 SETI League members building and operating their own observing stations. For conference details, visit [www.setileague.org/admin/meet2001.htm](http://www.setileague.org/admin/meet2001.htm). □□


**ACTIVE**  
 ELECTRONIC COMPONENTS DEPOT

**OVER 115,000 ELECTRONIC COMPONENTS AVAILABLE!**

**More than 5,000 products on display!**

Active has the widest selection of the latest electronics and production supplies, all in a local, easy-to-shop store near you.

**Serving the electronic needs of engineers, technicians, hobbyists, MRO and students for over 30 years.**



- Electronic Components
- Semiconductors
- Passive Components
- Test & Measure Equipment
- Wire and Cable
- Hand Tools
- Soldering Equipment
- Chemicals
- Books and much more!

**Visit an Active Store near you!**

<b>BAITIMORE</b> 6714 Ritchie Hwy Glen Burnie, MD 21061 Tel.: (410) 863-0070 Fax: (410) 863-0075 <a href="mailto:active.baltimore@future.ca">active.baltimore@future.ca</a>	<b>CHERRY HILL</b> 1871 Route 70 East Cherry Hill, NJ 08003 Tel.: (856) 424-7070 Fax: (856) 424-7722 <a href="mailto:active.cherry.hill@future.ca">active.cherry.hill@future.ca</a>	<b>DETROIT</b> 29447 Five Mile Road Livonia, MI 48154 Tel.: (734) 525-0153 Fax: (734) 525-1015 <a href="mailto:active.detroit@future.ca">active.detroit@future.ca</a>	<b>SEATTLE</b> 13107 Northrup Way Bellevue, WA 98005 Tel.: (425) 881-8191 Fax: (425) 883-6820 <a href="mailto:active.seattle@future.ca">active.seattle@future.ca</a>
<b>CAMBRIDGE</b> 73 First Street Cambridge, MA 02141 Tel: (617) 864-3588 Fax: (617) 864-0855 <a href="mailto:active.cambridge@future.ca">active.cambridge@future.ca</a>	<b>CHICAGO</b> 1776 West Golf Road Mt. Prospect, IL 60056 Tel.: (847) 640-7713 Fax: (847) 640-7613 <a href="mailto:active.chicago@future.ca">active.chicago@future.ca</a>	<b>LONG ISLAND</b> 3075 Veterans Mem. Hwy. Ronkonkoma, NY 11779 Tel.: (631) 471-5400 Fax: (631) 471-5410 <a href="mailto:active.long.island@future.ca">active.long.island@future.ca</a>	<b>WOBURN</b> 11 Cummings Park Woburn, MA 01801 Tel.: (781) 932-0050 Fax: (781) 933-8884 <a href="mailto:active.woburn@future.ca">active.woburn@future.ca</a>

**Active has it... When you need it!** [www.activestores.com](http://www.activestores.com)



---

# Letters to the Editor

---

## Class-E RF Power Amplifiers (Jan/Feb 2001)

Please note the following correction on p. 12, left column, Eq 1:

$$R_{\text{load}} = R - [ESR_{L2} + ESR_{C2} + 1.365 R_{\text{on}} + 0.2116 ESR_{C1}]$$

$R$  is the value obtained from Eq 6 or 6A when using for  $P$  the procedure described at "Briefly:" in the three lines above Eq 1.—*Nathan O. Sokal, WA1HQC, Design Automation, 4 Tyler Rd, Lexington, MA 02420-2404; NathanSokal@compuserve.com*

## Wave Mechanics of Transmission Lines, Part 1 (Jan/Feb 2001)

Doug,

In my Jan/Feb 2001 article, I neglected to acknowledge Mr. William Klocko, N3WK, for his discussions regarding the subject of wave reflections in transmission line systems. My conversations with Bill on this subject were of great value. I would like to acknowledge him here and offer my apologies for that oversight.—*Steve Best, VE9SRB, 48 Perimeter Rd, Manchester, NH 03103-3327; srbest@att.net*

Dear Steven and Doug,

Just a quick note to tell you how much I enjoyed the first of this series in *QEX*. I appreciate the painstaking way you led me through the algebra, step by step, with no intuitive leaps in the dark. I like the way transmission-line loss was included at the very outset and was truly delighted with the way an infinite series dropped out as the equation for  $V_{\text{fwd}}$ . I've never seen such a clear and intuitive description before, let me congratulate you on that.—*Chris Cadogan, G3XWB, 8 Horncliffe Close, Rawtenstall Rossendale, Lancs BB4 6EE, Great Britain; chris@cadogan.u-net.com*

## On the Impedance Transformation Properties of a $\pi$ Network

In *QEX*, Sep/Nov 1995, William Sabin, W0IYH, described a standard IEEE procedure for measuring the output resistance of amplifiers and networks (see his Eq 8). This procedure involves making a small change in load resistance and measuring the resulting difference in load voltage and current. The output resistance is then determined by dividing the voltage difference by the current difference,  $R_{\text{OUT}} = dE/dI$ . I have used this procedure successfully for measuring the output resistance of class B and C amplifiers. In every instance where the loading of the amplifier was initially adjusted for delivery of all available power into the load with a given level of drive,  $R_{\text{OUT}} = R_{\text{LOAD}}$  at various levels of drive and delivered power.

After looking more closely at the concept, in his letter to the editor, *QEX*, May/June 2000, Mr. Sabin now asserts that this procedure will not give the correct answer, because the  $p$  network does not behave as a perfect transformer. He asserts that with a change in load resistance, we do not get the correct answer for the loss-less dynamic output resistance of the tube because of the  $\pi$  network's imperfect transformer action.

That distorts the objective of the IEEE procedure from obtaining the output resistance of the  $p$  network to obtaining the source resistance of the tube, which is not what the IEEE procedure obtains. We are not interested in the source resis-

tance of the tube, we are only interested in the source resistance seen at the output of the  $p$  network, that is, at the coax connector. Mr. Sabin states that the output resistance at the coax connector is also incorrect using this procedure; but my measurements show that this is not true. On the contrary, using the IEEE "small load-variation" method yields the correct network output resistance measured at the coax. The introduction of reactance at the input of the  $p$  network, plus the non-corresponding variation of the input resistance caused by deviation from the true transformer ratio is irrelevant to obtaining the network output resistance measured at the coax output connector.

In his letter in *QEX*, Sept/Oct 2000, Mr. Sabin presented a graph, his Fig 2, that plots output resistance of a  $p$  network versus  $r_p$ , the tube's lossless dynamic output resistance. His intent is to show how impedance transformation through a  $\pi$  network deviates from that through a perfect transformer. In this he is correct, the deviation does occur but not in the manner shown in his Fig 2, which is irrelevant in determining the network output resistance.

The data appearing in Fig 2 are interesting, but misleading for the following reason. A change in the internal resistance of the source cannot change the output resistance of the network while in normal operation, as the data in his Fig 2 would have us believe. The dependent and independent variables in the graph are reversed in relation to normal functioning of the network. In network operation, the load impedance is the independent variable that determines the dependent variable: the network input impedance. In his Fig 2, the source resistance  $r_p$  is shown erroneously as the independent variable, and the output impedance is shown erroneously as the dependent variable. This is incorrect because, as stated above, a change of internal resistance in the source cannot affect the output impedance of the network that is left undisturbed after proper adjustment.

A change in source resistance, in relation to the input impedance of the network, can only affect the amount of voltage applied at the input of the network and thus the amount of power delivered. A change in the load impedance terminating a network can change the network-input impedance, however, irrespective of the source resistance.

The data in Fig 2 are obtained by looking rearward at the output of the network. In looking rearward at the output, Fig 2 can be interpreted correctly only by considering that the direction of energy flow in the network is reversed from the normal flow: from the source to the load. In a configuration that would yield the data appearing in Fig 2, the  $x$ -axis values of ' $r_p$ ' would be functioning as load resistances, not source resistances. The  $y$ -axis resistances and reactances would be the resulting values of input impedance obtained while looking rearward into the network from original output terminals. In other words, if physical measurements were made rearward from the output to verify the data of Fig 2, real physical resistors of values that appear on the  $x$ -axis would be required as terminating loads at the network input. Then, when impedance measurements are taken at the network output, the values of resistance and reactance indicated on the  $y$ -axis would appear as network input impedances, not load impedances.

As a final point, measuring the change in load voltage and current resulting from a small change in load resistance to determine the output resistance of a network is in no way related to measuring rearward into the network, nor does it involve the tube source resistance in any way. Measuring the results of a change in load resistance occurs with the energy flowing in the normal direction, from the source forward through the network and into the load, contrary to the opposite direction of flow when measuring rearward as indicated

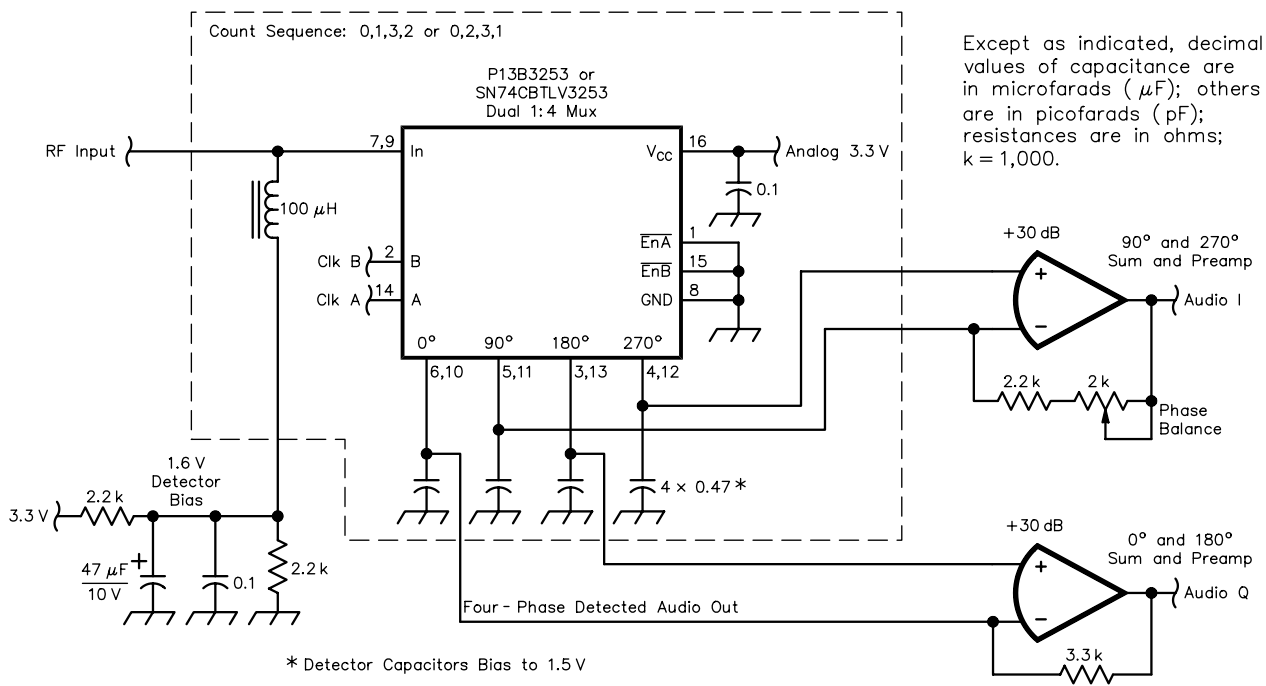


Fig 1—A schematic of N7VE's commutating mixer.

in Fig 2. Consequently, the objection to the standard IEEE load-variation method of determining the output resistance of networks is unfounded.—Walter Maxwell, W2DU, 243 Cranor Ave, DeLand, FL 32720-3914; w2du@iag.net

### Notes on "Ideal" Commutating Mixers (Nov/Dec 1999)

Doug,

Have you heard of my "Tayloe" detector? (See Fig 1.) It is a commutating quadrature detector that has only 0.9 dB of [conversion] loss. I just thought of this as I read your article. My detector produces only a difference, not a sum, and the 0.9 dB comes from the integration effect described in your article.

Fig 1 is a schematic of the detector. The topology of the design is the same as a switched-capacitor filter. Think of the input resistance as the characteristic impedance of the system, nominally 50  $\Omega$ . The detector is driven by a two-bit counter to switch at a frequency four times the detection frequency. This allows a  $1/4$ -cycle of input RF to be averaged on each of the four detection capacitors in sequence. For example, the 0° output gets the average of the first  $1/4$  cycle of RF, the 90° output gets the average of the second  $1/4$  cycle, and so forth, for all  $1/4$ -cycle segments.

Note that the 0° and 180° outputs are negatives of each other, as are the 90° and 270° outputs. These can then be summed using the differential inputs of a pair of op amps to produce a 0° ("I") and 90° ("Q") output. The differential inputs to the op amp yield an additional 6 dB of gain. The I and Q outputs can be used with a 90° audio phase-shift network to receive single sideband.

Each of the four detected outputs has a 200- $\Omega$  effective source impedance. This is because the 50- $\Omega$  driving RF impedance is only seen 25% of the time at each of the detection capacitors. This 200- $\Omega$  effective impedance is also used as the input impedance to the op amps, so their gain is 3300/

200 or 16.5 $\times$ —about 24 dB. The differential input yields an additional 6 dB of gain for a total of 30 dB from each op amp.

Notice that the circuit has been optimized to eliminate resistors in the signal path. This allows for an ultra-low-noise detection/preamplifier combination. Currently, my best receiver has -143-dBm sensitivity in a 500-Hz bandwidth, but my noise spreadsheet calculations indicate -146 dBm may be achievable.

Since the input frequency is being integrated onto the detection capacitor, only the difference frequency is produced. This is unlike a normal mixer that produces both a sum and difference. The net result is that each of the four detected voltage signals is only 0.9 dB down from the original signal, having a 200- $\Omega$  source impedance instead of the original 50- $\Omega$  signal; 0.9 dB is about a factor of 0.9 $\times$ . This loss factor is derived from the integration of a 90° segment of the peak of a sine wave. If each output is on for less than  $1/4$  cycle, this average detected loss will decrease further, but the effective source impedance will also increase.

Because the detector has such a very low loss, very sensitive receivers can be built without resorting to the use of RF preamplifiers. Since no preamplifier is used, strong signal handling is easy to achieve. Furthermore, since the multiplexer uses low-level digital driving signals, high-performance receivers that consume very little current can be built. One of my transceivers consumes only 11 mA at 12 V dc, but has 120 dB of blocking dynamic range and a +20-dBm IP3. That design emphasizes low current drain for portable use; better performance is possible if that is not a limitation.—Dan Tayloe, N7VE; 14240 S 7th St, Phoenix, AZ 85048; Arizona ScQRPions; dtayloe@home.com

Dear Dan,

Thank you. I recall we got a letter from P. T. Anderson, KC1HR, back in the Jul/Aug 1999 issue that dealt with something similar. The technique seems to hold significant promise for experimenters who want excellent dynamic



range from their gear—Doug Smith, KF6DX, [kf6dx@arrl.org](mailto:kf6dx@arrl.org).

## Signals, Samples and Stuff, Part 2 (May/June 1998)

Dear Mr. Smith,

I very much enjoyed reading your *QEX* article. An Amateur Radio friend found it for me when I asked him if he had seen anything on frequency synthesizers that may give me a start on replacing the failed PLL in my ICOM R71A.

Is there anywhere that I can get the complete circuit diagram, and perhaps the artwork, for the synthesizer (including the VFO)? If not, I'm sure I will go on to produce something using the design described as, being a broad-

cast-band DXer who listens only in exalted-carrier mode, the 1-Hz steps discussed sound heavenly!—*Brian Dodgson, Melbourne, Australia; [bigbird@melbpc.org.au](mailto:bigbird@melbpc.org.au)*

Hi Brian,

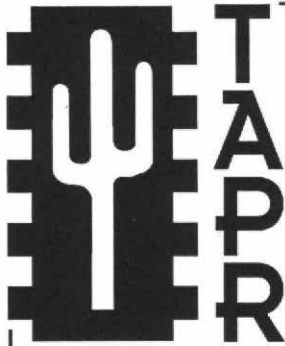
Thanks for your note. The DDS part of my design appears near the end of Chapter 18 of the 2001 ARRL Handbook, sans artwork. The VCO appears in the article you cite. While I can't supply the rest of it at this time, we published a couple other articles last year that may fill your bill. They are: S. Hageman, "Build This 250-MHz Synthesized Signal Source," Jan/Feb 2000; R. Peterson, WA6NUT, "A PLL Spur Eliminator for DDS VFOs," Jul/Aug 2000—Doug Smith, KF6DX

## Next Issue in QEX/Communications Quarterly

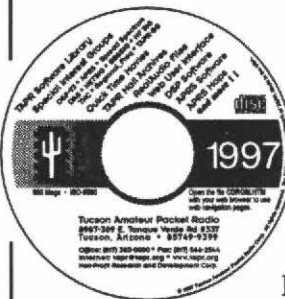
Is your personal computer powered on, but sitting idle most of the time? If so, you can engage it in useful scientific research without much ado. In our next issue, award-winning author H. Paul Shuch, N6TX, shows how digital signal processing contributes to the search for extraterrestrial radio signals. Specifically, Paul details a method of multi-processing wherein many separate computers around the world participate in various sets of calculations during

those idle periods. A lot of filtering and correlation is needed to sort the chaff from the wheat, so to speak, when it comes to reducing the vast array of data gathered by Earth's giant radio telescopes. "Distributed Processing Goes Galactic" tells how it's done and how you can get aboard. If you think that's not part of Amateur Radio, just look at what amateur astronomers like Percival Lowell (1855-1916) have done for their cause over the years.

ARRL Technical Advisor [Walt Maxwell, W2DU](#), returns to *QEX* with his analysis of how amplifiers deliver their power. The process seems familiar to many of us; but when you dig into the details, you find it's not so simple. Walt explains and he includes new data to support his conclusions.



Join the effort in developing Spread Spectrum Communications for the amateur radio service. Join TAPR and become part of the largest packet radio group in the world. TAPR is a non-profit amateur radio organization that develops new communications technology, provides useful/affordable kits, and promotes the advancement of the amateur art through publications, meetings, and standards. Membership includes a subscription to the *TAPR Packet Status Register* quarterly newsletter, which provides up-to-date news and user/technical information. Annual membership US/Canada/Mexico \$20, and outside North America \$25.

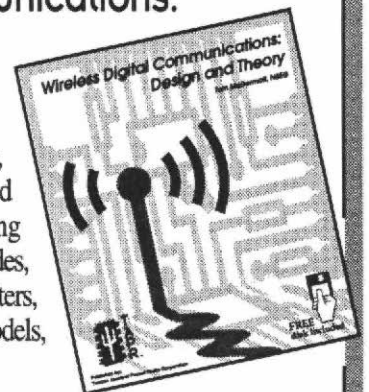


### TAPR CD-ROM

Over 600 Megs of Data in ISO 9660 format. TAPR Software Library: 40 megs of software on BBSs, Satellites, Switches, TNCs, Terminals, TCP/IP, and more! 150Megs of APRS Software and Maps. RealAudio Files. Quicktime Movies. Mail Archives from TAPR's SIGs, and much, much more!

### Wireless Digital Communications: Design and Theory

Finally a book covering a broad spectrum of wireless digital subjects in one place, written by Tom McDermott, N5EG. Topics include: DSP-based modem filters, forward-error-correcting codes, carrier transmission types, data codes, data slicers, clock recovery, matched filters, carrier recovery, propagation channel models, and much more! Includes a disk!



### Tucson Amateur Packet Radio

8987-309 E. Tanque Verde Rd #337 • Tucson, Arizona • 85749-9399  
Office: (940) 383-0000 • Fax: (940) 566-2544 • Internet: [tapr@tapr.org](mailto:tapr@tapr.org) [www.tapr.org](http://www.tapr.org)  
Non-Profit Research and Development Corporation

# RSGB PRODUCTS

Imported by ARRL— from the Radio Society of Great Britain



## Communication Reference

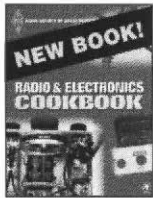
Packed with technical information!



### Radio Communication Handbook

One of the most comprehensive guides to the theory and practice of Amateur Radio communication. Find the latest technical innovations and techniques, from LF (including a new chapter for LowFERS!) to the GHz bands. For professionals and students alike. 820 pages.

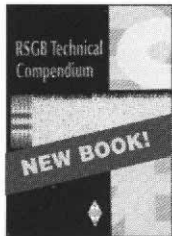
ARRL Order No. 5234—\$53



### Radio & Electronics Cookbook

Build up your electronics skills and knowledge with this unique collection of electronic projects, ideal for all levels of experimenters. Quick, rewarding construction projects. 319 pages.

ARRL Order No. RREC—\$28



### RSGB Technical Compendium

A collection of proven and experimental radio equipment designs, and practical advice (articles from 12 editions of *RadCom* 1999). 288 pages.

ARRL Order No. RTCP—\$30



### More Editions!

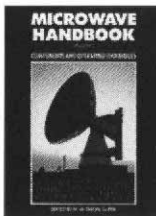
#### Technical Topics Scrapbook

Invaluable collections of experimental HF/VHF antennas, circuit ideas, radio lore, general hints and comments—all from the popular *RadCom* magazine column, *Technical Topics*.

1985-1989 edition, Order No. RT85—\$18

1990-1994 edition, Order No. 7423—\$25

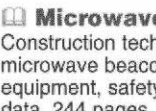
1995-1999 edition, Order No. RT95—\$25



#### Microwave Handbook, Volume 1

Operating techniques, system analysis and propagation, microwave antennas, transmission line and components, microwave semiconductors and tubes. 200 pages.

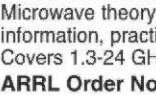
ARRL Order No. 2901—\$22



#### Microwave Handbook, Volume 2

Construction techniques, common equipment, microwave beacons and repeaters, test equipment, safety, filters and additional circuit data. 244 pages.

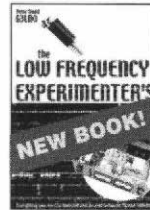
ARRL Order No. 3606—\$35



#### Microwave Handbook, Volume 3

Microwave theory and practice, reference information, practical designs, hints and tips. Covers 1.3-24 GHz. 284 pages.

ARRL Order No. 3975—\$35



### The LF Frontier!

#### The Low Frequency Experimenter's Handbook

Invaluable reference and techniques for transmitting and receiving between 50 and 500 kHz. 112 pages.

ARRL Order No. RLFS—\$32



#### RadCom 99 on CD-ROM

Includes all twelve issues of *RadCom* magazine published in 1999, with fully searchable keyword index.

ARRL Order No. RC99—\$33



#### VHF/UHF Handbook

The theory and practice of VHF/UHF operating and transmission lines. Background on antennas, EMC, propagation, receivers and transmitters, and construction details for many projects. Plus, specialized modes such as data and TV. 317 pages.

ARRL Order No. 6559—\$35

## Antennas



### HOT New Book!

#### Backyard Antennas

With a variety of simple techniques, you can build high performance antennas. Create compact multi-band antennas, end-fed and center-fed antennas, rotary beams, loops, tuning units, VHF/UHF antennas, and more! 208 pages.

ARRL Order No. RBYA—\$32



### Pocket Guide!

#### Your Guide to Propagation

This handy, easy-to-read guide takes the mystery out of radio wave propagation. It will benefit anyone who wants to understand how to get better results from their station.

ARRL Order No. 7296—\$17



### Outstanding Antennas!

#### HF Antenna Collection

Articles from RSGB's *RadCom* magazine. Single- and multi-element horizontal and vertical antennas, very small transmitting and receiving antennas, feeders, tuners and more. 240 pages.

ARRL Order No. 3770—\$18



### Antennas for every situation!

#### HF Antennas for All Locations

Design and construction details for hundreds of

antennas, including some unusual designs. Don't let a lack of real estate keep you off the air! 322 pages.

ARRL Order No. 4300—\$15

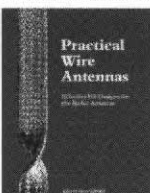


#### The Antenna Experimenter's Guide

Build and use simple RF equipment to measure antenna impedance, resonance and performance. General antenna construction methods, how

to test theories, and using a computer to model antennas. 158 pages.

ARRL Order No. 6087—\$30



#### Practical Wire Antennas

The practical aspects of HF wire antennas: how the various types work, and how to buy or build one that's right for you. Marconis, Windoms, loops, dipoles and even underground

antennas! The final chapter covers matching systems. 100 pages. Order No. R878—\$17

Order Toll Free  
**1-888-277-5289**  
[www.arrrl.org/shop](http://www.arrrl.org/shop)

Shipping: US orders add \$5 for one item, plus \$1 for each additional item (\$10 max.). International orders add \$2.00 to US rate (\$12.00 max.). US orders shipped via UPS.

## Operating



#### The VHF/UHF DX Book

Assemble a VHF/UHF station, and learn about VHF/UHF propagation, operating techniques, transmitters, power amplifiers and EMC. Includes designs for VHF and UHF transverters, power supplies, test equipment and

much more. 448 pages. Order No. 5668—\$35



### New Award Rules!

#### RSGB IOTA Directory 2000

Everything you need to know to enjoy collecting islands for the popular worldwide IOTA (Islands on the Air) award.

ARRL Order No. RA00—\$16

tel: 860-594-0355 fax: 860-594-0303

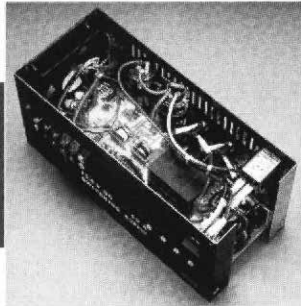
e-mail: [pubsales@arrrl.org](mailto:pubsales@arrrl.org)

World Wide Web: <http://www.arrrl.org/>

**ARRL** 225 Main St., Newington, CT 06111-1494

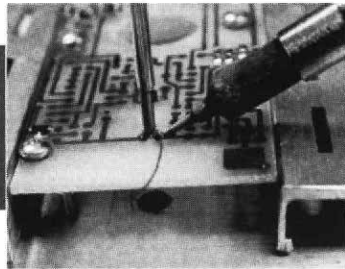


# THE ARRL HANDBOOK Use it, and you'll tackle Amateur Radio state of the art. 2001



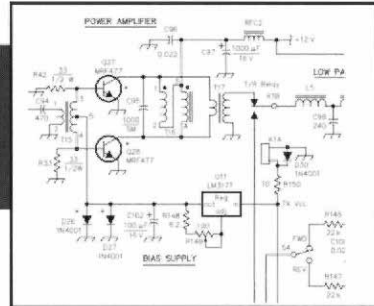
## Technology

This latest edition features up to date discussions and explanations in applied electronics and communications. The contents are enhanced by more than a thousand drawings, photos, and tables. Learn how to put new technology to work. Explore a new chapter on digital signal processing.



## Projects

The ARRL Handbook is a winning combination of informative theory and practical projects—for a variety of skill levels. Includes PC-board layouts and templates for weekend projects, and contact information for parts suppliers and manufacturers. Build to success!

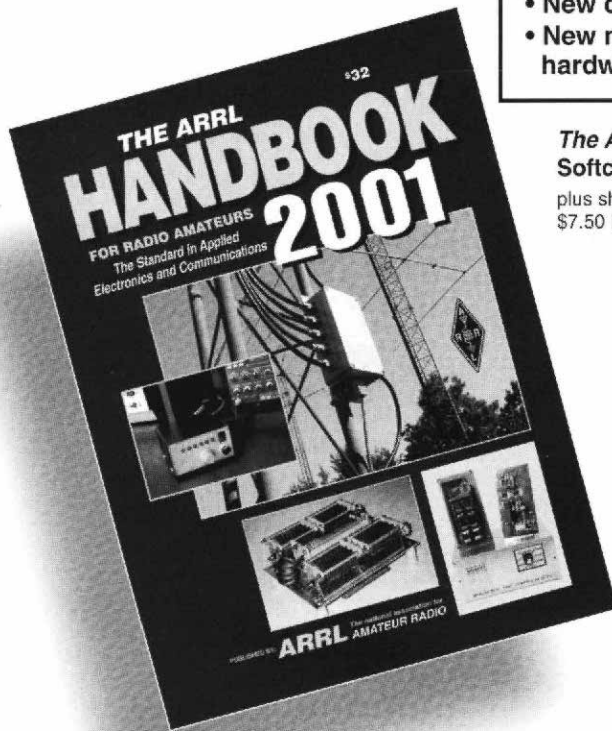


## Reliability

Experts in many fields have labored to make this edition the best ever! See for yourself why generations of hams and others interested in radio electronics have trusted The ARRL Handbook.

## ALWAYS UPDATED!

- New chapter on DSP
- Computer connector pinouts
- New material on computer hardware
- New remote antenna switch project



*The ARRL Handbook for Radio Amateurs*  
Softcover. ARRL Order No. 1867 ..... \$32  
plus shipping: \$6 US (UPS).  
\$7.50 International (surface mail).

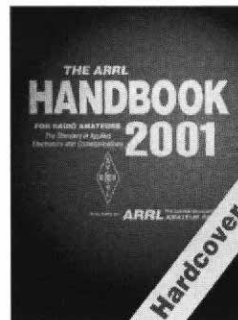


## *The ARRL Handbook CD for Radio Amateurs*

Version 5.0—for Windows and Macintosh\*  
View, Search and Print from the entire 2001 edition book!  
**CD-ROM.**

ARRL Order No. 1883 ..... \$39.95  
plus shipping: \$4 US (UPS).  
\$5.50 International (surface mail).

\*Some supplementary software utilities included, for Windows and DOS only.



## *The ARRL Handbook for Radio Amateurs* Hardcover.

ARRL Order No. H186..... \$49.95  
plus shipping: \$7 US (UPS).  
\$8.50 International (surface mail).

Sales Tax is required for shipments to CT, MI, VA, CA and Canada.



**ARRL** The national association for  
AMATEUR RADIO

225 Main Street, Newington, CT 06111-1494 tel: 860-594-0355 fax: 860-594-0303  
e-mail: pubsales@arrl.org World Wide Web: <http://www.arrl.org/>

In the US call our toll-free number **1-888-277-5289** 8 AM-8 PM Eastern time Mon.-Fri.

QEX 1/2001

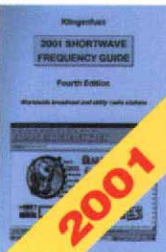





# ARRL Marketplace!



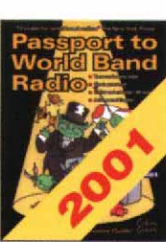
These publications have been added to the ARRL Library...  
so you can add them to yours!



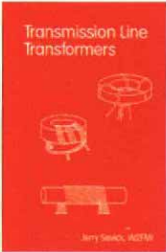
**2001 Shortwave Frequency Guide**  
Completely up-to-date shortwave radio guide. Tune into worldwide broadcast and utility radio stations. Find clandestine, domestic, and international stations. Thousands of entries, and a superb alphabetical list of stations. User-friendly! Totally revised-from scratch!  
**ARRL Order No. SWG1—\$34.95**



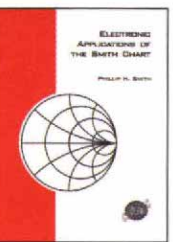
**The 2001 Super Frequency List CD-ROM**  
More than 39,700 entries cover both broadcast and utility stations, from 0 to 30 MHz. Hundreds of fascinating new color screenshots. Connects easily to leading receiver control programs. Browse through data in milliseconds! Search for specific frequencies, countries, stations, languages, call signs, and times as well. Requires Microsoft Windows.  
**ARRL Order No. SFC1—\$24.95**



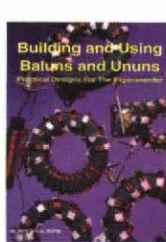
**Passport to World Band Radio 2001**  
Popular guide of worldwide radio schedules. It zeros in on news, sports and entertainment from Afghanistan to Zambia, and includes award-winning ratings of world band radios and "how-to" articles by experts. Includes Passport's Blue Pages, listing every station, everywhere—at a glance.  
**ARRL Order No. PWB1—\$19.95**



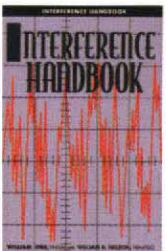
**Transmission Line Transformers**  
This book stands alone in its coverage of the subject of broadband transmission line transformers. Many configurations of Ruthroff and Guanella types of transformers are described with complete performance measurements and construction details.  
**ARRL Order No. 7245—\$34**



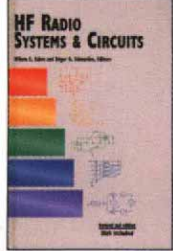
**Electronic Applications of the Smith Chart**  
The legendary Smith Chart inventor's original, classic reference book describing how the chart is used for designing lumped element (inductors and capacitors) and transmission line circuits (coaxial, waveguide, stripline or microstrip lines). Includes tutorial material on transmission line theory and behavior, circuit representation on the chart, matching networks, network transformations and broadband matching.  
**ARRL Order No. 7261—\$59**



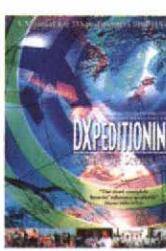
**Building and Using Baluns and Ununs**  
Practical Designs for the Experimenter! Transmission line transformer theory, design, and construction. Includes hundreds of examples for dipoles, Yagis, log periodics, beverages, multi-band antennas, antenna tuners, and more.  
**ARRL Order No. 7644—\$19.95**



**Interference Handbook**  
Locate and solve interference problems of every type. Suppression circuits for interfering devices are discussed in detail, and protection techniques for home entertainment equipment. THE book for power-line interference problems!  
**ARRL Order No. 6015—\$14**



**HF Radio Systems & Circuits**  
Includes Software! Comprehensive coverage of system definition and performance requirements down to the individual circuit elements that make up radio transmitters and receivers. Thorough attention is given to key circuits like oscillators, synthesizers, filters and amplifiers, speech processing, AGC systems, high linearity amplifiers, and solid state power amplifiers.  
**ARRL Order No. 7253—\$75**



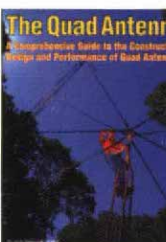
**DXpeditioning — Behind the Scenes**  
Learn what it takes to operate from a rare DX location. Covers every aspect of DXpeditioning, from planning and traveling, to QSLing. Based on many real-life experiences, including the Spratly Island (9M0C) effort.  
**ARRL Order No. DXBS—\$28**



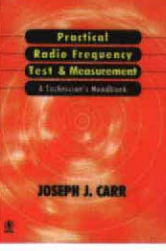
**Microcontroller Projects with Basic Stamps**  
Complete guide to developing practical solutions with these tiny microprocessors. A wealth of example projects. Includes software.  
**ARRL Order No. 7865—\$44.95**



**winSMITH 2.0**  
An easy-to-use, flexible computerized Smith Chart. Accelerate your RF and microwave designs! Unlock a greater understanding of transmission lines and simple matching problems. 3.5-inch installation diskette. Requires Microsoft Windows.  
**ARRL Order No. 7946—\$80**



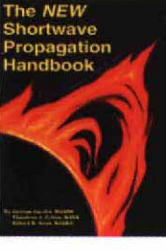
**The Quad Antenna**  
An authoritative book on the design, construction, characteristics and applications of quad antennas. Covers all aspects of this popular, but often misunderstood antenna.  
**ARRL Order No. QUAD—\$15.95**



**Practical Radio Frequency Test & Measurement**  
Learn the basics of performing tests and measurements used in radio-frequency systems installation, proof of performance, maintenance, and troubleshooting. Provides immediate applications, test set-ups, procedures, and interpretation of results.  
**ARRL Order No. 7954—\$34.95**

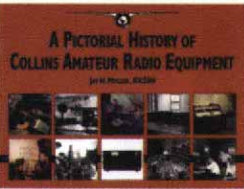


**33 Simple Weekend Projects**  
A wide-ranging collection of do-it-yourself electronics projects. Useful accessories for VHF FMing, projects for satellite communications, CW, simple antennas, and a complete HF station you can build for around \$100!  
**ARRL Order No. 7628—\$15.95**



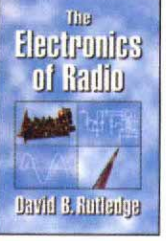
**The NEW Shortwave Propagation Handbook**  
Understand how HF signals propagate, and learn about sunspots and ionospheric predictions. Make productive use of the radio spectrum, regardless of the time of day, season, or sunspot cycle. Filled with illustrations, photos, charts and tables!  
**ARRL Order No. 7636—\$19.95**

**A Pictorial History of Collins Amateur Radio Equipment**  
The most complete history of Collins equipment is told with hundreds of pictures (many in color) and in the words of the men who made it happen. Travel from the pre-war era through the 1980's, and enjoy an upclose profile of Arthur A. Collins.  
**ARRL Order No. 7830—\$39.95**



**Order Toll Free 1-888-277-5289**  
[www.arrl.org/shop](http://www.arrl.org/shop)

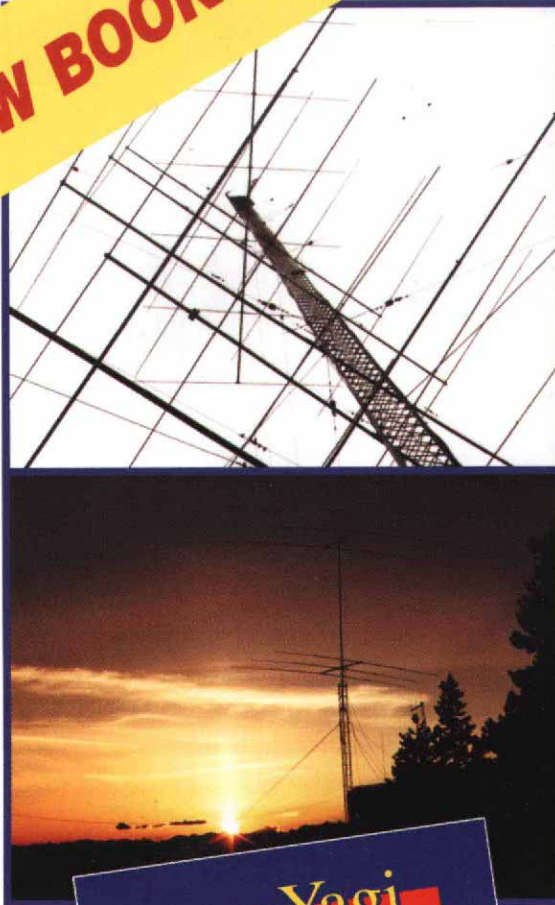
**Shipping and Handling instructions:** US orders add \$5 for one item, plus \$1 for each additional item (\$10 max.). US orders are shipped via UPS. International orders add \$2.00 to the US shipping rate (\$12.00 max.). Orders are shipped via surface mail. Other shipping options are available. Please call or write for information.  
**Sales Tax** is required for shipments to CT and MI 6% (including S/H), VA 4.5% (excluding S/H), CA (add applicable tax, excluding S/H) and Canada (excluding S/H).



**The Electronics of Radio**  
An introduction to analog radio electronics, through the design and construction of a radio transceiver (the NorCal 40A). A structured (college-level) approach describes basic electronic components and simple circuits, filters, amplifiers, oscillators, mixers, and antennas. Includes circuit simulation software (diskette), *Puff*.  
**ARRL Order No. ERAD—\$44.95**



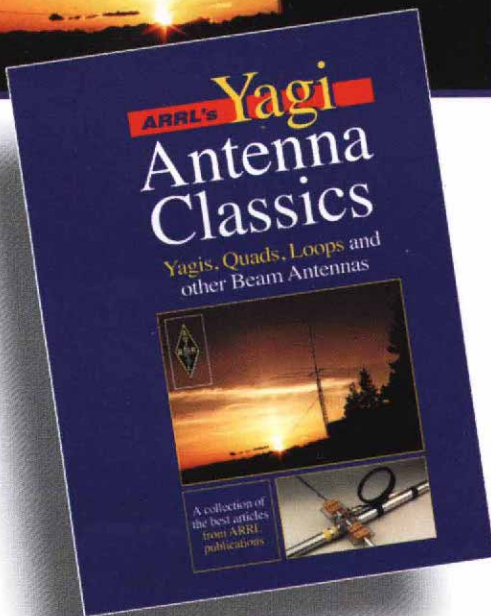
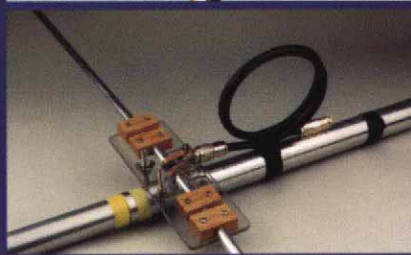
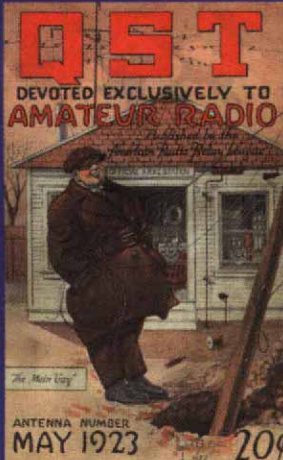
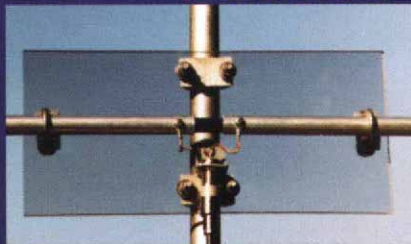
**NEW BOOK!**



# ARRL's Yagi Antenna Classics



**Directional antennas**  
— superior communications



**Nine chapters cover some of the most effective antennas...Yagis, Quads, Loops, and other Beam Antennas**

Enjoy this collection of some of the very best articles from *QST*, *QEX*, *NCJ* and other ARRL publications. The beam antennas covered in this book will provide the reader with a historical perspective, new and ambitious ideas, and computer-optimized designs for all-around best performance.

**Read about beams** or actually build one of your own! **Discover a wealth of ideas** from some of the leaders in antenna design and experimentation of the last 70 years. **See classic ads and photos** from the pages of *QST*.

Available from your ARRL Publication Dealer!

### Contents

- **Monobanders:** Beams for your favorite band
- **Multibanders:** Beams that cover two or more bands
- **HF, VHF and UHF Beams:** From 80 meters to 2304 MHz
- **Computer Modeling:** Optimize your beam's performance
- **Towers, Masts and Guys:** Your beam needs solid support
- **The "WOW" Factor:** Can you believe this?

**ARRL's Yagi Antenna Classics**  
ARRL Order No. 8187...\$17.95  
plus shipping: \$5.00 US (UPS)  
\$7.00 International (surface mail)  
Sales Tax is required for shipments to CT, MI, VA, CA and Canada.

**ARRL** The national association for **AMATEUR RADIO** 225 Main Street, Newington, CT 06111-1494 tel: 860-594-0355 fax: 860-594-0303  
e-mail: [pubsales@arrl.org](mailto:pubsales@arrl.org) World Wide Web: <http://www.arrl.org/>

In the US call our toll-free number **1-888-277-5289** 8 AM-8 PM Eastern time Mon.-Fri.